DEVELOPMENT OF MONITORING AND TREATMENT TECHNOLOGIES TO COMBAT HARMFUL ALGAE BLOOMS

By

Shardula Gawankar

A DISSERTATION

Submitted to
Michigan State University
in partial fulfillment of the requirements
for the degree of

Environmental Engineering – Doctor of Philosophy

2023

ABSTRACT

Lake Erie has been affected by harmful algal blooms for decades. In 2014, this resulted in the plant having to shut down its intake after toxic cyanotoxins were found in source water. Such occurrences are becoming more common across the globe. U.S. EPA has established regulations for microcystin, the most common form of cyanotoxin. Climate change is predicted to increase the occurrence of other types of cyanotoxins, such as saxitoxins, which are not regulated by the U.S. EPA. Hence, the removal and monitoring of cyanotoxins, produced by harmful algae blooms, in water is of utmost importance to protect public health.

The efficacy of oxidation varies greatly for each of the cyanotoxins due to their different chemical structures. There is presently no oxidation process that a water treatment plant can implement that is proven to simultaneously remove all the cyanotoxins (microcystin, saxitoxin, cylindrospermopsin, and anatoxin) from drinking water. Thus, water treatment plants that are currently designed to remove microcystins are not protected against all forms of cyanotoxins. The investigation of the removal of these cyanotoxins using innovative treatment technologies requires a detection method that is sensitive and capable of detecting all the variants of cyanotoxins. The detection of saxitoxin is particularly challenging as compared to other cyanotoxins due to its low molecular mass and highly polar nature. Hydrophilic interaction liquid chromatography coupled with mass spectrometry (HILIC-MS) has the ability to provide specific detection through mass differentiation, which makes it an ideal tool for the quantitative analysis of saxitoxin and its variants. Hence, a method was developed to extract and detect saxitoxin from water using HILIC-MS in conjunction with weak cation exchange solid phase extraction (SPE), to provide a sensitive and reliable quantification of saxitoxins.

However, the application of LC/MS for the detection of cyanotoxins in treatment studies is not cost effective as the cost of instrumentation is high, its operation requires high skill, and cyanotoxin standards have limited access and are expensive. Hence, a screening technique has been developed which uses methylene blue to identify the reaction kinetics of persulfate and peroxide oxidation in the presence of ferrous chloride and to optimize parameters, which can be helpful in predicting the degradation of cyanotoxins under similar conditions. Catalyst activated persulfate and peroxide oxidation produce sulfate and hydroxyl radicals, which can degrade a wide range of recalcitrant chemicals and hence are preferred in water and wastewater treatment. The screening technique was validated by investigating the degradation of microcystin-LR. The notable advantages of developing this screening technique are: (i) reduced cost of analysis as methylene blue can be detected in real time by measuring its absorbance, and (ii) can perform multiple trials in short time due to ease of analysis. This screening technique was also applied to iron oxide coated ceramic membranes in combination with persulfate oxidation to understand the degradation kinetics.

ACKNOWLEDGEMENTS

I would like to express my deepest gratitude to Dr. Susan Masten for her excellent mentoring and guidance through the latter half of my PhD program. I am extremely grateful for her dedication towards making me reach the finish line and believe that I could not have achieved the completion of this program without her support. She is my role model and I hope to carry forward the research ethics and passion for teaching that she has instilled in me.

I would also like to express my deepest appreciation to Dr. Rebecca Lahr who believed in me to persevere and taught me excellent organizational skills. She always welcomed my ideas and supported my passion for working with cyanotoxins. I am also thankful to my other committee members, Dr. Hui Li and Dr. Joan Rose for their valuable feedback and insight into overcoming challenges faced in my research.

I also am grateful for the support from my friends and family throughout my PhD program. My parents have been my pillars of strength and their belief in me has made me persevere through this journey. Shivam Bajaj has been a wonderful friend who has constantly motivated me and trusted my ability to succeed. Lastly, I would like to recognize my dog for being my emotional support and providing joy during difficult times.

TABLE OF CONTENTS

CHAPTER 1 : Review Of The Occurrence, Treatment Technologies, And Detection Methods For Saxitoxins

ABSTRACT

Saxitoxins are a group of cyanotoxins, which are produced by freshwater cyanobacteria and marine dinoflagellates. They have the highest potency (LD50 of 10 $\mu g/kg$ in mice) among the cyanotoxins. They are neurotoxic and act by inhibiting the supply of sodium ions into cells, resulting in paralysis and death by respiratory arrest in humans. The increasing occurrence of saxitoxins in freshwaters, a result of climate change and the presence of excess nutrients, is becoming a concern for water treatment owing to its structural properties which make it resistant to oxidation at pH < 8.4. Hence, it is crucial to be able to monitor these toxins in surface and drinking water to protect public health. The polar nature of saxitoxins makes it difficult to use traditional reverse phase LC/MS for quantification and the existing ELISA method is unable to detect the different variants of saxitoxin. The aim of this review is to outline the current state of knowledge related to the occurrence of saxitoxins in freshwaters and treatment technologies that are successful in removing saxitoxins from water, while also providing a critical assessment of the detection methods to provide a basis for further development.

INTRODUCTION

Harmful algal blooms (HABs) result from the excessive growth of cyanobacteria (also referred to as blue-green algae, although cyanobacteria are not true algae) in freshwater and seawater. HABs can adversely affect human life, fish, shellfish, marine mammals, and birds. Cyanotoxins can be classified as hepatotoxins (e.g., microcystins and cylindrospermopsin) and neurotoxins (e.g., saxitoxins and anatoxins). This review focuses on saxitoxins that are produced by several freshwater cyanobacterial species, including *Anabaena*, *Aphanizomenon*, and *Lyngbya*.

The increasing occurrence of saxitoxins in freshwater reservoirs (Grachev et al., 2018; Kaas & Henriksen, 2000; Loftin et al., 2016; Molica et al., 2002) and drinking water sources (AWWA, 2016; Ohio EPA, 2021), coupled with their high human toxicity (intraperitoneal LD_{50} of $10\ \mu g/kg$ in mice) (Wiberg & Stephenson, 1960) present a pressing need for the development of strategies to monitor and mitigate these HABs. Toward this goal, it is essential to develop a standard method for monitoring saxitoxins, as has been done for microcystins and cylindrospermopsin (J.A. Shoemaker et al., 2015; U.S. EPA, 2015d).

The biological and analytical detection methods of saxitoxins (Humpage et al., 2010; J. Li & Persson, 2021; Rutkowska et al., 2019), treatment methods focused on the removal of saxitoxins (da Silva et al., 2022), and the occurrence and fate of saxitoxins in freshwater (Christensen & Khan, 2020) have been reviewed separately but there does not exist a single comprehensive review of all of the above elements, with implications for water treatment authorities. Hence, this review updates and provides a comprehensive review of the global occurrence of saxitoxins in freshwaters, treatment technologies for removal of saxitoxins from drinking water. It also includes the detection methods that can be applied for the monitoring of saxitoxins and its variants in water.

Structure of Saxitoxin

Saxitoxin, also referred to as the paralytic shellfish toxin (PST), is a neurotoxin. Saxitoxins are produced by freshwater cyanobacteria such as *Anabaena*, *Cylindrospermopsis*, *Aphanizomenon*, *Planktothrix*, and *Lyngbya*, and by eukaryotic dinoflagellates in marine environments (Ballot et al., 2017; Cusick & Sayler, 2013; Pearson et al., 2010; Wiese et al., 2010). Fifteen freshwater species of cyanobacteria have been identified as saxitoxin producers (Christensen & Khan,

2020). *Aphanizomenon flos-aquae* was the first freshwater cyanobacterium identified as a saxitoxin producer in the late 1960s (Jackim & Gentile, 2021; Onodera et al., 1997).

The more than 50 different variants of PSTs have a common backbone of tetrahydropurine ring that can be substituted at the C11, N1, and C13 positions and are classified into 3 major categories based on the functional group (R_4) at the C13 position: carbamoyl ($R_4 = CO - NH_2$), decarbamoyl ($R_4 = H$), and N-sulfocarbamoyl ($R_4 = CO - NH - SO_3^-$), shown here in the order of decreasing toxicity (Genenah & Shimizu, 1981; Raposo et al., 2020; Shimizu et al., 1981). The positively charged guanidinium groups present on the tetrahydropurine ring and the hydroxyl group at C12 have a high affinity to bind to the sodium channels on cell membranes, which inhibits the supply of sodium ions into cells, leading to paralysis and death by respiratory arrest (Aráoz et al., 2010; Llewellyn, 2006; Strichartz, 1984). The potency of each variant is different and there have been several studies that have tried to evaluate the relative toxicity of PSTs (Genenah & Shimizu, 1981; Oshima, 1995; Schantz, 1986; Vale et al., 2008). In order to reduce the discrepancy of the toxicities derived from different studies, the Panel on Contaminants in the Food Chain proposed Toxicity Equivalent Factors (TEF) as a measure to compare the potency of the variants of saxitoxin (Alexander et al., 2009). The most common variants of saxitoxin along with their TEF are listed in Table 1-1.

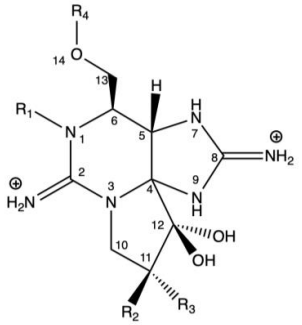

Figure 1-1: Structure of saxitoxin.

Table 1-1: Variants of saxitoxin and their toxicity equivalent factor.

Group	Toxin	R_1	R_2	R_3	R_4	TEF
Carbamoyl	STX	–H	–H	–H	$–OC–NH_2$	1.0
	NeoSTX	–OH	–H	–H	$–OC–NH_2$	1.0
	GTX1	–OH	–H	$–OSO_3^-$	$–OC–NH_2$	1.0
	GTX2	–H	–H	$–OSO_3^-$	$–OC–NH_2$	0.4
	GTX3	–H	$–OSO_3^-$	–H	$–OC–NH_2$	0.6
	GTX4	–OH	$–OSO_3^-$	–H	$–OC–NH_2$	0.7
Decarbamoyl	dcSTX	–H	–H	–H	–H	1.0
	dcNeoSTX	–OH	–H	–H	–H	0.4
	dcGTX1	–OH	–H	$–OSO_3^-$	–H	NA*
	dcGTX2	–H	–H	$–OSO_3^-$	–H	0.2
	dcGTX3	–H	$–OSO_3^-$	–H	–H	0.4
	dcGTX4	–OH	$–OSO_3^-$	–H	–H	NA
N-sulfocarbamoyl	GTX5	–H	–H	–H	$–OC–NH–SO_3^-$	0.1
	GTX6	–OH	–H	–H	$–OC–NH–SO_3^-$	0.1
	C1	–H	–H	$–OSO_3^-$	$–OC–NH–SO_3^-$	NA
	C2	–H	$–OSO_3^-$	–H	$–OC–NH–SO_3^-$	0.1
	C3	–OH	–H	$–OSO_3^-$	$–OC–NH–SO_3^-$	NA
	C4	–OH	$–OSO_3^-$	–H	$–OC–NH–SO_3^-$	0.1

*Not available

Toxicity and Fate of Saxitoxin in Water

Saxitoxins are the most toxic of all cyanotoxins known to date, with the lowest LD_{50} value (as shown in Table 1-2). The four major cyanotoxins – microcystins, cylindrospermopsin, anatoxin-a, and saxitoxins have been listed on the Contaminant Candidate List 4 (CCL4) and List 5 (CCL5) by the U.S. EPA. However, drinking water health advisories by the U.S. EPA have been established only for microcystins and cylindrospermopsin (U.S. EPA, 2015b, 2015a).

Table 1-2: Toxicities and drinking water guidelines of different cyanotoxins.

Cyanotoxin	**LD_{50} (i.p. mice)**		**Drinking water guidelines (ug/L)**		
Microcystin-LR	50 μg/kg	(Carmichael et al., 1990; Dittmann & Wiegand, 2006; Krishnamurthy et al., 1986; Pearson et al., 2010)	1	*Provisional guideline value provided by WHO*	(World Health Organization (WHO), 2017)
			1.6	*Ohio Threshold for drinking water*	(Ohio EPA, 2020)
			0.1	*Short-term, chronic, and subchronic Health Based Value for Minnesota*	(Minnesota Department of Health, 2015)
			1.3	*Australian Drinking Water Guideline*	(NHMRC Australia & NRMMC Australia, 2022)
			1.5 (total microcystins)	*Guideline for Canadian Drinking Water Quality*	(Health Canada, 2022)
Nodularin	30 – 60 μg/kg	(Carmichael & Boyer, 2016)	3	*New Zealand provisional maximum acceptable value*	(Drinking-Water Standards for New Zealand 2005 (Revised 2018), 2018)
Cylindrospermopsin	200 μg/kg after 120 hours	(Buratti et al., 2017)	1	*New Zealand provisional maximum acceptable value*	(Kouzminov et al., 2007)

Table 1-2 (cont'd)

			1	*Oregon provisional guideline*	(Farrer et al., 2015)
			3	*Ohio Threshold for drinking water*	(Ohio EPA, 2020)
			3	*Drinking Water Health Advisory for Cylindrosper mopsin*	(U.S. EPA, 2015c)
Anatoxin-a	200 – 375 µg/kg	(Carmichael et al., 1990; Carmichael & Boyer, 2016)	6	*New Zealand provisional acceptable value*	(Kouzminov et al., 2007)
			3	*Oregon provisional guideline*	(Farrer et al., 2015)
			1.6	*Ohio Threshold for drinking water*	(Ohio EPA, 2020)
Anatoxin-a(s)	20 – 40 µg/kg	(Carmichael et al., 1990; Carmichael & Boyer, 2016)	1	*New Zealand provisional acceptable value*	(Kouzminov et al., 2007)
Saxitoxin	10 µg/kg	(Buratti et al., 2017; Carmichael & Boyer, 2016; Pearson et al., 2010; Wiberg & Stephenson, 1960)	3	*New Zealand provisional acceptable value*	(Kouzminov et al., 2007)
			1	*Oregon provisional guideline*	(Farrer et al., 2015)
			1.6	*Ohio Threshold for drinking water*	(Ohio EPA, 2020)

Saxitoxins are hydrophilic polar compounds that are known to be basic due to the presence of guanidinium groups. The guanidinium group at C7,8,9 has a pKa of 8.24 and that at C1,2,3 has a pKa of 11.28 (Hall et al., 1990a; Rogers & Rapoport, 1980; Schantz, 1986; Strichartz, 1984). At a neutral pH, the saxitoxin molecule carries a bivalent positive charge which, upon a rise in pH, changes as the C8 guanidinium group donates a hydronium ion (Shimizu et al., 1981; Strichartz, 1984). Even with a low octanol-water partitioning coefficient (Kow) of <0.001, saxitoxins can be bioaccumulated in fish and animals through the gut caused by the alkaline environment (pH >8.22) which results in deprotonation of the guanidinium group of saxitoxins at C7,8,9, resulting in the molecule losing its polarity and hence becoming more prone to diffusion across the lipid bilayer (Llewellyn 2006).

Saxitoxins are very unstable in nature and are likely to undergo chemical transformation to the other toxic variants of saxitoxin (Jones & Negri, 1997; Negri et al., 1997). Saxitoxins are known to survive for periods up to 18 months at low pH conditions and at temperatures of 4 °C or lower (Alfonso et al., 1994). Upon heating and in acidic pH conditions, this toxin is capable of increasing toxicity by transforming into more toxic variants, but rapidly transforms to lose toxicity in basic pH environments (Jones & Negri, 1997; Nagashima et al., 1991). The persistence of saxitoxins in non-sterile water has been observed for around 90 days with an increase in toxicity at 90 days and that in water filtered through a 0.2 μm membrane filterwas even longer (Jones & Negri, 1997). Saxitoxins are resistant to bacterial degradation in the environment (Tang et al., 2012) with the exception of certain marine bacterial isolates obtained from toxic mussels that achieved > 90% degradation of saxitoxins in 3 days (Donovan et al., 2008).

OCCURRENCE OF SAXITOXINS

HABs occur due to a variety of influencing factors such as nutrient content, temperature, topography, and ecology of a water body. Nutrients such as phosphorus and nitrogen play a very important role in the growth of HABs. It is not only the addition of these nutrients into the water body that drives the increase in HABs, but also the change in the ratio of these nutrients. The high nitrogen to phosphorus ratio, a result of a 3-fold increase in nitrogen fertilizer as compared to phosphorus, is conducive for the growth of HABs (Glibert & Burford, 2017). The outcome of this increased nitrogen to phosphorus ratio greatly increases the formation of HABs because agricultural run-off is a primary contributor of nutrients into freshwaters among other sources like the atmosphere, wastewater treatment plants, and industrial waste. In some cases, organisms also play a role in increasing algal growth, for example in Lake Erie, zebra mussels capture phosphorus from the sediment and reintroduce it in water (Walker, 2014). This in turn increases the nutrient content, which facilitates HAB growth and its dominance in the ecosystem.

There is a strong relation between climate change and rise in HABs which can be supported by the factors specified below (Bullerjahn et al., 2016; J. C. Ho & Michalak, 2020; Jöhnk et al., 2008; Michalak et al., 2013). Most significantly, climate change causes a rise in temperatures, which is preferred by most HAB species and makes them dominant over other types of algae. The warmer temperatures also increase stratification in the water body, favoring the formation of HABs. Furthermore, the higher temperatures cause an increase in phosphorus loading, which as mentioned before, plays a crucial role in formation of HABs. Another consequence of climate change is an increase in precipitation, which can be expected to increase the likelihood of nutrient runoff into water bodies, ultimately resulting in an increase in occurrence of HABs (J. C. Ho & Michalak, 2020; Michalak et al., 2013). Evidence of the effects of global warming is

supported by studies that indicate a rise in HAB cyanobacteria in temperate zones due to an increase in temperature (Sinha et al., 2012; Wiedner et al., 2007).

Among the many cyanobacterial species that produce HABs, *Anabaena*, *Cylindrospermopsis*, *Aphanizomenon*, *Planktothrix*, and *Lyngbya*, are some examples of those that produce saxitoxins in freshwaters. A review by Christensen and Khan (2020) provides a comprehensive list of cyanobacterial species producing saxitoxins. Table 1-3 provides a summary of the global occurrence of cyanobacterial species that produced saxitoxins in freshwaters. With respect to the prevalence of saxitoxins, a study reviewing the global occurrence of cyanotoxins found saxitoxins to be present in 8% of the 1118 reported instances of cyanotoxins, with the highest percentage of saxitoxins i.e., 21%, occurring in Australia and New Zealand (Svirčev et al., 2019). A national study conducted by the U.S. EPA in 2007 on 1161 lakes and reservoirs found saxitoxin to be present in 7.7% of the samples with a mean concentration of $0.061\ \mu g/L$; however, saxitoxin producers were present at a high percentage, i.e., 79% of the samples (Loftin et al., 2016). Given the increasing rate of climate change coupled with this high percentage of saxitoxin producers, it is anticipated that the percentage of saxitoxin detections in freshwaters will rise drastically.

The production of saxitoxins in freshwaters is largely influenced by environmental factors, such as temperature, light intensity, conductivity, water hardness, and nutrient presence (Burford et al., 2016; Carneiro et al., 2009, 2013; Castro et al., 2004). High nitrogen to phosphorus ratios have been shown to result in at least a 3 fold increase in the production of saxitoxin by *Alexandrium tamarense* (Granéli & Flynn, 2006). The positive correlation of saxitoxin production with higher TN:TP ratio was also reported by Moraes et al. (2021) while on the other hand, phosphorus limitation was reported to have increased the saxitoxin concentration in both

Alexandrium sp. and *R. raciborskii* species, suggesting saxitoxin production to be a form of survival strategy (Moraes et al., 2021). Turbidity had a negative correlation with saxitoxin concentrations (Moraes et al., 2021). Global warming has resulted in increased drought periods, especially in semi-arid conditions like those in Northeast Brazil. This prolonged drought period causes intense evaporation which leads to high salt concentrations in water bodies, which in turn results in higher saxitoxin production for a certain period (Carneiro et al., 2013). A positive correlation between conductivity and saxitoxin concentrations was also found in Peri Coastal Lake (Brentano et al., 2016). Consequently, the production of saxitoxins in higher salt concentrations and in alkaline conditions, suggest that the toxin is linked to maintaining homeostasis of the cyanobacterial cell (Pomati et al., 2004). Saxitoxin production was found to be highest at a temperature of $25℃$ with high light intensity ($> 100\ \mu mol$ photons$/m^2 s$) (Mesquita et al., 2019), while another study discovered a positive correlation of low temperature and cold stress conditions with saxitoxin production (Kim et al., 2021).

Table 1-3: Global occurrence of saxitoxin and its variants along with the associated cyanobacteria in freshwaters.

Year	**Location**	**Cyanobacteria**	**Variants of Saxitoxin**	**Method of Detection**	**Reference**
1990 - 1993	Murray-Darling basin, Victoria Australia	*Anabaena circinalis*	STX, GTX1-6, dcGTX2, dcGTX3, and C1-2	HPLC and Fast Atom Bombardment (FAB)-MS	(Baker & Humpage, 1994; Humpage et al., 1994)
1993	Guntersville reservoir, Alabama, USA	*Lyngbya wollei*	dcSTX, dcGTX2, dcGTX3	HPLC-FLD	(Carmichael et al., 1997; Onodera et al., 1997)
1994	Farm dam near Forbes, New South Wales, Australia	*Anabaena circinalis*	C1-2, dcGTX2, dcGTX3, GTX2-5, STX, dcSTX	HPLC-FLD	(Negri et al., 1995)

Table 1-3 (cont'd)

1994	96 freshwater ponds and lakes, Denmark	*Anabaena lemmermannii* (dominant species)	STX, GTX1-5, dcSTX, neoSTX	HPLC-FLD	(Kaas & Henriksen, 2000)
1994 - 1996	2 reservoirs in State of São Paulo, Brazil	*Cylindrospermopsis racibroskii*	STX, neoSTX,	HPLC-FLD and HPLC-ESIMS	(Lagos et al., 1999)
1996	Montargil reservoir in Portugal	*Aphanizomenon flos-aquae, Microcystis aeruginosa*	STX, neoSTX, dcSTX, GTX5-6	HPLC-FLD and LC/MS	(Pereira et al., 2000)
1996	Crestuma-Lever reservoir in Portugal	*Aphanizomenon flos-aquae, Microcystis aeruginosa*	GTX1, GTX3-4	HPLC-FLD	(Ferreira et al., 2001)
1997	Lake Varese, Italy	*Planktothrix* sp.	STX	HPLC-FLD and LC/MS	(Pomati et al., 2000)
2000	Armano Ribeiro Gonçalves reservoir and Pataxó channel, Brazil	*Cylindrospermopsis raciborskii*	STX, GTX, C1-2	HPLC-FLD	(Costa et al., 2006)
2002 - 2003	Finnish freshwater in south-Eastern and Central Finland	*Anabaena lemmermannii*	STX	HPLC-FLD and LC/MS	(Rapala et al., 2005)
2005 - 2008	Recreational area of Champs-sur-Marne at Paris, France	*Aphanizomenon gracile, Aphanizomenon flos-aquae*	STX, neoSTX	HILIC-MS	(Ledreux et al., 2010)
2006	Lakes and reservoirs in Missouri, Iowa, Kansas, and Minnesota (USA)	*Anabaena, Aphanizomenon , Planktothrix*	N/A[a]	ELISA	(Graham et al., 2010)

Table 1-3 (cont'd)

2008 – 2009	Lake Pamvotis, Greece	*Aphanizomenon flos-aqua*	N/A[a]	ELISA	(Gkelis et al., 2014)
2009	Lake Atitlan, Guatemala	*Lyngbya*	N/A[a]	ELISA	(Rejmánková et al., 2011)
2009	Arctic freshwaters in northern Baffin Island	*Scytonema* cf. *crispum*, *Lyngbya wollei*	N/A[a]	ELISA	(Kleinteich et al., 2013)
2009 – 2011	Reservoirs in Rio Grande do Norte, Brazil	*Cylindrospermopsis raciborskii*, *Planktothrix agardhii*, *Aphanizomenon gracile*, *Anabaena circinalis*	N/A[a]	ELISA	(Fonseca et al., 2015)
2010	Lake Baikal, Russia	*Anabaena lemmermannii*	N/A[a]	ELISA	(Belykh et al., 2015)
2010	19 lakes and reservoirs in Czech Republic	*Anabaena* sp., *Aphanizomenon* sp.	N/A[a]	ELISA	(Jančula et al., 2014)
2011	Drinking-water pre-treatment reservoir and lakes in a recreational reserve of The Groynes in South Island, New Zealand	*Scytonema* cf. *crispum*	STX, neoSTX, GTX1-5, dcSTX, dcGTX2-3	HPLC-FLD	(Smith et al., 2011)
2014	The Vistonis lake, Greece	*Aphanizomenon favaloroi*	STX, neoSTX	HILIC-MS/MS	(Moustaka-Gouni et al., 2017)

Table 1-3 (cont'd)

2014 - 2015	Lakes Gauštvinis, Jieznas, and Širvys in Lithuania	*Aphanizomenon gracile*	STX	HILIC-MS/MS	(Karosienė et al., 2020)
2016	Karla reservoir, Greece	*Aphanizomenon favaloroi, Cylindrospermopsis raciborskii*	N/A[a]	ELISA	(Papadimitriou et al., 2018)
2017	Irkutsk reservoir, Russia	*Anabaena lemmermannii*	STX	HPLC-MS and ELISA	(Grachev et al., 2018)
2017 - 2018	Peri Lake, Brazil	*Cylindrospermopsis raciborskii*	STX, neoSTX, dcSTX, GTX1-5	HPLC-FLD	(Ramos et al., 2021)
2018	5 lakes in northern Zealand, Denmark	*Anabaena lemmermannii*	STX, GTX, dcSTX, neoSTX, dc-neoSTX	HPLC-FLD	(Podduturi et al., 2021)
2019 - 2020	Lake Taihu, China	*Dolichospermum, Apanizomenon, and Oscillatoria*	N/A[a]	ELISA	(H. Li et al., 2022)

[a]Measured in terms of total saxitoxins

TREATMENT OF SAXITOXINS

Most studies on the removal of saxitoxins from drinking water are limited to laboratory scale and have been summarized in Table 1-4 (Coral et al., 2011; Newcombe & Nicholson, 2002; Nicholson et al., 2003; Orr et al., 2004; Rositano et al., 2001). The efficacy of each treatment method is dependent on the chemistry of saxitoxin molecule. With an increase in pH (>8.24), the saxitoxin molecule donates a hydronium ion from the C8 guanidinium group; this deprotonated form exists in equilibrium with a ketone that forms when the gemdiol group is dehydrated (Figure 1-2; (Hall et al., 1990b; Shimizu et al., 1981; Strichartz, 1984).

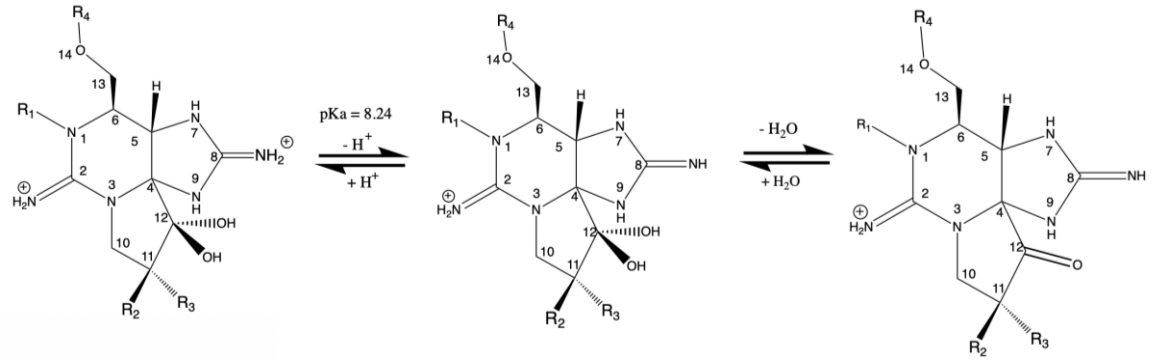

Figure 1-2: Effect of pH on the saxitoxin molecule.

Saxitoxins with a deprotonated C-8 guanidinium group are susceptible to oxidation, which explains their degradation even by hypochlorite at pH > 8 (Newcombe & Nicholson, 2002; Nicholson et al., 2003; Rogers & Rapoport, 1980); A pH of > 8.5 along with a residual free chlorine concentration of 0.5 mg/L was required for > 90% removal of saxitoxins (Newcombe & Nicholson, 2002; Nicholson et al., 2003). However, this is not a typical pH condition for water treatment plants drawing their source from surface waters that do not employ chemical softening. The majority of saxitoxin variants were resistant to batch ozone treatment within a pH range of 7 – 8 at a residual ozone concentration of 0.5 mg/L for 10 mins (Newcombe & Nicholson, 2002; Orr et al., 2004; Rositano et al., 2001). Total and extracellular saxitoxin concentrations remained unchanged after treatment with potassium permanganate (0.5 mg/L) in natural waters at pH ~8 (Ho et al. 2009). STX and GTX2/3 were susceptible to photolysis at a pH of 8 and not at a pH of 6, and the study also suggested that hydroxyl radical was not a significant contributor in the degradation, implying that the toxins did not undergo hydrolysis or direct photolysis (Kurtz, 2021).

The only study that evaluated catalytic wet peroxide oxidation (CWPO) of saxitoxin showed that only 60% removal of STX occurred after 5 hours of reaction as compared to 100% removal of microcystin-RR in 1.5 hour reaction time (Munoz et al., 2019).

Adsorption using granulated activated carbon (GAC) with an empty bed contact time of 15 mins completely removed all the high potency saxitoxins i.e., STX, dc-STX, and GTX2-3 (Orr et al., 2004). GAC with greater amount of mesopores favor higher adsorption of saxitoxins (Silva Buarque et al., 2015). The Langmuir isotherm is best known to describe the kinetics of adsorption of saxitoxin onto GAC (Capelo-Neto & Silva Buarque, 2016). During adsorption by powdered activated carbon (PAC), an increase in the carbon dose and contact time were correlated with higher removal efficiency of saxitoxins (L. Ho et al., 2009; Shi et al., 2012). In addition, a pH > 8 resulted in higher removal rate of saxitoxins (Rorar et al., 2022; Shi et al., 2012). Absorption was highest at a pH of 10.7 when the saxitoxin molecule was in its neutral form, suggesting that dispersive and H-bonding interactions played a dominant role during adsorption of saxitoxin and the effect of NOM on the adsorption reduced as pH increased (Shi et al., 2012). Higher initial concentrations of saxitoxin were shown to be related to higher removal percentage using PAC (Rorar et al., 2022). In a review on adsorption process for saxitoxin, the key parameters that governed adsorption were: (i) the type, chemical structure, pore size, and the surface area of the adsorbent, (ii) molecular weight of the variant of saxitoxin, (iii) pH of the water during the adsorption process, and (iv) the organic matter present in the sample (da Silva et al., 2022). The same study also ranked the efficiency of adsorbents that have been studied in the past for saxitoxin in the following order: wood-based PAC > bituminous PAC > lignite PAC > coconut shell GAC > chitin > oyster shell powder.

When the removal of saxitoxin and its variants was investigated on two types of nanofiltration membranes, NF-90 and NF-270, the NF-90 membrane showed higher removal in comparison to the NF-270. The higher hydrophobicity coupled with smaller average pore

diameter favored higher removal and prevented a decline in the permeate flux (Coral et al., 2011).

Table 1-4: Summary of treatment methods used for the removal of saxitoxins.

Treatment Method	Removal efficiency	Experimental conditions	Reference
Chlorination	>99.1 Order of degradation is as follows: STX > C2 > GTX3 ~ C1 ~ GTX2	• Experiments performed on Murray River water filtered through 1.2 μm glass microfiber filter and ultrapure water • pH 8 • Free chlorine concentration was 3 mg/L	(Zamyadi et al., 2010)
Ozonation	Continuous O_3 – 31% of GTX5, 22% of C1-2, 77% of dc-STX Batch O_3 – 86% of dc-STX	• Experiments performed on raw water from water treatment plant • Residual O_3 concentration of 0.5 mg/L in batch treatment	(Orr et al., 2004)
Potassium Permanganate	No removal	• Experiments performed on Myponga reservoir water • pH 7.7 • Potassium permanganate dosed at 0.5 mg/L resulting in a residual of ~ 0.16 mg/L after 1 hour	(L. Ho et al., 2009)
Activated carbon (GAC)	100% of dc-STX, STX, GTX2-3, and GTX5 94 – 100% of dcGTX2-3 74% of C1-2	• Experiments performed on raw water from water treatment plant. • GAC columns packed to achieve empty bed contact time of 15 mins.	(Orr et al., 2004)

Table 1-4 (cont'd)

Activated carbon (PAC)	> 99% STX	• Experiment performed on spiked DI water • WPH (bituminous coal-based PAC) dosed at $\mathbf{10\ mg/L}$. • pH 10.7 • Equilibration time was 24 hours	(Shi et al., 2012)
Nanofiltration	100% of neoSTX, dcSTX, and STX	• Experiments performed on surface water samples mixed with lysed *Cylindrospermopsis raciborskii* culture • pH of sample water was 6 • Pressure of 8 bar applied to the membrane • Total filtration time was 180 mins	(Coral et al., 2011)

METHODS FOR DETECTION OF SAXITOXINS

Evolution of Chromatographic Detection of Saxitoxins

Ingestion of toxic shellfish has been the primary route of exposure of saxitoxins to humans, resulting in the focus of most studies being on detecting saxitoxin in shellfish samples. The mouse bioassay (MBA) was the earliest biological method that was developed and standardized for the detection of saxitoxins (Sommer & Meyer, 1937). However, the Limit of Detection (LOD) of the method is 40 μg STX/100 g shellfish, equivalent to a concentration of 200 $\mu g/L$ saxitoxin in water, which is well beyond WHO's 3 $\mu g/L$ drinking water guideline (World Health Organization, 2019). In addition, the method's use of live animals combined with its lack of sensitivity, which is essential to detect low concentrations of saxitoxin, and inconsistent results, resulted in a search for alternative methods.

Saxitoxins inherently lack fluorescence, which previously limited its detection by analytical methods like gas chromatography and spectrometry. However, Bates and Rapoport (Bates & Rapoport, 1975) developed a technique that involved alkaline hydrogen peroxide oxidation of saxitoxin to yield fluorescent by-products, which formed a basis for further advancement in development of analytical methods for saxitoxin detection. The incorporation of this fluorometric method in a post-column reaction system that involved the separation of saxitoxins by high pressure liquid chromatography (HPLC) was first brought about by Sullivan (Sullivan & Wekell, 1984). However, this method was only limited to detecting GTX 1-6, STX, and neoSTX, and not capable of separating N-sulfocarbomyl-11-hydroxysulfate toxins (C1-C4). This was resolved in Oshima's study involving post column derivatization liquid chromatography (LC) that could detect as many as 15 variants of saxitoxin (Oshima, 1995; Oshima et al., 1989).

While Oshima's method used periodic acid for oxidizing the saxitoxins after chromatographic injection, Lawrence set up a method to oxidize the toxins with peroxide prior to injection (Lawrence et al., 1995). This precolumn oxidation of saxitoxins, also known as "Lawrence method" (Lawrence et al., 2005) was later adopted as the AOAC Official Method 2005.06.

Another discovery of using electrospray ionization-mass spectrometry (ESI-MS) to detect saxitoxins proved beneficial as it meant that the direct detection of the toxins was possible without oxidation. Also, since saxitoxin is basic, it provided strong $[M + H]^+$ ions which can be effectively detected by ESI-MS (Quilliam et al., 1989). The combination of liquid chromatography and mass spectrometry (LC/MS) is one of the most preferred analytical methods to quantify toxins with high sensitivity and selectivity. However, LC/MS has proved to be a challenge for detection of saxitoxins due to the following reasons: (i) variants of saxitoxins exist in a wide range of charge states which makes it difficult to perform simultaneous

chromatographic separations for all variants, (ii) the polar nature of saxitoxins prevents the retention of these toxins on reversed phase columns without the use of volatile ion-pairing agents such as heptafluorobutyric acid, and (iii) low sensitivity can occur due to the use of ion-pairing agents which can result in an increase in background noise and also decrease the electrospray ionization efficiency (Dell'Aversano et al., 2004; Quilliam, 1996; Quilliam et al., 2001). A recent study used dansyl chloride (DNS) for the chemical derivatization of STX followed by quantification using ultra high-performance LC coupled with heated electrospray ionization and Q-Exactive mass spectrometer, which provided a method detection limit of $0.01\ \mu g/L$ (Roy-Lachapelle et al., 2015). The method also used strong cation exchange SPE for the clean-up of sample matrix and concentration of analytes achieving recoveries between $86 - 90\%$ for STX.

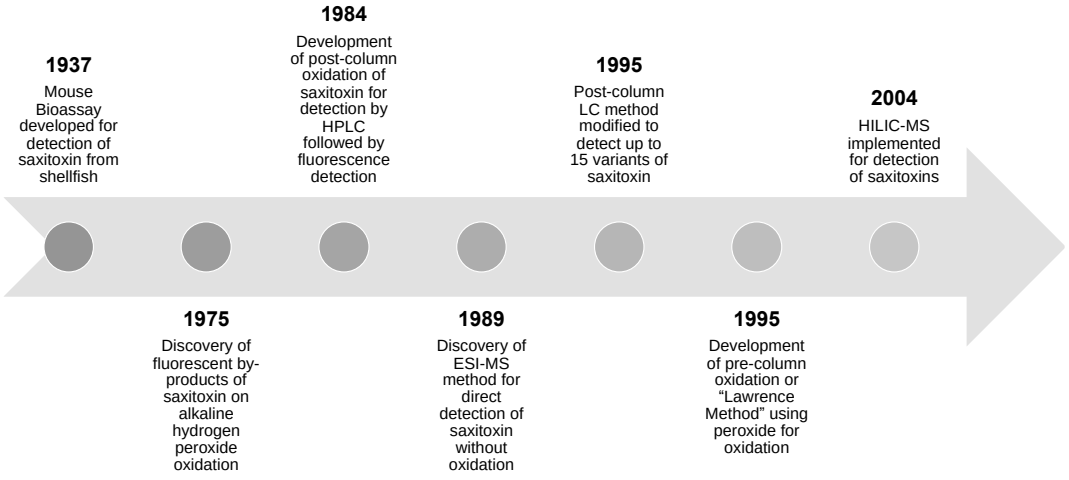

Figure 1-3: Timeline representing evolution of chromatographic detection methods for saxitoxin.

Hydrophilic Interaction Liquid Chromatography (HILIC)

To overcome the challenges posed by LC/MS, an alternate separation method was sought out that would allow for the simultaneous detection of all saxitoxin variants in a single analysis while also providing high sensitivity. Hence, hydrophilic interaction liquid chromatography coupled with electrospray ionization tandem mass spectrometry (HILIC-MS), which is well

suited for the separation of polar compounds like saxitoxins, was implemented for the analysis of saxitoxins (Dell'Aversano et al., 2004). In HILIC-MS (Buszewski & Noga, 2012), the stationary phase is a polar compound e.g., amide, which is capable of easily absorbing polar solvents like water. The polarity of the stationary phase increases with a layering of polar solvent, which attracts polar analytes like saxitoxin. The retention of saxitoxin is also dependent on the polarity of the mobile phase. Hence, the gradient is designed such that the mobile phase is composed of lower polarity solvents like acetonitrile in the start to facilitate retention, with a gradual increase in high polar solvents like water to enable elution of saxitoxin from the column (see Figure 1-4). The use of formate buffers is necessary to achieve a good peak shape and also decrease the retention time (Quilliam et al., 2001).

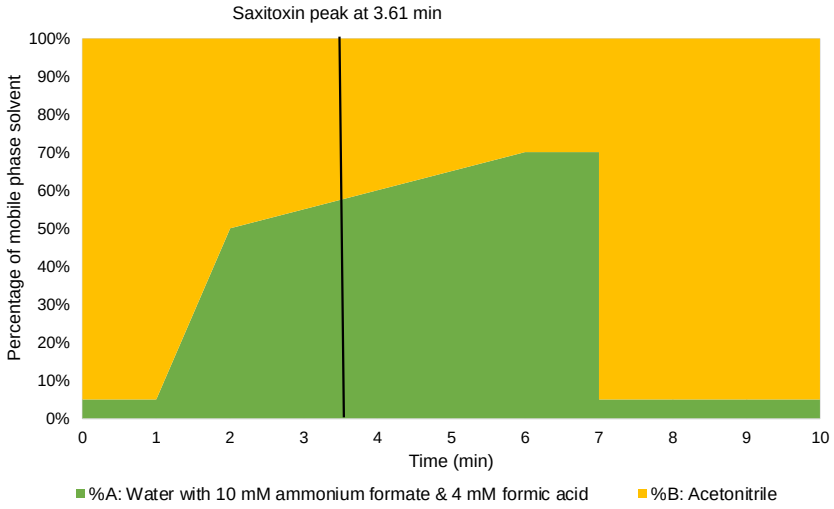

Figure 1-4: Liquid Chromatography gradient of saxitoxin (Column used: Acquity BEH Amide, $100 \times 2.1\ mm, 1.7\ \mu M$).

Dell'Aversano et al. (Dell'Aversano et al., 2004) were the first to test the suitability of the HILIC-MS detection method on field cyanobacterial cell samples containing *Anabaena circinalis* and *Cylindrospermopsis raciborskii*. This study obtained a LOD of $17.96\ \mu g/L$ for STX. They were also able to detect other variants like GTX2&3, dcSTX, dcGTX2&3, and C1-2 in the

cyanobacterial field samples. In another study, Johnson et al. (Johnson et al., 2009) extracted and quantified STX and neoSTX from human urine. The toxins were extracted from human urine matrix using weak cation exchange solid phase extraction to proceed with detection using HILIC-MS. After achieving a recovery of 90% in the extraction step, the LOD achieved by this study for STX was 4.8 $\mu g/L$. This study was further implemented in an online-solid phase extraction LC/MS/MS method wherein an even lower LOD of 1.01 $\mu g/L$ was achieved (Bragg et al., 2015). The authors also claim that using the online method reduced the time required for sample preparation (1 hr online versus 3 hr offline). While Dell'Aversano et al. (Dell'Aversano et al., 2004, 2005) were the first to develop the HILIC-MS method for quantification of saxitoxins, their method run time was long with STX being detected at 20.3 minutes. Hence, Halme et al. (Halme et al., 2012) developed a method for the fast and quantitative analysis of STX, achieving a retention time of 6.5 minutes and a LOD of 3 $\mu g/L$. The developed method was also verified by application on freeze dried *Alexandrium Ostenfeldii* samples.

A novel extraction method using a combination of silica and strong cation exchange SPE was developed to extract saxitoxins from food and water (Jansson & Åstot, 2015). The method was able to detect saxitoxin concentrations as low as 10 $\mu g/L$ in water, milk, and orange juice using HILIC-MS after extraction. To ensure accurate and sensitive measurement of saxitoxins from urine samples, polyamide was used as a HILIC SPE material for clean-up of samples prior to detection using HILIC-MS (Xu et al., 2018). The LOD achieved by this method for saxitoxin was 0.2 $\mu g/L$ with SPE recoveries ranging between $90\% - 120\%$. A zwitterionic HILIC column was used for the first time for separation of saxitoxins following its extraction from freshwater samples using carbon based SPE (Haddad et al., 2019). The study obtained a 53% recovery of STX through SPE and a method detection limit of 0.22 ng/L STX from water. Vo

Duy et al. optimized an on-line enrichment method using hydrophilic-lipophilic balance based adsorbents coupled with HILIC-MS to detect saxitoxin concentrations in parts-per-trillion levels from freshwater samples (Vo Duy et al., 2022). Upon evaluation of matrix effects, the absorptive losses by using glass fiber filters as well as glass autosampler vials were found to be maximum. The developed method was validated on surface water samples, achieving a LOD of $0.72\ ng/L$ for STX. In another study, seawater samples were used to analyze STX by performing SPE using silica cartridges for the filtrate, achieving a recovery of $\sim 19\%$, followed by detection using HILIC coupled with heated electrospray ionization and Q-Exactive mass spectrometer, resulting in a LOD of $0.5\ \mu g/L$ (Bosch-Orea et al., 2021).

Enzyme-linked Immunosorbent Assay (ELISA)

ELISA is a type of detection method in the form of a biochemical assay that uses antibodies that are raised based on the target analyte. The concentration of toxins is measured based on a colorimetric reaction. Since the assay is designed to detect the antibody on the plate, the signal is inversely proportional to the amount of toxins present in the sample. ELISA is a popular alternative to LC/MS due its sensitivity, rapidity, and ease of use. The evolution of assays developed for detection of saxitoxins have been summarized in previous reviews (Cusick & Sayler, 2013; Humpage et al., 2010; Usleber et al., 2001). Since this detection method has been researched extensively over the years, it has led to the commercialization of several ELISA kits (J. Li & Persson, 2021). The popular choice is 96-well ELISA plate by Abraxis which can detect saxitoxins from freshwater and seawater samples as well as shellfish samples, with sample preparation. The LOD of ELISA test kit is $0.015\ \mu g/L$ for STX present in water samples without prior sample preparation.

Table 1-5: Comparison between ELISA and HILIC-MS methods for detecting saxitoxins from water.

Comparison Factor	HILIC-MS	ELISA
Sample preparation	Samples need to be cleaned up using SPE and reconstituted into the mobile phase solvents of the HILIC-MS system.	No sample preparation necessary. Dilutions can be made is range falls beyond the linear detection range.
Typical Cost/sample	$9.33 Cost breakdown: • Cost/hour for using the Q-ToF located in Michigan State University = $\$56$ • Run time per saxitoxin sample = 10 mins • Total samples run in 1 hour = 6 • Cost/sample $= \frac{\$56}{6} = \$9.33$ • Additional cost for sample preparation not included in the above cost breakdown	$5.57 Cost breakdown: • Cost of 96-well plate = $\$535$ • Cost/sample $= \frac{\$535}{96} = \$5.57$
Time	Can run 6 samples per hour The addition of blank samples between high concentration samples to prevent carryover increases the total time	Approximately 2 hours per plate (10 – 96 samples)
LOD	Varies depending on the method and enrichment by solid-phase extraction ($0.72\ ng/L$ - $0.5\ \mu g/L$)	$0.015\ \mu g/L$

Table 1-5 (cont'd)

Limitations	• High cost of analysis • Sample matrix needs to be changed to match the mobile phase solvents of the LC system • Requires a trained and skilled personnel in LC/MS/MS to perform analysis • Total time of analysis depends on the method and can exceed several hours	• High cross-reactivity of dcSTX and GTX2&3 (23% - 29%) • LOD can be affected if the above toxins are present in the water sample • Not capable of quantifying the individual variants of saxitoxins • Requires access to a plate reader to measure the absorbance of the samples
Advantages	• Depending on the availability of standards, can quantify the variants of saxitoxin • High accuracy in measurement • Matrix effects can be reduced by sample preparation techniques	• A quick method to check the presence of saxitoxins in samples • Does not need any prior skills or knowledge of the method to perform the measurement • Kits are readily available for purchase

Although the HILIC-MS and ELISA methods are sensitive and reliable methods for detection of saxitoxin, they cannot be applied in the field for the rapid measurement of saxitoxins. Hence, research has gained a new direction in detection of saxitoxin, which involves the use of biosensors. Biosensors are equipped with bioreceptors and signal processing unit, that allow for the measurement of signal changes that are caused by the interaction between the bioreceptor and the target material (Conroy et al., 2009). Bioreceptors in the form in antibodies, aptamers, and nanomaterials are designed, creating two broad categories of biosensors: electrochemical and optical biosensors, which have been applied for detection of saxitoxins from freshwater and sea water (Park et al., 2022).

CONCLUSION

Saxitoxins, possessing neurotoxicity, are the most potent of all cyanotoxins with over 50 different variants. The most common and well-known route of exposure to humans has been through ingestion of toxic shellfish, giving saxitoxin the popular terminology of paralytic shellfish toxins (PSTs). Saxitoxins were predominantly produced in marine environments by dinoflagellates but are now increasingly being detected in freshwaters, produced by cyanobacteria. Cyanobacterial growth is largely related to nutrient pollution of freshwater bodies and is also a result of climate change. Through the knowledge presented in this review, it is evident that climate change is not only responsible for increasing the occurrence of saxitoxin producing cyanobacteria in freshwaters but is also a promoter of saxitoxin production. Given the inevitable effects of climate change, a foreseeable increase in saxitoxins in expected in the future, which is reason enough for the U.S. EPA to establish a drinking water health advisory for saxitoxins which will thereby necessitate its monitoring, hence protecting our drinking water. The treatment technologies reviewed in this paper have only been studied at the laboratory scale and there is enough evidence to suggest that most treatment methods employed by water treatment plants are incapable of removing the toxicity of the saxitoxin molecule. With a rise in HABs in temperate regions, there are increased chances of cyanotoxins entering the source water of many drinking water treatment plants, posing a challenge for their simultaneous removal. Microcystins, the chemistry of which is different from saxitoxins, have been the focus of oxidative treatment for majority of water treatment plants, which cannot be applied for treatment of saxitoxins. Hence, it is crucial to develop a treatment technology which can reliably remove all cyanotoxins.

The treatment of saxitoxins comes with another challenge posed by the polar saxitoxins, i.e., its monitoring in water. Unlike microcystins, saxitoxins lack inherent fluorescence and are unable to be retained on reversed phase columns, which makes it challenging to detect saxitoxins by chromatography or spectrometry without chemical derivatization/oxidation. The additional step of chemical derivatization/oxidation reduces signal efficiency and selectivity of the variants of saxitoxin. The development of HILIC-MS for detection of saxitoxins has exceeded all other detection methods in terms of sensitivity, selectivity, and time efficiency. However, the cost of instrumentation is very high and requires highly skilled personnel for operation of these instruments, which creates a major limitation for water treatment operators. ELISA is a preferred alternative for detection of saxitoxins due to its ease-of-use and sensitivity but is incapable of quantifying the variants of saxitoxin. The structure of saxitoxin makes the development of sample pretreatment techniques, like SPE, just as difficult as analytical methods used for detection of saxitoxins. However, since saxitoxins are present at low concentrations in surface waters, it is essential to develop concentration methods with a good recovery that can lead to their successful quantification. Hence, it is evident that there is still much progress to be made in the monitoring and detection of saxitoxins from water which can serve the purpose of regulation in water treatment plants, to protect public health.

REFERENCES

Alexander, J., Benford, D., Cockburn, A., Cravedi, J., Dogliotti, E., Domenico, A. Di, Fernández-Cruz, M. L., Fink-gremmels, J., Fürst, P., Galli, C., Grandjean, P., Gzyl, J., Heinemeyer, G., Johansson, N., Mutti, A., Schlatter, J., Leeuwen, R. Van, Peteghem, C. Van, & Verger, P. (2009). Marine Biotoxins in Shellfish – Saxitoxin group. The EFSA Journal, 1019, 1–76.

Alfonso, A., Louzao, M. C., Vieytes, M. R., & Botana, L. M. (1994). Comparative study of the stability of saxitoxin and neosaxitoxin in acidic solutions and lyophilized samples. Toxicon, 32(12), 1593–1598. https://doi.org/10.1016/0041-0101(94)90318-2

Aráoz, R., Molgó, J., & Tandeau de Marsac, N. (2010). Neurotoxic cyanobacterial toxins. Toxicon, 56(5), 813–828. https://doi.org/10.1016/j.toxicon.2009.07.036

AWWA. (2016). Cyanotoxins in US Drinking Water: Occurrence, Case Studies and State Approaches to Regulation Cyanotoxins in US Drinking Water. September.

Baker, P. D., & Humpage, A. R. (1994). Toxicity associated with commonly occurring cyanobacteria in surface waters of the murray-darling basin, australia. Marine and Freshwater Research, 45(5), 773–786. https://doi.org/10.1071/MF9940773

Ballot, A., Bernard, C., & Fastner, J. (2017). Saxitoxin and Analogues. In Handbook of Cyanobacterial Monitoring and Cyanotoxin Analysis (pp. 148–154). John Wiley and Sons, Ltd. https://doi.org/10.4081/aiol.2017.7221

Bates, H. A., & Rapoport, H. (1975). A Chemical Assay for Saxitoxin, the Paralytic Shellfish Poison. Journal of Agricultural and Food Chemistry, 23(2), 237–239. https://doi.org/10.1021/jf60198a016

Belykh, O. I., Gladkikh, A. S., Sorokovikova, E. G., Tikhonova, I. v., Potapov, S. A., & Butina, T. v. (2015). Saxitoxin-Producing cyanobacteria in Lake Baikal. Contemporary Problems of Ecology, 8(2), 186–192. https://doi.org/10.1134/S199542551502002X

Bosch-Orea, C., Sanchís, J., & Farré, M. (2021). Analysis of highly polar marine biotoxins in seawater by hydrophilic interaction liquid chromatography coupled to high resolution mass spectrometry. MethodsX, 8(101370). https://doi.org/10.1016/j.mex.2021.101370

Bragg, W. A., Lemire, S. W., Coleman, R. M., Hamelin, E. I., & Johnson, R. C. (2015). Detection of human exposure to saxitoxin and neosaxitoxin in urine by online-solid phase extraction-liquid chromatography-tandem mass spectrometry. Toxicon, 99, 118–124. https://doi.org/10.1016/j.toxicon.2015.03.017

Brentano, D. M., Giehl, E. L. H., & Petrucio, M. M. (2016). Abiotic variables affect STX concentration in a meso-oligotrophic subtropical coastal lake dominated by Cylindrospermopsis raciborskii (Cyanophyceae). Harmful Algae, 56, 22–28. https://doi.org/10.1016/j.hal.2016.03.017

Bullerjahn, G. S., McKay, R. M., Davis, T. W., Baker, D. B., Boyer, G. L., D'Anglada, L. V., Doucette, G. J., Ho, J. C., Irwin, E. G., Kling, C. L., Kudela, R. M., Kurmayer, R., Michalak, A. M., Ortiz, J. D., Otten, T. G., Paerl, H. W., Qin, B., Sohngen, B. L., Stumpf, R. P., … Wilhelm, S. W. (2016). Global solutions to regional problems: Collecting global expertise to address the problem of harmful cyanobacterial blooms. A Lake Erie case study. Harmful Algae, 54, 223–238. https://doi.org/10.1016/j.hal.2016.01.003

Buratti, F. M., Manganelli, M., Vichi, S., Stefanelli, M., Scardala, S., Testai, E., & Funari, E. (2017). Cyanotoxins: producing organisms, occurrence, toxicity, mechanism of action and human health toxicological risk evaluation. Archives of Toxicology, 91(3), 1049–1130. https://doi.org/10.1007/s00204-016-1913-6

Burford, M. A., Beardall, J., Willis, A., Orr, P. T., Magalhaes, V. F., Rangel, L. M., Azevedo, S. M. F. O. E., & Neilan, B. A. (2016). Understanding the winning strategies used by the bloom-forming cyanobacterium Cylindrospermopsis raciborskii. Harmful Algae, 54, 44–53. https://doi.org/10.1016/j.hal.2015.10.012

Buszewski, B., & Noga, S. (2012). Hydrophilic interaction liquid chromatography (HILIC)-a powerful separation technique. Analytical and Bioanalytical Chemistry, 402(1), 231–247. https://doi.org/10.1007/s00216-011-5308-5

Capelo-Neto, J., & Silva Buarque, N. M. (2016). Simulation of saxitoxins adsorption in full-scale GAC filter using HSDM. Water Research, 88, 558–565. https://doi.org/10.1016/j.watres.2015.10.048

Carmichael, W. W., & Boyer, G. L. (2016). Health impacts from cyanobacteria harmful algae blooms: Implications for the North American Great Lakes. Harmful Algae, 54, 194–212. https://doi.org/10.1016/j.hal.2016.02.002

Carmichael, W. W., Evans, W. R., Yin, Q. Q., Bell, P., & Moczydlowski, E. (1997). Evidence for paralytic shellfish poisons in the freshwater cyanobacterium Lyngbya wollei (Farlow ex Gomont) comb. nov. Applied and Environmental Microbiology, 63(8), 3104–3110.

Carmichael, W. W., Mahmood, N. A., & Hyde, E. G. (1990). Natural Toxins from Cyanobacteria (Blue-Green Algae). In Marine Toxins: Origin, Structure, and Molecular Pharmacology (pp. 87–106). https://doi.org/10.1021/bk-1990-0418.ch006

Carneiro, R. L., Dos Santos, M. E. V., Pacheco, A. B. F., & De Oliveira E Azevedo, S. M. F. (2009). Effects of light intensity and light quality on growth and circadian rhythm of saxitoxins production in Cylindrospermopsis raciborskii (Cyanobacteria). Journal of Plankton Research, 31(5), 481–488. https://doi.org/10.1093/plankt/fbp006

Carneiro, R. L., Pacheco, A. B. F., & De Oliveira E Azevedo, S. M. F. (2013). Growth and saxitoxin production by cylindrospermopsis raciborskii (cyanobacteria) correlate with water hardness. Marine Drugs, 11(8), 2949–2963. https://doi.org/10.3390/md11082949

Castro, D., Vera, D., Lagos, N., García, C., & Vásquez, M. (2004). The effect of temperature on growth and production of paralytic shellfish poisoning toxins by the cyanobacterium

Cylindrospermopsis raciborskii C10. Toxicon, 44(5), 483–489. https://doi.org/10.1016/j.toxicon.2004.06.005

Christensen, V. G., & Khan, E. (2020). Freshwater neurotoxins and concerns for human, animal, and ecosystem health: A review of anatoxin-a and saxitoxin. Science of the Total Environment, 736, 139515. https://doi.org/10.1016/j.scitotenv.2020.139515

Conroy, P. J., Hearty, S., Leonard, P., & O'Kennedy, R. J. (2009). Antibody production, design and use for biosensor-based applications. Seminars in Cell and Developmental Biology, 20(1), 10–26. https://doi.org/10.1016/j.semcdb.2009.01.010

Coral, L. A., Proença, L. A. de O., de Jesus Bassetti, F., & Lapolli, F. R. (2011). Nanofiltration membranes applied to the removal of saxitoxin and congeners. Desalination and Water Treatment, 27(1–3), 8–17. https://doi.org/10.5004/dwt.2011.2034

Costa, I. A. S., Azevedo, S. M. F. O., Senna, P. A. C., Bernardo, R. R., Costa, S. M., & Chellappa, N. T. (2006). Occurrence of toxin-producing cyanobacteria blooms in a Brazilian semiarid reservoir. Brazilian Journal of Biology, 66(1 B), 211–219. https://doi.org/10.1590/S1519-69842006000200005

Cusick, K. D., & Sayler, G. S. (2013). An overview on the marine neurotoxin, saxitoxin: Genetics, molecular Targets, methods of detection and ecological functions. Marine Drugs, 11(4), 991–1018. https://doi.org/10.3390/md11040991

da Silva, M. B., Vianna, M. T. G., & Marques, M. (2022). Adsorption Processes Applied for the Removal of Saxitoxins in Water: a Literature Review (2010–2022). Water, Air, and Soil Pollution, 233(12). https://doi.org/10.1007/s11270-022-06010-z

Dell'Aversano, C., Eaglesham, G. K., & Quilliam, M. A. (2004). Analysis of cyanobacterial toxins by hydrophilic interaction liquid chromatography-mass spectrometry. Journal of Chromatography A, 1028(1), 155–164. https://doi.org/10.1016/j.chroma.2003.11.083

Dell'Aversano, C., Hess, P., & Quilliam, M. A. (2005). Hydrophilic interaction liquid chromatography-mass spectrometry for the analysis of paralytic shellfish poisoning (PSP) toxins. Journal of Chromatography A, 1081(2), 190–201. https://doi.org/10.1016/j.chroma.2005.05.056

Dittmann, E., & Wiegand, C. (2006). Cyanobacterial toxins - Occurrence, biosynthesis and impact on human affairs. Molecular Nutrition and Food Research, 50(1), 7–17. https://doi.org/10.1002/mnfr.200500162

Donovan, C. J., Ku, J. C., Quilliam, M. A., & Gill, T. A. (2008). Bacterial degradation of paralytic shellfish toxins. Toxicon, 52(1), 91–100. https://doi.org/10.1016/j.toxicon.2008.05.005

Farrer, D., Counter, M., Hillwig, R., & Cude, C. (2015). Health-based cyanotoxin guideline values allow for cyanotoxin-based monitoring and efficient public health response to cyanobacterial blooms. Toxins, 7(2), 457–477. https://doi.org/10.3390/toxins7020457

Ferreira, F. M. B., Soler, J. M. F., Fidalgo, M. L., & Fernández-Vila, P. (2001). PSP toxins from Aphanizomenon flos-aquae (cyanobacteria) collected in the Crestuma-Lever reservoir (Douro river, northern Portugal). Toxicon, 39(6), 757–761. https://doi.org/10.1016/S0041-0101(00)00114-8

Fonseca, J. R., Vieira, P. C. S., Kujbida, P., & Costa, I. A. S. da. (2015). Cyanobacterial occurrence and detection of microcystins and saxitoxins in reservoirs of the Brazilian semi-arid. Acta Limnologica Brasiliensia, 27(1), 78–92. https://doi.org/10.1590/s2179-975x2814

Genenah, A. A., & Shimizu, Y. (1981). Specific Toxicity of Paralytic Shellfish Poisons. Journal of Agricultural and Food Chemistry, 29(6), 1289–1291. https://doi.org/10.1021/jf00108a047

Gkelis, S., Papadimitriou, T., Zaoutsos, N., & Leonardos, I. (2014). Anthropogenic and climate-induced change favors toxic cyanobacteria blooms: Evidence from monitoring a highly eutrophic, urban Mediterranean lake. Harmful Algae, 39, 322–333. https://doi.org/10.1016/j.hal.2014.09.002

Glibert, P., & Burford, M. (2017). Globally Changing Nutrient Loads and Harmful Algal Blooms: Recent Advances, New Paradigms, and Continuing Challenges. Oceanography, 30(1), 58–69. https://doi.org/10.5670/oceanog.2017.110

Grachev, M., Zubkov, I., Tikhonova, I., Ivacheva, M., Kuzmin, A., Sukhanova, E., Sorokovikova, E., Fedorova, G., Galkin, A., Suslova, M., Netsvetayeva, O., Eletskaya, E., Pogadaeva, T., Smirnov, V., Ivanov, A., Shagun, V., Minaev, V., & Belykh, O. (2018). Extensive Contamination of Water with Saxitoxin Near the Dam of the Irkutsk Hydropower Station Reservoir (East Siberia, Russia). Toxins, 10(10), 402. https://doi.org/10.3390/toxins10100402

Graham, J. L., Loftin, K. A., Meyer, M. T., & Ziegler, A. C. (2010). Cyanotoxin mixtures and taste-and-odor compounds in cyanobacterial blooms from the midwestern united states. Environmental Science and Technology, 44(19), 7361–7368. https://doi.org/10.1021/es1008938

Granéli, E., & Flynn, K. (2006). Chemical and Physical Factors Influencing Toxin Content. Ecology of Harmful Algae, 189, 229–241. https://doi.org/10.1007/978-3-540-32210-8_18

Haddad, S. P., Bobbitt, J. M., Taylor, R. B., Lovin, L. M., Conkle, J. L., Chambliss, C. K., & Brooks, B. W. (2019). Determination of microcystins, nodularin, anatoxin-a, cylindrospermopsin, and saxitoxin in water and fish tissue using isotope dilution liquid chromatography tandem mass spectrometry. Journal of Chromatography A, 1–9. https://doi.org/10.1016/j.chroma.2019.03.066

Hall, S., Strichartz, G., Moczydlowski, E., Ravindran, A., & Reichardt, P. B. (1990a). Chapter 3 The Saxitoxins Structures and Key Properties.

Hall, S., Strichartz, G., Moczydlowski, E., Ravindran, A., & Reichardt, P. B. (1990b). The Saxitoxins: Sources, Chemistry and Pharmacology. In Marine Toxins: Origin, Structure, and Molecular Pharmacology (pp. 29–65).

Halme, M., Rapinoja, M. L., Karjalainen, M., & Vanninen, P. (2012). Verification and quantification of saxitoxin from algal samples using fast and validated hydrophilic interaction liquid chromatography-tandem mass spectrometry method. Journal of Chromatography B: Analytical Technologies in the Biomedical and Life Sciences, 880(1), 50–57. https://doi.org/10.1016/j.jchromb.2011.11.015

Health Canada. (2022). Guidelines for Canadian Drinking Water Quality - Summary Tables, Water and Air Quality Bureau. https://www.canada.ca/en/health-canada/services/environmental-workplace-health/reports-publications/water-quality.html

Ho, J. C., & Michalak, A. M. (2020). Exploring temperature and precipitation impacts on harmful algal blooms across continental U.S. lakes. Limnology and Oceanography, 65(5), 992–1009. https://doi.org/10.1002/lno.11365

Ho, L., Tanis-Plant, P., Kayal, N., Slyman, N., & Newcombe, G. (2009). Optimising water treatment practices for the removal of Anabaena circinalis and its associated metabolites, geosmin and saxitoxins. Journal of Water and Health, 7(4), 544–556. https://doi.org/10.2166/wh.2009.075

Humpage, A. R., Magalhaes, V. F., & Froscio, S. M. (2010). Comparison of analytical tools and biological assays for detection of paralytic shellfish poisoning toxins. Analytical and Bioanalytical Chemistry, 397(5), 1655–1671. https://doi.org/10.1007/s00216-010-3459-4

Humpage, A. R., Rositano, J., Bretag, A. H., Brown, R., Baker, P. D., Nicholson, B. C., & Steffensen, D. A. (1994). Paralytic shellfish poisons from australian cyanobacterial blooms. Marine and Freshwater Research, 45(5), 761–771. https://doi.org/10.1071/MF9940761

J.A. Shoemaker, Tettnhorst, D. R., & Cruz, A. de la. (2015). Method 544: Determination of Microcystins and Nodularin in Drinking Water by Solid Phase Extraction and Liquid Chromatography/Tandem Mass Spectrometry (LC/MS/MS). United States Environmental Protection Agency.

Jackim, E., & Gentile, J. (2021). Toxins of a Blue-Green Algae : Similarity to Saxitoxin. Science, 162(3856), 915–916.

Jančula, D., Straková, L., Sadílek, J., Maršálek, B., & Babica, P. (2014). Survey of cyanobacterial toxins in Czech water reservoirs-the first observation of neurotoxic saxitoxins. Environmental Science and Pollution Research, 21(13), 8006–8015. https://doi.org/10.1007/s11356-014-2699-9

Jansson, D., & Åstot, C. (2015). Analysis of paralytic shellfish toxins, potential chemical threat agents, in food using hydrophilic interaction liquid chromatography-mass spectrometry. Journal of Chromatography A, 1417, 41–48. https://doi.org/10.1016/j.chroma.2015.09.029

Jöhnk, K. D., Huisman, J., Sharples, J., Sommeijer, B., Visser, P. M., & Stroom, J. M. (2008). Summer heatwaves promote blooms of harmful cyanobacteria. Global Change Biology, 14(3), 495–512. https://doi.org/10.1111/j.1365-2486.2007.01510.x

Johnson, R. C., Zhou, Y., Statler, K., Thomas, J., Cox, F., Hall, S., & Barr, J. R. (2009). Quantification of saxitoxin and neosaxitoxin in human urine utilizing isotope dilution tandem mass spectrometry. Journal of Analytical Toxicology, 33(1), 8–14. https://doi.org/10.1093/jat/33.1.8

Jones, G. J., & Negri, A. P. (1997). Persistence and Degradation of Cyanobacterial Paralytic Shellfish Poisons (PSPs) in Freshwaters. Water Research, 31(3), 525–533.

Kaas, H., & Henriksen, P. (2000). Saxitoxins (PSP toxins) in Danish lakes. Water Research, 34(7), 2089–2097. https://doi.org/10.1016/S0043-1354(99)00372-3

Karosienė, J., Savadova-Ratkus, K., Toruńska-Sitarz, A., Koreivienė, J., Kasperovičienė, J., Vitonytė, I., Błaszczyk, A., & Mazur-Marzec, H. (2020). First report of saxitoxins and anatoxin-a production by cyanobacteria from Lithuanian lakes. European Journal of Phycology, 55(3), 327–338. https://doi.org/10.1080/09670262.2020.1734667

Kim, H., Park, H., Wang, H., Yoo, H. Y., Park, J., & Ki, J. S. (2021). Low temperature and cold stress significantly increase saxitoxins (Stxs) and expression of stx biosynthesis genes sxta4 and sxtg in the dinoflagellate alexandrium catenella. Marine Drugs, 19(6). https://doi.org/10.3390/md19060291

Kleinteich, J., Wood, S. A., Puddick, J., Schleheck, D., Küpper, F. C., & Dietrich, D. (2013). Potent toxins in Arctic environments - Presence of saxitoxins and an unusual microcystin variant in Arctic freshwater ecosystems. Chemico-Biological Interactions, 206(2), 423–431. https://doi.org/10.1016/j.cbi.2013.04.011

Kouzminov, A., Ruck, J., & Wood, S. A. (2007). New Zealand risk management approach for toxic cyanobacteria in drinking water. Australian and New Zealand Journal of Public Health, 31(3), 275–281. https://doi.org/10.1111/j.1467-842X.2007.00061.x

Krishnamurthy, T., Carmichael, W. W., & Sarver, E. W. (1986). Toxic peptides from freshwater cyanobacteria (blue-green algae). I. Isolation, purification and characterization of peptides from Microcystis aeruginosa and Anabaena flos-aquae. Toxicon, 24(9), 865–873. https://doi.org/10.1016/0041-0101(86)90087-5

Kurtz, T. D. (2021). The Photodegradation of Saxitoxins in Surface Waters. University of Colorado Boulder.

Lagos, N., Onodera, H., Zagatto, P. A., Andrinolo, D., Azevedo, S. M. F. Q., & Oshima, Y. (1999). The first evidence of paralytic shellfish toxins in the freshwater cyanobacterium Cylindrospermopsis raciborskii, isolated from Brazil. Toxicon, 37(10), 1359–1373. https://doi.org/10.1016/S0041-0101(99)00080-X

Lawrence, J. F., Menard, C., & Cleroux, C. (1995). Evaluation of prechromatographic oxidation for liquid chromatographic determination of paralytic shellfish poisons in shellfish. Journal of AOAC International, 78(2), 514–520. https://doi.org/10.1016/j.paid.2011.03.037

Lawrence, J. F., Niedzwiadek, B., & Menard, C. (2005). Quantitative Determination of Paralytic Shellfish Poisoning Toxins in SHellfish using Prechromatographic Oxidation and Liquid Chromatography with Fluorescence Detection: Collaborative Study. Journal of AOAC International, 88(6), 1714–1732.

Ledreux, A., Thomazeau, S., Catherine, A., Duval, C., Yéprémian, C., Marie, A., & Bernard, C. (2010). Evidence for saxitoxins production by the cyanobacterium Aphanizomenon gracile in a French recreational water body. Harmful Algae, 10(1), 88–97. https://doi.org/10.1016/j.hal.2010.07.004

Li, H., Gu, X., Chen, H., Mao, Z., Shen, R., Zeng, Q., & Ge, Y. (2022). Co-occurrence of multiple cyanotoxins and taste-and-odor compounds in the large eutrophic Lake Taihu, China: Dynamics, driving factors, and challenges for risk assessment. Environmental Pollution, 294(73), 118594. https://doi.org/10.1016/j.envpol.2021.118594

Li, J., & Persson, K. M. (2021). Quick detection method for paralytic shellfish toxins (PSTs) monitoring in freshwater - A review. Chemosphere, 265(November), 128591. https://doi.org/10.1016/j.chemosphere.2020.128591

Llewellyn, L. E. (2006). Saxitoxin, a toxic marine natural product that targets a multitude of receptors. Natural Product Reports, 23(2), 200–222. https://doi.org/10.1039/b501296c

Loftin, K. A., Graham, J. L., & Meyer, M. T. (2016). Cyanotoxins in inland lakes of the United States : Occurrence and potential recreational health risks in the EPA National Lakes Assessment 2007. Harmful Algae, 56, 77–90.

Mesquita, M. C. B., Lürling, M., Dorr, F., Pinto, E., & Marinho, M. M. (2019). Combined effect of light and temperature on the production of saxitoxins in Cylindrospermopsis raciborskii strains. Toxins, 11(1). https://doi.org/10.3390/toxins11010038

Michalak, A. M., Anderson, E. J., Beletsky, D., Boland, S., Bosch, N. S., Bridgeman, T. B., Chaffin, J. D., Cho, K., Confesor, R., Daloglu, I., DePinto, J. V., Evans, M. A., Fahnenstiel, G. L., He, L., Ho, J. C., Jenkins, L., Johengen, T. H., Kuo, K. C., LaPorte, E., … Zagorski, M. A. (2013). Record-setting algal bloom in Lake Erie caused by agricultural and meteorological trends consistent with expected future conditions. Proceedings of the National Academy of Sciences, 110(16), 6448–6452. https://doi.org/10.1073/pnas.1216006110

Minnesota Department of Health. (2015). Toxicological Summary for Microcystin-LR.

Molica, R., Onodera, H., García, C., Rivas, M., Andrinolo, D., Nascimento, S., Meguro, H., Oshima, Y., Azevedo, S., & Lagos, N. (2002). Toxins in the freshwater cyanobacterium Cylindrospermopsis raciborskii (Cyanophyceae) isolated from Tabocas reservoir in Caruaru, Brazil, including demonstration of a new saxitoxin analogue. Phycologia, 41(6), 606–611. https://doi.org/10.2216/i0031-8884-41-6-606.1

Moraes, M. A. B., Rodrigues, R. A. M., Schlüter, L., Podduturi, R., Jørgensen, N. O. G., & Calijuri, M. C. (2021). Influence of environmental factors on occurrence of cyanobacteria and

abundance of saxitoxin-producing cyanobacteria in a subtropical drinking water reservoir in brazil. Water (Switzerland), 13(12). https://doi.org/10.3390/w13121716

Moustaka-Gouni, M., Hiskia, A., Genitsaris, S., Katsiapi, M., Manolidi, K., Zervou, S. K., Christophoridis, C., Triantis, T. M., Kaloudis, T., & Orfanidis, S. (2017). First report of Aphanizomenon favaloroi occurrence in Europe associated with saxitoxins and a massive fish kill in Lake Vistonis, Greece. Marine and Freshwater Research, 68(4), 793–800. https://doi.org/10.1071/MF16029

Munoz, M., Nieto-Sandoval, J., Cirés, S., de Pedro, Z. M., Quesada, A., & Casas, J. A. (2019). Degradation of widespread cyanotoxins with high impact in drinking water (microcystins, cylindrospermopsin, anatoxin-a and saxitoxin) by CWPO. Water Research, 163. https://doi.org/10.1016/j.watres.2019.114853

Nagashima, Y., Noguchi, T., Tanaka, M., & Hashimoto, K. (1991). Thermal Degradation of Paralytic Shellfish. Journal of Food Science, 56(6), 1572–1575.

National Health and Medical Research Council (Australia), N., & Natural Resource Management Ministerial Council (Australia), N. (2022). Australian Drinking Water Guidelines Version 3.8. National Health and Medical Research Council.

Negri, A. P., Jones, G. J., Blackburn, S. I., Oshima, Y., & Onodera, H. (1997). Effect of Culture and Bloom Development and of Sample Storage on Paralytic Shellfish Poisons in the Cyanobacterium Anabaena Circinalis. Journal of Phycology, 33(1), 26–35. https://doi.org/10.1111/j.0022-3646.1997.00026.x

Negri, A. P., Jones, G. J., & Hindmarsh, M. (1995). Sheep mortality associated with paralytic shellfish poisons from the cyanobacterium Anabaena circinalis. Toxicon, 33(10), 1321–1329. https://doi.org/10.1016/0041-0101(95)00068-W

Newcombe, G., & Nicholson, B. (2002). Treatment options for the saxitoxins class of cyanotoxins. Water Science and Technology: Water Supply, 2(5–6), 271–275.

Nicholson, B. C., Morrall, J., Woods, T. A., Papageorgiou, J., Kapralos, C., Shaw, G. R., Senogles, P. J., Wickramasinghe, W., Moore, M. R., Davis, B. C., & Eaglesham, G. K. (2003). Chlorination for degrading saxitoxins (paralytic shellfish poisons) in water. Environmental Technology (United Kingdom), 24(11), 1341–1348. https://doi.org/10.1080/09593330309385678

Ohio EPA. (2020). Public Water System Harmful Algal Bloom Response Strategy.

Ohio EPA. (2021). Harmful Algal Blooms (HAB): Information for Public Water Systems. https://epa.ohio.gov/ddagw/HAB

Onodera, H., Satake, M., Oshima, Y., Yasumoto, T., & Carmichael, W. W. (1997). New saxitoxin analogues from the freshwater filamentous cyanobacterium Lyngbya wollei. Natural Toxins, 5(February), 146–151. https://doi.org/10.1002/1522-7189(1997)5:4<146::AID-NT4>3.0.CO;2-V

Orr, P. T., Jones, G. J., & Hamilton, G. R. (2004). Removal of saxitoxins from drinking water by granular activated carbon, ozone and hydrogen peroxide - Implications for compliance with the Australian drinking water guidelines. Water Research, 38(20), 4455–4461. https://doi.org/10.1016/j.watres.2004.08.024

Oshima, Y. (1995). Postcolumn Derivatization Liquid Chromatographic Method for Paralytic Shellfish Toxins. Journal of AOAC International, 78(2), 528–532.

Oshima, Y., Sugino, K., & Yasumoto, T. (1989). Latest Advances in HPLC Analysis of Paralytic Shellfish Toxins. Mycotoxins and Phycotoxins ’88, 319–326.

Papadimitriou, T., Katsiapi, M., Vlachopoulos, K., Christopoulos, A., Laspidou, C., Moustaka-Gouni, M., & Kormas, K. (2018). Cyanotoxins as the “common suspects” for the Dalmatian pelican (Pelecanus crispus) deaths in a Mediterranean reconstructed reservoir. Environmental Pollution, 234, 779–787. https://doi.org/10.1016/j.envpol.2017.12.022

Park, J. A., Seo, Y., Sohn, H., Park, C., Min, J., & Lee, T. (2022). Recent Trends in Biosensors Based on Electrochemical and Optical Techniques for Cyanobacterial Neurotoxin Detection. Biochip Journal, 16(2), 146–157. https://doi.org/10.1007/s13206-022-00054-3

Pearson, L., Mihali, T., Moffitt, M., Kellmann, R., & Neilan, B. (2010). On the chemistry, toxicology and genetics of the cyanobacterial toxins, microcystin, nodularin, saxitoxin and cylindrospermopsin. In Marine Drugs (Vol. 8, Issue 5). https://doi.org/10.3390/md8051650

Pereira, P., Onodera, H., Andrinolo, D., Franca, S., Araújo, F., Lagos, N., & Oshima, Y. (2000). Paralytic shellfish toxins in the freshwater cyanobacterium Aphanizomenon flos-aquae, isolated from Montargil reservoir, Portugal. Toxicon, 38(12), 1689–1702. https://doi.org/10.1016/S0041-0101(00)00100-8

Podduturi, R., Schlüter, L., Liu, T., Osti, J. A. S., Moraes, M. de A. B., & Jørgensen, N. O. G. (2021). Monitoring of saxitoxin production in lakes in Denmark by molecular, chromatographic and microscopic approaches. Harmful Algae, 101(January). https://doi.org/10.1016/j.hal.2020.101966

Pomati, F., Rossetti, C., Manarolla, G., Burns, B. P., & Neilan, B. A. (2004). Interactions between intracellular Na+ levels and saxitoxin production in Cylindrospermopsis raciborskii T3. Microbiology, 150(2), 455–461. https://doi.org/10.1099/mic.0.26350-0

Pomati, F., Sacchi, S., Rossetti, C., Giovannardi, S., Onodera, H., Oshima, Y., & Neilan, B. A. (2000). The Freshwater Cyanobacterium Planktothrix Sp. FP1: Molecular Identification and Detection of Paralytic Shellfish P oisoning Toxins. Journal of Phycology, 36(3), 553–562.

Quilliam, M. A. (1996). Liquid Chromatography-Mass Spectrometry of Seafood Toxins. Journal of Chromatography Library, 59, 415–444. https://doi.org/10.1037//0003-066X.46.5.506

Quilliam, M. A., Hess, P., & Dell’Aversano, C. (2001). Recent Developments in the Analysis of Phycotoxins by Liquid Chromatography-Mass Spectrometry. Mycotoxins and Phycotoxins in Perspective at the Turn of the Century, 383–391.

Quilliam, M. A., Thomson, B. A., Scott, G. J., & Siu, K. W. M. (1989). Ion-spray mass spectrometry of marine neurotoxins. Rapid Communications in Mass Spectrometry, 3(5), 145–150. https://doi.org/10.1002/rcm.1290030508

Ramos, T. K., Costa, L. D. F., Yunes, J. S., Resgalla, C., Barufi, J. B., Bastos, E. de O., Horta, P. A., & Rörig, L. R. (2021). Saxitoxins from the freshwater cyanobacterium Raphidiopsis raciborskii can contaminate marine mussels. Harmful Algae, 103. https://doi.org/10.1016/j.hal.2021.102004

Rapala, J., Robertson, A., Negri, A. P., Berg, K. A., Tuomi, P., Lyra, C., Erkomaa, K., Lahti, K., Hoppu, K., & Lepistö, L. (2005). First report of saxitoxin in Finnish lakes and possible associated effects on human health. Environmental Toxicology, 20(3), 331–340. https://doi.org/10.1002/tox.20109

Raposo, M. I. C., Gomes, M. T. S. R., Botelho, M. J., & Rudnitskaya, A. (2020). Paralytic Shellfish Toxins (PST)- Transforming Enzymes : A Review. Toxins, 12, 1–20.

Rejmánková, E., Komárek, J., Dix, M., Komárková, J., & Girón, N. (2011). Cyanobacterial blooms in Lake Atitlan, Guatemala. Limnologica, 41(4), 296–302. https://doi.org/10.1016/j.limno.2010.12.003

Rogers, R. S., & Rapoport, H. (1980). The pKa's of Saxitoxin. Journal of the American Chemical Society, 102(24), 7335–7339. https://doi.org/10.1021/ja00544a030

Rorar, J., Garcia, L. D., & Cutright, T. (2022). Removal of saxitoxin and anatoxin-a by PAC in the presence and absence of microcystin-LR and/or cyanobacterial cells. Journal of Environmental Sciences. https://doi.org/10.1016/j.jes.2022.08.015

Rositano, J., Newcombe, G., Nicholson, B., & Sztajnbok, P. (2001). Ozonation of nom and algal toxins in four treated waters. Water Research, 35(1), 23–32. https://doi.org/10.1016/S0043-1354(00)00252-9

Roy-Lachapelle, A., Solliec, M., & Sauvé, S. (2015). Determination of BMAA and three alkaloid cyanotoxins in lake water using dansyl chloride derivatization and high-resolution mass spectrometry. Analytical and Bioanalytical Chemistry, 407(18), 5487–5501. https://doi.org/10.1007/s00216-015-8722-2

Rutkowska, M., Płotka-Wasylka, J., Majchrzak, T., Wojnowski, W., Mazur-Marzec, H., & Namieśnik, J. (2019). Recent trends in determination of neurotoxins in aquatic environmental samples. TrAC - Trends in Analytical Chemistry, 112, 112–122. https://doi.org/10.1016/j.trac.2019.01.001

Schantz, E. J. (1986). Chemistry and Biology of Saxitoxin and Related Toxins. Annals of the New York Academy of Sciences, 479(1), 15–23. https://doi.org/10.1111/j.1749-6632.1986.tb15557.x

Shi, H., Ding, J., Timmons, T., & Adams, C. (2012). PH effects on the adsorption of saxitoxin by powdered activated carbon. Harmful Algae, 19, 61–67. https://doi.org/10.1016/j.hal.2012.05.008

Shimizu, Y., Hsu, C. ping, & Genenah, A. (1981). Structure of Saxitoxin in Solutions and Stereochemistry of Dihydrosaxitoxins. Journal of the American Chemical Society, 103(3), 605–609. https://doi.org/10.1021/ja00393a017

Silva Buarque, N. M., De Brito Buarque, H. L., & Capelo-Neto, J. (2015). Adsorption kinetics and diffusion of Saxitoxins on granular-activated carbon: Influence of pore size distribution. Journal of Water Supply: Research and Technology - AQUA, 64(3), 344–353. https://doi.org/10.2166/aqua.2015.140

Sinha, R., Pearson, L. A., Davis, T. W., Burford, M. A., Orr, P. T., & Neilan, B. A. (2012). Increased incidence of Cylindrospermopsis raciborskii in temperate zones - Is climate change responsible? Water Research, 46(5), 1408–1419. https://doi.org/10.1016/j.watres.2011.12.019

Smith, F. M. J., Wood, S. A., van Ginkel, R., Broady, P. A., & Gaw, S. (2011). First report of saxitoxin production by a species of the freshwater benthic cyanobacterium, Scytonema Agardh. Toxicon, 57(4), 566–573. https://doi.org/10.1016/j.toxicon.2010.12.020

Sommer, H., & Meyer, K. F. (1937). Paralytic Shell-Fish Poisoning. Arch. Pathol., 24, 560–598.

Strichartz, G. R. (1984). Structural determinations of the affinity of saxitoxin for neuronal sodium channels: Electrophysiological studies on frog peripheral nerve. Journal of General Physiology, 84(August 1984), 281–305. https://doi.org/10.1085/JGP.84.2.281

Sullivan, J. J., & Wekell, M. M. (1984). Determination of Paralytic Shellfish Poisonning Toxins by High Pressure Liquid Chromatography. Seafood Toxins American Chemical Society, May 1968, 198–205.

Svirčev, Z., Lalić, D., Bojadžija Savić, G., Tokodi, N., Drobac Backović, D., Chen, L., Meriluoto, J., & Codd, G. A. (2019). Global geographical and historical overview of cyanotoxin distribution and cyanobacterial poisonings. Archives of Toxicology, 93(9), 2429–2481. https://doi.org/10.1007/s00204-019-02524-4

Tang, T., Hoefel, D., Mosisch, T., & Ho, L. (2012). Assessing the fate and biodegradation of cyanobacterial metabolites in australian waters. Water Practice and Technology, 7(4). https://doi.org/10.2166/wpt.2012.064

U.S. EPA. (2015a). Drinking Water Health Advisory for the Cyanobacterial Microcystin Toxins (Issue June).

U.S. EPA. (2015b). Drinking Water Health Advisory for the Cyanobacterial Toxin Cylindrospermopsin (Issue June).

U.S. EPA. (2015c). Drinking Water Health Advisory for the Cyanobacterial Toxin Cylindrospermopsin.

U.S. EPA. (2015d). Method 545: Determination of cylindrospermopsin and anatoxin-a in drinking water by liquid chromatography electrospray ionization tandem mass spectrometry (LC/ESI-MS/MS).

Usleber, E., Dietrich, R., Bürk, C., Schneider, E., & Märtlbauer, E. (2001). Immunoassay Methods for Paralytic Shellfish Poisoning Toxins. Journal of AOAC International, 84(5), 1649–1656. https://academic.oup.com/jaoac/article/84/5/1649/5656903

Vale, C., Alfonso, A., Vieytes, M. R., Romarís, X. M., Arévalo, F., Botana, A. M., & Botana, L. M. (2008). In vitro and in vivo evaluation of paralytic shellfish poisoning toxin potency and the influence of the pH of extraction. Analytical Chemistry, 80(5), 1770–1776. https://doi.org/10.1021/ac7022266

Vo Duy, S., Munoz, G., Dinh, Q. T., Zhang, Y., Simon, D. F., & Sauvé, S. (2022). Fast screening of saxitoxin, neosaxitoxin, and decarbamoyl analogues in fresh and brackish surface waters by on-line enrichment coupled to HILIC-HRMS. Talanta, 241. https://doi.org/10.1016/j.talanta.2022.123267

Walker, H. W. (2014). Harmful Algae Blooms in Drinking Water: Removal of Cyanobacterial Cells and Toxins (1st ed.). CRC Press.

Drinking-water standards for New Zealand 2005 (revised 2018), Ministry of Health (2018).

Wiberg, G. S., & Stephenson, N. R. (1960). Toxicologic studies on paralytic shellfish poison. Toxicology and Applied Pharmacology, 2(6), 607–615. https://doi.org/10.1016/0041-008X(60)90078-8

Wiedner, C., Rücker, J., Brüggemann, R., & Nixdorf, B. (2007). Climate change affects timing and size of populations of an invasive cyanobacterium in temperate regions. Oecologia, 152(3), 473–484. https://doi.org/10.1007/s00442-007-0683-5

Wiese, M., D'Agostino, P. M., Mihali, T. K., Moffitt, M. C., & Neilan, B. A. (2010). Neurotoxic alkaloids: Saxitoxin and its analogs. Marine Drugs, 8(7), 2185–2211. https://doi.org/10.3390/md8072185

World Health Organization, W. (2019). Cyanobacterial toxins: Saxitoxins Background document for development of WHO Guidelines for Drinking-water Quality and Guidelines for Safe Recreational Water Environments.

World Health Organization (WHO). (2017). Guidelines for Drinking-water Quality: fourth edition incorporating the first addendum (4th ed.).

Xu, X. min, Huang, B. fen, Xu, J. jiao, Cai, Z. xuan, Zhang, J., Chen, Q., & Han, J. L. (2018). Fast and quantitative determination of saxitoxin and neosaxitoxin in urine by ultra performance liquid chromatography-triple quadrupole mass spectrometry based on the cleanup of solid phase extraction with hydrophilic interaction mechanism. Journal of Chromatography B: Analytical Technologies in the Biomedical and Life Sciences, 1072(November 2017), 267–272. https://doi.org/10.1016/j.jchromb.2017.11.032

Zamyadi, A., Ho, L., Newcombe, G., Daly, R. I., Burch, M., Baker, P., & Prévost, M. (2010). Release and oxidation of cell-bound saxitoxins during chlorination of Anabaena circinalis cells. Environmental Science and Technology, 44(23), 9055–9061. https://doi.org/10.1021/es102130b

CHAPTER 2 : Detection Of Saxitoxin From Drinking Water Using Solid Phase Extraction And Hydrophilic Interaction Liquid Chromatography – Mass Spectrometry

ABSTRACT

Saxitoxin is a potent neurotoxin which can cause paralytic shellfish poisoning (i.e., binding to sodium channels on cell membranes and inhibiting the supply of sodium ions into cells). These are produced by marine dinoflagellates and freshwater cyanobacteria, typically in tropical regions. However, climate change is predicted to increase the occurrence of saxitoxins in temperate regions. This is concerning as saxitoxins, the most potent of all cyanotoxins, are not regulated for monitoring and removal by drinking water treatment plants. The detection of saxitoxin is challenging as compared to other cyanotoxins due to its low molecular mass and highly polar nature.

The research objective of this study was to develop a sensitive and reliable method for the detection of saxitoxin from water samples. A Quadrupole/Time of Flight instrument and a Quadrupole/Orbitrap instrument was used to detect saxitoxins using HILIC-MS. The lowest concentration of saxitoxin (STX) that could be detected using HILIC-MS was 1.5 nM ($0.45\ \mu g/L$). Weak cation exchange (WCX) cartridges were tested to examine the recovery of the toxin during extraction from reagent water. The recovery percentage of saxitoxin from reagent water and tap water ranged from $64\% - 69\%$ with a 10X concentration of STX. This study also helped identify loss of saxitoxin due to sorption to glass as well as drying after extraction, indicating that for further development, these steps should be avoided. The use of internal standard (L-arginine amide) was also beneficial in normalizing any losses due to sorption.

INTRODUCTION

Saxitoxin, also referred to as the paralytic shellfish toxin (PST), is a neurotoxin that is produced by marine dinoflagellates and freshwater cyanobacteria. Saxitoxin and its structural variants act by binding to sodium channels on cell membranes and inhibiting the supply of sodium ions into cells which leads to paralysis and death by respiratory arrest (Aráoz et al., 2010). Detections of saxitoxin producing cyanobacteria from tropical or sub-tropical origins are increasing in temperate regions like Michigan, Alabama and Northeast Germany (Ballot et al., 2010; Chaffin et al., 2019; Hong et al., 2006; Onodera et al., 1997). Furthermore, agricultural run-off coupled with an increasing surface water temperature due to global warming makes Lake Erie, a source of drinking water for 12 million people in U.S.A. and Canada, a potential hub for saxitoxin production in the future (Sinha et al., 2012). Saxitoxins have been detected in freshwaters of the United States and also in some cases in treated drinking water (AWWA, 2016; Loftin et al., 2016).

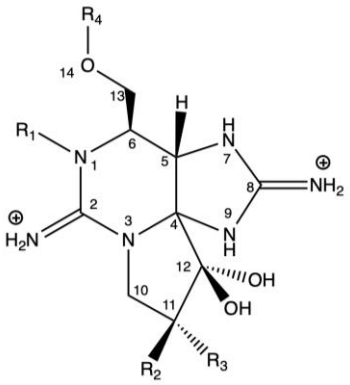

Toxin	R_1	R_2	R_3	R_4	Relative Toxicity
STX	- H	- H	- H	-OC-NH_2	1
NEO	- OH	- H	- H	-OC-NH_2	0.92
GTX1	- OH	- H	- OSO_3^-	-OC-NH_2	0.99
GTX2	- H	- H	- OSO_3^-	-OC-NH_2	0.36
GTX3	- H	- OSO_3^-	- H	-OC-NH_2	0.64
GTX4	- OH	- OSO_3^-	- H	-OC-NH_2	0.73
GTX5	- H	- H	- H	-OC-NH-SO_3^-	0.06
GTX6	- OH	- H	- H	-OC-NH-SO_3^-	0.06
C1	- H	- H	- OSO_3^-	-OC-NH-SO_3^-	0.01
C2	- H	- OSO_3^-	- H	-OC-NH-SO_3^-	0.01

Figure 2-1: Structure of saxitoxin and its variants with relative toxicities (Oshima, 1995).

Mouse bioassay (MBA) was the early biological method that was developed and standardized for the detection of saxitoxins (Sommer & Meyer, 1937). This method soon lost demand due to its use of live animals and slow results. Eventually, analytical methods like HPLC and LC-MS gained popularity due to their relatively quick and accurate analysis (Halme & Vanninen, 2013). Since saxitoxin is a highly polar compound, it cannot be retained on a reverse phase column in the absence of ion-pairing reagents. The use of ion-pairing reagents is not ideal due to the interference in signal causing reduced detection sensitivity. Hence, hydrophilic interaction liquid chromatography coupled with electrospray ionization tandem mass spectrometry (HILIC-MS) was implemented for the analysis of saxitoxins (Dell'Aversano et al., 2005).

Monitoring of saxitoxins in the source and drinking water is performed using the enzyme-linked immunosorbent assay (ELISA) method, which is well known for its ease of use, rapidity of single target analysis, and sensitivity, providing a detection limit of $0.02\ \mu g/L$. However, ELISA offers poor selectivity of analytes and the possible cross-reactivity of saxitoxin variants makes the test unreliable for quantitative analysis (Humpage et al., 2010). The ability of HILIC-MS to provide specific detection through mass differentiation makes it an ideal tool for the quantitative analysis of saxitoxin variants.

Most studies that used HILIC-MS for the detection of saxitoxins derived their source of extraction from shellfish because historically the threat to humans by saxitoxins was primarily via food due to the ability of saxitoxins to bioaccumulate in shellfish (Cusick & Sayler, 2013; Levin, 1991). For the determination of human exposure to saxitoxin, urine is used as an extraction source for the detection by HILIC-MS (Bragg et al., 2015; Johnson et al., 2009; Xu et al., 2018). Due to the rise in number of detections of saxitoxin producing cyanobacteria in freshwaters, researchers have developed methods to detect saxitoxins from algal cell cultures

(Dell'Aversano et al., 2004; Lajeunesse et al., 2012; Velzeboer et al., 2000). The low concentrations of saxitoxins in surface water requires extensive pre-concentration for successful detection on LC/MS. However, since the studies mentioned above used sources other than water, their extraction methods involved minimal pre-concentration or clean-up steps.

The basic nature of saxitoxin, originating from the guanidinium groups of the toxin, suggests that carboxylate weak-cation exchange resins will be capable of retaining the toxin (Hall & Reichardt, 1984). Existing methods for WCX SPE, which have been used for extraction of saxitoxins from human urine and plasma (Bragg et al., 2015; Eangoor et al., 2015; Johnson et al., 2009; Peake et al., 2016), were modified in our study so as to achieve extraction from approximately 100 mL of water. Hence, this study aimed to extract saxitoxins from 100 mL of water using weak-cation exchange (WCX) solid-phase extraction (SPE). The implementation of HILIC-MS in combination with WCX SPE is expected to provide an accurate, reliable, and sensitive detection of saxitoxins from water.

METHODS

Materials

Certified calibration solution of STX was purchased from National Research Council of Canada. HPLC grade acetonitrile (CAS# 75-0-8) and methanol (CAS# 67-56-1) were purchased from Sigma Aldrich (St. Louis, Missouri, USA). Ammonium formate (certified ACS) (CAS# 540-69-2), formic acid, 99%, Optima™ LC/MS grade (CAS# 64-18-6), and ammonium hydroxide (certified ACS plus) (CAS# 1336-21-6, 7664-41-7, and 7732-18-5) were obtained from Fisher Scientific (Fair Lawn, New Jersey, USA). Ultrapure water was prepared using the GenPure water system from ThermoFisher Scientific. Restek™ 2.0 mL amber autosampler vials (part # 21142) and Restek™ polypropylene vial inserts (part # 06-718-933) were purchased from Fisher

Scientific (Fair Lawn, New Jersey, USA). Potassium phosphate dibasic trihydrate, $\geq 99.0\%$ (CAS# 16788-57-1; Sigma Aldrich®, St. Louis, Minnesota, USA) and potassium phosphate monobasic, white crystals (CAS# 7778-77-0; Michigan State University Chemistry Store, East Lansing, Michigan, USA) were used to prepare a 0.05 M phosphate buffer with a resulting pH of 7.10. Ammonium acetate (CAS# 631-61-8; Sigma Aldrich®, St. Louis, Minnesota, USA) and acetic acid, glacial (certified ACS) (CAS# 64-19-7; Fisher Scientific, Fair Lawn, New Jersey, USA) were used to prepare 0.05 M acetate buffer with a resulting pH of 5.85.

Sample Preparation using SPE

The concentration of STX in the certified standard was $66.3\ \mu M$, which was used to preparing standards and for spiking into samples for this study.

The following cartridges were used for initial testing: Phenomenex™ (Torrance, California, USA) WCX (8B-S035-FCH), United Chemical Technologies (UCT, Bristol, Pennsylvania, USA) WCX (EUCCX156), Waters HLB (186003365), Waters™ (Milford, Massachusetts, USA) WCX (186002498), and Biotage® (Charlotte, North Carolina, USA) Evolute WCX (612-0050-CXG). Biotage® VacMaster™ 10 manifold was used to perform SPE. Several methods were tested on the above cartridges to achieve maximum recovery and detailed descriptions of these methods are provided in Table 2-1. When the eluents were dried, a SpeedVac system was used. Dried extracts were then reconstituted with 95% acetonitrile and 5% ultrapure water containing $10\ mM$ ammonium formate and $4\ mM$ formic acid to prepare for detection using UPLC/MS/MS. Aliquots of $100\ \mu L$ were dispensed in the polypropylene vial inserts which were placed inside autosampler vials.

Instrumentation

STX was measured by UPLC/MS using a Waters Xevo G2-XS (QToF) or Thermo Q-Exactive (Orbitrap). Liquid chromatography (LC) separation was achieved using an Acquity BEH Amide, 1.7 μm, 100×2.1 mm column with a flow rate of 0.3 mL/min. The mobile phase solvents were A) 10 mM ammonium formate in ultrapure water (pH 2.8) and B) acetonitrile. The total run time was 10 minutes with the following gradient: (i) 95% of B was held for 2 minutes, (ii) A was increased to 50% at 2 minutes and held for 4 minutes, (iii) a further increase of A to 70% was made at the 6th minute and held for 1 minute, and (iv) B was brought back up to 95% at 7th minute and held until the end of the run. Positive mode was applied for electrospray ionization and the injection volume was 10 μL for both mass spectrometry (MS) instruments. The QToF instrument parameters consisted of the following: capillary voltage = 3 kV, sampling cone = 30, source temperature = 100℃, desolvation temperature = 350℃, cone gas flow = 50 $L/hour$, and desolvation gas flow = 600 $L/hour$. Some of the functional parameters of QToF were as follows: mass range = 190 – 1500, target enhancement mass = 300.00, and mass correction was applied using Leu-enkephalin as the lock mass reference compound. The full MS-SIM mode on the Orbitrap included the following parameters: resolution setting = 70,000, AGC target = 3,000,000, maximum inject time = 200 ms, scan range = 100 – 1500 m/z. The heated electrospray ion source parameters used for the Orbitrap are as follows: Sheath gas flow rate = 50, Aux gas flow rate = 13, sweap gas flow rate = 3, spray voltage = 3.5 kV, capillary temperature = 263℃, and aux has heater temperature = 425℃.

METHOD DEVELOPMENT

Evaluation of SPE Cartridge and Procedure

With a goal of achieving maximum recovery, different types of cartridges were tested as shown in Table 1. WCX cartridges were expected to have higher recoveries as compared to HLB due to the chemistry of the sorbent that allows for retention of polar analytes like saxitoxins. At a pH between 6 – 8, the carboxylic acid ligand of the stationary phase of the cartridge would be deprotonated, allowing the formation of an ionic bond with the positively charged C-8 and C-2 guanidinium groups of STX (Figure 2-2). Formic acid was added to the eluent to contribute H^+ ions in the matrix which would replace the STX molecule, resulting in elution of the analyte. However, even with the addition of formic acid, the recovery percentage was very low (< 10%). Alternatively, the elution of STX could also occur if the pH is high enough (> 8.4) for the STX molecule to be deprotonated (Hall et al., 1990b; Strichartz, 1984). Hence, ammonium hydroxide was added to the elution solvent in one of the trials, which was observed to result in no recovery of STX. Since some the elution solvents could not be injected into LC/MS, the samples were required to be dried using a SpeedVac prior to injection. The dried samples were then reconstituted with the same solvent mixture used for preparation of standards. Through several trials, the recovery did not exceed 30%. Hence, the drying of eluents was eliminated, and the elution solvent was selected such that it could be directly injected into the LC/MS without requiring additional modification. Consequently, the recoveries of STX drastically improved resulting in > 80% recovery of STX using 3 different cartridges as shown in Table 2-1. This led to the conclusion that there was a considerable loss of STX during the drying step.

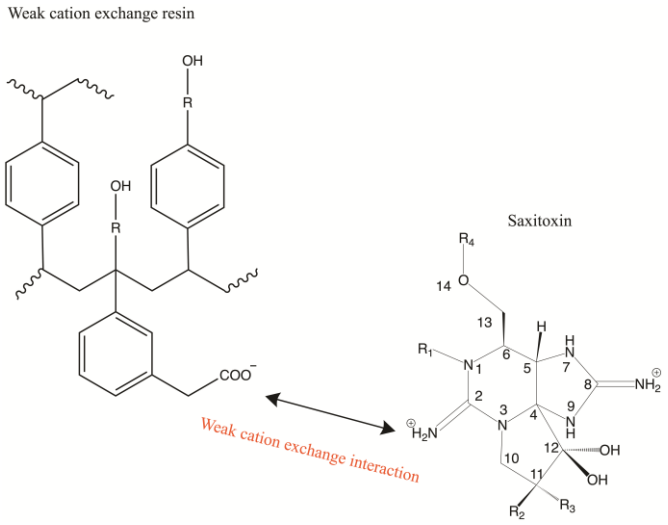

Figure 2-2: Retention chemistry of saxitoxin with weak cation exchange (WCX) resin

Table 2-1: Summary of SPE trials performed to evaluate recovery of STX using different cartridges.

Cartridge	**Sample Preparation**	**SPE steps**	**Recovery**
Phenomenex WCX	6 mL sample with 0.05 M phosphate buffer (pH 7.10) and 0.033 μM STX	1. Cartridges pre-treated with 15 mL 0.05 M phosphate buffer (pH 7.10) 2. Conditioned with 15 mL methanol 3. Equilibrated with 15 mL 0.05 M phosphate buffer (pH 7.10) 4. Sample loaded on cartridge (vacuum = 7 – 10 in Hg) 5. Cartridge washed with 6 mL ultrapure water followed by 6 mL methanol 6. Cartridge dried for 5 min under high vacuum (vacuum = 20 in Hg) 7. Cartridge eluted with 6 mL 95% methanol and 5% ammonium hydroxide 8. Eluents dried and reconstituted with 100 μL of dilution solvent*	0%

Table 2-1 (cont'd)

Phenomenex WCX	6 mL sample with 0.033 μM STX	1. Cartridge pre-treated with 15 mL 0.05 M phosphate buffer (pH 7.10) 2. Conditioned with 15 mL methanol followed by 15 mL of 95% methanol and 5% formic acid 3. Equilibrated with 15 mL 0.05 M phosphate buffer (pH 7.10) 4. Sample loaded on cartridge (vacuum = 7 – 10 in Hg) 5. Cartridge washed with 15 mL ultrapure water followed by 6 mL methanol 9. Cartridge dried for 5 min under high vacuum (vacuum = 20 in Hg) 6. Cartridge eluted with 6 mL 95% methanol and 5% formic acid 7. Eluents dried and reconstituted with 100 μL of dilution solvent	25 – 30% recovery within replicates
Phenomenex WCX	1 mL sample with 1 μM STX	1. Cartridge pre-treated with 15 mL 0.05 M acetate buffer (pH 5.85) 2. Conditioned with 15 mL methanol followed by 6 mL of 50% methanol, 45% ultrapure water, and 5% formic acid 3. Equilibrated with 15 mL 0.05 M acetate buffer (pH 5.85) 4. Sample loaded on cartridge (no vacuum applied) 5. Cartridge washed with 6 mL methanol 6. Cartridge dried for 5 min under high vacuum (vacuum = 20 in Hg) 7. Cartridge eluted with 6 mL of 50% methanol, 45% ultrapure water, and 5% formic acid 8. Eluents dried and reconstituted with 100 μL of dilution solvent	~10%

Table 2-1 (cont'd)

Phenomenex WCX	1 mL sample with 0.5 μM STX	1. Cartridge pre-treated with 15 mL 0.05 M acetate buffer (pH 5.85) 2. Conditioned with 15 mL methanol followed by 6 mL of 90% methanol and 10% formic acid 3. Equilibrated with 15 mL 0.05 M acetate buffer (pH 5.85) 4. Sample loaded on cartridge (no vacuum applied) 5. Cartridge washed with 6 mL methanol 6. Cartridge dried for 5 min under high vacuum (vacuum = 20 in Hg) 7. Cartridge eluted with 6 mL of 90% methanol and 10% formic acid 8. Eluents dried and reconstituted with 100 μL of dilution solvent	< 10%
UCT WCX	1 mL sample with 0.5 μM STX	1. Conditioned with 15 mL methanol 2. Equilibrated with 15 mL 0.05 M phosphate buffer (pH 7.10) 3. Sample loaded on cartridge (no vacuum applied) 4. Cartridge washed with 6 mL ultrapure water followed by 6 mL acetonitrile 5. Cartridge dried for 5 min under high vacuum (vacuum = 20 in Hg 6. Cartridge eluted with 6 mL of 95% methanol and 5% formic acid 7. Eluents dried and reconstituted with 100 μL of dilution solvent	~10%
Phenomenex WCX	100 mL sample with 4.8 nM STX	1. Conditioned with 5 mL methanol 2. Equilibrated with 5 mL ultrapure water 3. Sample loaded on cartridge (vacuum = 7 – 10 in Hg) 4. Cartridge washed with 6 mL ultrapure water 5. Cartridge eluted with 10 mL of 95% acetonitrile and 5% formic acid	85.5%

Table 2-1 (cont'd)

Waters WCX	100 mL sample with 4.8 nM STX	1. Conditioned with 5 mL methanol 2. Equilibrated with 5 mL ultrapure water 3. Sample loaded on cartridge (vacuum = 7 – 10 in Hg) 4. Cartridge washed with 6 mL ultrapure water 5. Cartridge eluted with 10 mL of 95% acetonitrile and 5% formic acid	93%
Biotage WCX	100 mL sample with 4.8 nM STX	1. Conditioned with 5 mL methanol 2. Equilibrated with 5 mL ultrapure water 3. Sample loaded on cartridge (vacuum = 7 – 10 in Hg) 4. Cartridge washed with 6 mL ultrapure water 5. Cartridge eluted with 10 mL of 95% acetonitrile and 5% formic acid	93%

*dilution solvent – 95% acetonitrile + 5% ultrapure water containing 10 mM ammonium formate and 4 mM formic acid

The recovery of STX using Biotage WCX cartridges was further evaluated for ultrapure water and was also compared to tap water. In one of the experiments (Day 1), the internal standard, i.e., L-arginine amide, used for HILIC-MS detection was added into the sample prior to extraction. As seen in Figure 3, the data were very inconsistent resulting in high standard deviation across 5 replicates. This can be explained by the chemistry of L-arginine amide, similar to that of STX, which makes it compete for retention on the stationary phase of the SPE. Hence, in the future experiments (Day 2), the L-arginine amide was not added in the samples prior to extraction. Based on the mean of 3 replicates for ultrapure water and tap water, it was surprising to see higher recovery in the tap water samples but the ultrapure samples displayed higher consistency within replicates as represented by the error bars (Figure 2-3). The statistical analysis performed

on the Day 2 data, using t-test, showed that the difference in means of the Genpure water recovery and tap water recovery is not significant at a 95% confidence interval (see Table 2-2 and Table 2-3).

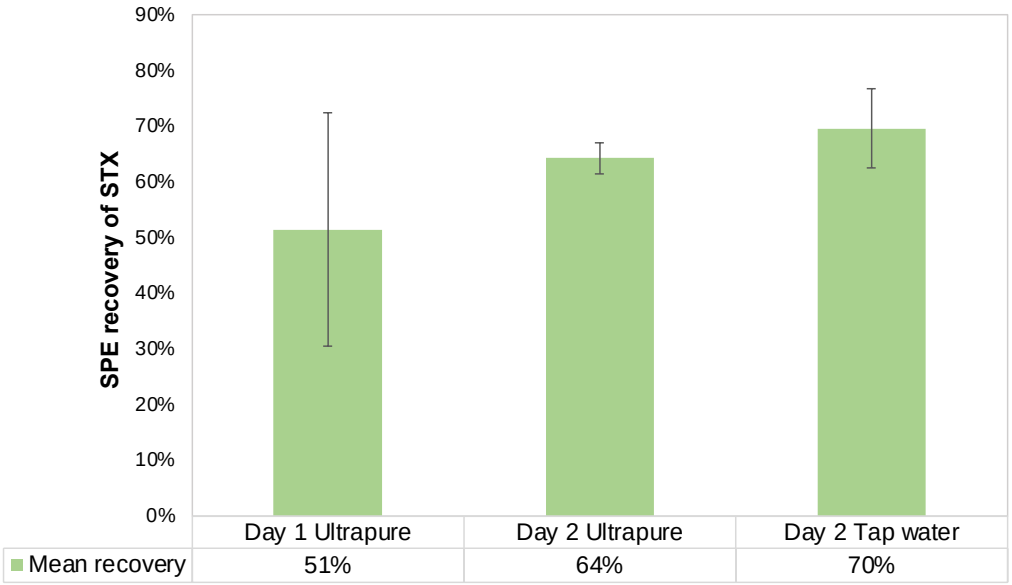

Figure 2-3: Recovery data for SPE of STX using Biotage WCX cartridges on different days with ultrapure water (Day 1: n = 5, Day 2: n = 3) and tap water (n = 3). Error bars represent standard deviation across replicates.

Detection by HILIC-MS

For developing the MS method, 1 μM STX, prepared in 95% acetonitrile and 5% water, was initially injected directly into the MS on Water TQ-D UPLC/MS/MS instrument. However, the toxin was not detected and hence the instrument was switched to Water Quattro Premier XE UPLC/MS/MS. The Acquity BEH Amide column was used for LC separation and target analysis was selected for MS providing a good signal strength for 1 μM STX. Details of mobile phase and gradient are provided in the "Instrumentation" section. The lowest concentration that was detected was 1 μM. Based on comparison with previous studies on HILIC-MS detection of STX, 1 μM was too high to be deemed as an acceptable detection limit. The instrument was then switched to Waters Xevo G2-XS (QToF), which provided better signal intensity, contributed by

the target enhancement feature which is characterized in the QToF. The other challenge that was encountered was the carryover of STX to blank samples, which implied that STX could have been sticking to surfaces, especially glass as all standards were prepared in glass vials. Glass consists of silanol (SiOH) groups that are deprotonated at a pH > 2 and become increasingly negative charged as the pH increases (Lowe et al., 2015). This negative charge attracts the positively charged guanidinium groups of saxitoxin at C2 and C8 position. Hence, the preparation material was switched from glass to polypropylene and the dilution solvent of the standards was amended to include 10 mM ammonium formate and 4 mM formic acid in the aqueous phase, which would increase the ionic strength of the solvent while also keeping the pH low (pH 3), limiting the adsorption of STX on surfaces. Carryover was still observed during a reproducibility check experiment wherein the concentration of STX increased with every sample that was run on the instrument, indicating that STX could be sticking to surfaces within the LC system. To combat this, the syringe wash was changed from just water to water containing 10 mM ammonium formate. Although this did not completely eliminate carryover, the data obtained were more consistent and the signal quality improved considerably resulting in a decrease in the STX detection limit to $0.125\ \mu M$. The minimum reporting level (MRL) was determined as $0.25\ \mu M$ by following the EPA quality control (QC) criteria as mentioned in the EPA method 544 (J.A. Shoemaker et al., 2015). The standard curve linear range was $0.125\ \mu M - 2\ \mu M$ with a $R^2 = 0.98$. Multiple blanks were required to be run between samples to eliminate any error due to carryover. A representative standard curve is shown in Figure 2-4.

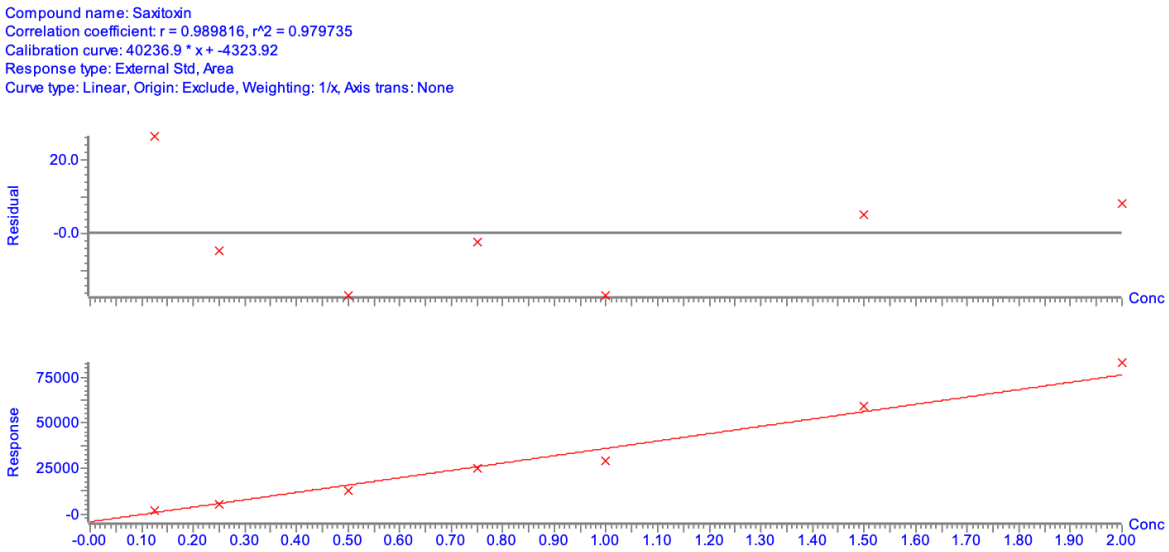

Figure 2-4: Representative standard curve for saxitoxin with a linear range of 0.125 μM to 2 μM.

To further increase the sensitivity, the scan time for MS was increased from 0.2 seconds to 0.4 seconds. This decreased the detection limit to 4.69 nM. However, this could not be established as the MRL as it failed to meet the criteria specified in EPA Method 544 (J.A. Shoemaker US EPA, Office of Research and Development et al., 2015), and hence to normalize any inconsistences created due to carryover, L-arginine amide was used as an internal standard. Following the incorporation of the internal standard, the instrument was changed from QToF to Orbitrap as the autosampler of the Orbitrap did not contain any glass components, further reducing the chances of STX sticking to glass surfaces. The lowest STX concentration that was detected on the Orbitrap was 1.5 nM and the standard curve linear range was 1.5 $nM - 96\ nM$ for STX with the inclusion of L-arginine amide in the standards. The peak area of the 1.5 nM STX peak is shown in Figure 2-5 and the representative standard curve is shown in Figure 2-6.

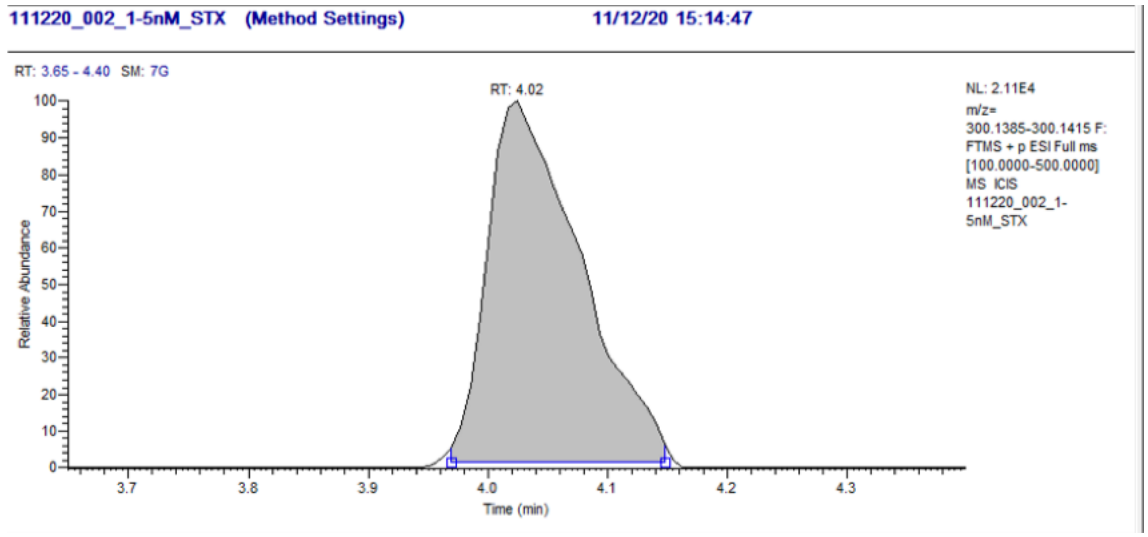

Figure 2-5: Chromatogram of 1.5 nM STX peak on the Orbitrap.

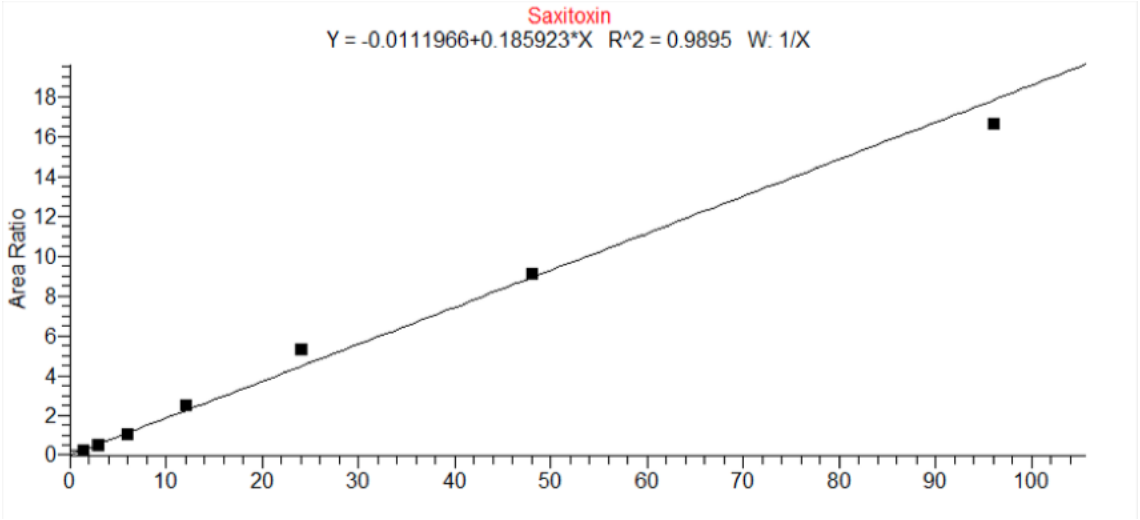

Figure 2-6: Representative standard curve for the linear range of $1.5\ nM - 96\ nM$ for STX on the Orbitrap.

DISCUSSION

The selection of WCX SPE and HILIC-MS was made based on the structure of saxitoxin and was also influenced by past literature focused on the detection of saxitoxins from different matrices (Bragg et al., 2015; Johnson et al., 2009). The protocols for SPE provided by the manufacturers of the WCX cartridges used in this study, could not be applied as stated to STX.

The method had to be modified in order to obtain maximum recovery. A notable finding through the SPE method development process was that drying of eluents containing STX resulted in a loss of the STX due to adsorption to the surfaces. Hence, minimal loss of STX can be achieved by using the same solvent for elution from WCX cartridges as that used for preparation of standards. Alternatively, if drying is necessary, methods like sonication would be required to redissolve the STX into the solvent used for reconstitution. To quantify the loss of STX due to drying, a comparison between recoveries with and without the drying step showed that the drying step resulted in recoveries of $10\% - 25\%$, whereas eliminating the drying step resulting in higher recoveries ranging from $80\% - 90\%$. The addition of internal standard, L-arginine amide, was explored before and after the extraction step. The resulting data for the internal standard added prior to SPE showed inconsistency in data whereas its addition after SPE, provided more consistency in data. The recoveries using Biotage WCX cartridge were 64.24% with a standard deviation of 0.02831 for reagent water, and 69.61% with a standard deviation of 0.07125 for tap water.

As seen with the HILIC-MS method development, the HILIC column, i.e., Acquity BEH Amide column, provided a good separation of the STX (shown in Figure 2-7). The QToF, due to its ability to perform target enhancement, was able to detect STX at low concentrations, i.e., $4.69\ nM$. The limitation with using the QToF was its use of glass autosampler components which adsorbed STX, resulting in carryover within the data. This resulted in inconsistency in the data. The adsorption of STX to glass vials was also recently demonstrated in a study in which the signal strength was considerably higher for samples in polypropylene vials as compared to the samples in glass vials (Vo Duy et al., 2022). This is consistent with our findings. The addition of the internal standards, L-arginine amide, along with switching to the Orbitrap instrument, which

did not consist of any glass components, increased the consistency of data. The lowest concentration of STX that was detected using the Orbitrap, while the LC column remained the same, was 1.5 nM. With the combination of WCX SPE and HILIC-MS, the developed method was able to detect STX concentrations as low as 4.8 nM prior to concentration, with the ability to detect concentrations as low as 0.3 nM based on the sensitivity of the HILIC-MS method.

FUTURE WORK & CONCLUSION

With the knowledge obtained through this study, one of the next steps would be to perform method validation, which involves the following QC testing: (i) precision demonstration by performing WCX SPE followed by HILIC-MS detection on 7 replicates of STX spiked samples with the relative standard deviation (RSD) of the samples to be < 30%, (ii) demonstration of accuracy by calculating the mean of same set of data used in (i) and checking if the recovery falls within $\pm$ 30% of the true value, and (iii) performing matrix addition on surface and tap water samples to ensure that the sample matrix does not affect the accuracy and precision of the method. The recovery of STX from surface waters also needs to be evaluated. While using surface water samples, an additional filtration step would be required for intracellular toxin release in which the samples would be filtered through a 0.45 μm membrane filter, followed by soaking the filtrate with the filter paper in methanol containing 20% water, and then mixing the soaking solvent into the filtered water. The selection of filter material should be made with caution as a study demonstrated that STX can be adsorbed by glass fiber, but not by nitrocellulose, nylon, polyethersulfone, and regenerated cellulose (Vo Duy et al., 2022).

The extraction and detection method described in this study can also be used to detect neoSTX, GTX1-6, and the decarbamoyl analogues, by increasing the total run time of samples on the HILIC-MS method to avoid peak overlap. The C-toxin variants of saxitoxin contain a sulfate

functional group in R_4 position (Figure 1) and a hydroxysulfate on C-11, which leads to these toxins having little or no charge within the pH range of 6 – 8, consequently resulting in lower binding capacity to carboxylic acid resins (Hall & Reichardt, 1984). To increase retention of the C-toxins during SPE, Jansson & Åstot (2015) used acid hydrolysis to convert C1&2 into GTX2&3 variants of saxitoxin. The use of an internal standard is crucial to normalize any errors during the sample run, resulting in higher precision of the data. While this study used L-arginine amide, there are better alternatives such as neoSTX-$^{15}N_7$ that are commercially available and that have been used in previous studied for detection of saxitoxin and its variants (Bragg et al., 2015; Vo Duy et al., 2022).

This study provides preliminary results that can be used for the development of a detection method for saxitoxins from large volumes, i.e., 100 mL of water, for the detection of low concentrations of saxitoxin in aqueous samples. With the integration of proper method validation techniques, it would be possible to standardize this method, similar to the one for microcystins, as mentioned in EPA method 544 (J.A. Shoemaker et al., 2015). When impacted by harmful algae blooms, this standardized method would serve as a resource for water utilities to monitor and regulate the presence of saxitoxins in drinking water, thus ensuring the protection of public health.

REFERENCES

Aráoz, R., Molgó, J., & Tandeau de Marsac, N. (2010). Neurotoxic cyanobacterial toxins. Toxicon, 56(5), 813–828. https://doi.org/10.1016/j.toxicon.2009.07.036

AWWA. (2016). Cyanotoxins in US Drinking Water: Occurrence , Case Studies and State Approaches to Regulation Cyanotoxins in US Drinking Water. September.

Ballot, A., Fastner, J., & Wiedner, C. (2010). Paralytic shellfish poisoning toxin-producing cyanobacterium Aphanizomenon gracile in Northeast Germany. Applied and Environmental Microbiology, 76(4), 1173–1180. https://doi.org/10.1128/AEM.02285-09

Bragg, W. A., Lemire, S. W., Coleman, R. M., Hamelin, E. I., & Johnson, R. C. (2015). Detection of human exposure to saxitoxin and neosaxitoxin in urine by online-solid phase extraction-liquid chromatography-tandem mass spectrometry. Toxicon, 99, 118–124. https://doi.org/10.1016/j.toxicon.2015.03.017

Chaffin, J. D., Mishra, S., Kane, D. D., Bade, D. L., Stanislawczyk, K., Slodysko, K. N., Jones, K. W., Parker, E. M., & Fox, E. L. (2019). Cyanobacterial blooms in the central basin of Lake Erie: Potentials for cyanotoxins and environmental drivers. Journal of Great Lakes Research, 45(2), 277–289. https://doi.org/10.1016/j.jglr.2018.12.006

Cusick, K. D., & Sayler, G. S. (2013). An overview on the marine neurotoxin, saxitoxin: Genetics, molecular Targets, methods of detection and ecological functions. Marine Drugs, 11(4), 991–1018. https://doi.org/10.3390/md11040991

Dell'Aversano, C., Eaglesham, G. K., & Quilliam, M. A. (2004). Analysis of cyanobacterial toxins by hydrophilic interaction liquid chromatography-mass spectrometry. Journal of Chromatography A, 1028(1), 155–164. https://doi.org/10.1016/j.chroma.2003.11.083

Dell'Aversano, C., Hess, P., & Quilliam, M. A. (2005). Hydrophilic interaction liquid chromatography-mass spectrometry for the analysis of paralytic shellfish poisoning (PSP) toxins. Journal of Chromatography A, 1081(2), 190–201. https://doi.org/10.1016/j.chroma.2005.05.056

Eangoor, P., Indapurkar, A., & Knaack, J. S. (2015). Development of a Solid Phase Extraction Method to Extract Gonyautoxins from Urine. 2–5.

Hall, S., & Reichardt, P. B. (1984). Cryptic Paralytic Shellfish Toxins. In Seafood Toxins (pp. 113–123). American Chemical Society.

Hall, S., Strichartz, G., Moczydlowski, E., Ravindran, A., & Reichardt, P. B. (1990). The Saxitoxins: Sources, Chemistry and Pharmacology. In Marine Toxins: Origin, Structure, and Molecular Pharmacology (pp. 29–65).

Halme, M., & Vanninen, P. (2013). Saxitoxin Analysis. Encyclopedia of Analytical Chemistry, 1–7. https://doi.org/10.1002/9780470027318.a9320

Hong, Y., Steinman, A., Biddanda, B., Rediske, R., & Fahnenstiel, G. (2006). Occurrence of the Toxin-producing Cyanobacterium Cylindrospermopsis raciborskii in Mona and Muskegon Lakes, Michigan. J. Great Lakes Res. Internat. Assoc. Great Lakes Res, 32(Who 1999), 645–652. https://doi.org/10.3394/0380-1330(2006)32[645:OOTTCC]2.0.CO;2

Humpage, A. R., Magalhaes, V. F., & Froscio, S. M. (2010). Comparison of analytical tools and biological assays for detection of paralytic shellfish poisoning toxins. Analytical and Bioanalytical Chemistry, 397(5), 1655–1671. https://doi.org/10.1007/s00216-010-3459-4

J.A. Shoemaker, Tettnhorst, D. R., & Cruz, A. de la. (2015). Method 544: Determination Of Microcystins And Nodularin In Drinking Water By Solid Phase Extraction And Liquid Chromatography/Tandem Mass Spectrometry (LC/MS/MS). United States Environmental Protection Agency.

Jansson, D., & Åstot, C. (2015). Analysis of paralytic shellfish toxins, potential chemical threat agents, in food using hydrophilic interaction liquid chromatography-mass spectrometry. Journal of Chromatography A, 1417, 41–48. https://doi.org/10.1016/j.chroma.2015.09.029

Johnson, R. C., Zhou, Y., Statler, K., Thomas, J., Cox, F., Hall, S., & Barr, J. R. (2009). Quantification of saxitoxin and neosaxitoxin in human urine utilizing isotope dilution tandem mass spectrometry. Journal of Analytical Toxicology, 33(1), 8–14. https://doi.org/10.1093/jat/33.1.8

Lajeunesse, A., Segura, P. A., Gélinas, M., Hudon, C., Thomas, K., Quilliam, M. A., & Gagnon, C. (2012). Detection and confirmation of saxitoxin analogues in freshwater benthic Lyngbya wollei algae collected in the St. Lawrence River (Canada) by liquid chromatography-tandem mass spectrometry. Journal of Chromatography A, 1219, 93–103. https://doi.org/10.1016/j.chroma.2011.10.092

Levin, R. E. (1991). Paralytic Shellfish Toxins: Their Origin, Characteristics and Methods of Detection: A Review. Journal of Food Biochemistry, 15(6), 405–417. https://doi.org/10.1111/j.1745-4514.1991.tb00425.x

Loftin, K. A., Graham, J. L., & Meyer, M. T. (2016). Cyanotoxins in inland lakes of the United States : Occurrence and potential recreational health risks in the EPA National Lakes Assessment 2007. Harmful Algae, 56, 77–90.

Lowe, B. M., Skylaris, C. K., & Green, N. G. (2015). Acid-base dissociation mechanisms and energetics at the silica-water interface: An activationless process. Journal of Colloid and Interface Science, 451, 231–244. https://doi.org/10.1016/j.jcis.2015.01.094

Onodera, H., Satake, M., Oshima, Y., Yasumoto, T., & Carmichael, W. W. (1997). New saxitoxin analogues from the freshwater filamentous cyanobacterium Lyngbya wollei. Natural Toxins, 5(February), 146–151. https://doi.org/10.1002/1522-7189(1997)5:4<146::AID-NT4>3.0.CO;2-V

Oshima, Y. (1995). Postcolumn Derivatization Liquid Chromatographic Method for Paralytic Shellfish Toxins. Journal of AOAC International, 78(2), 528–532.

Peake, R. W. A., Zhang, V. Y., Azcue, N., Hartigan, C. E., Shkreta, A., Prabhakara, J., Berde, C. B., & Kellogg, M. D. (2016). Measurement of neosaxitoxin in human plasma using liquid–chromatography tandem mass spectrometry: Proof of concept for a pharmacokinetic application. Journal of Chromatography B: Analytical Technologies in the Biomedical and Life Sciences, 1036–1037, 42–49. https://doi.org/10.1016/j.jchromb.2016.09.043

Sinha, R., Pearson, L. A., Davis, T. W., Burford, M. A., Orr, P. T., & Neilan, B. A. (2012). Increased incidence of Cylindrospermopsis raciborskii in temperate zones - Is climate change responsible? Water Research, 46(5), 1408–1419. https://doi.org/10.1016/j.watres.2011.12.019

Sommer, H., & Meyer, K. F. (1937). Paralytic Shell-Fish Poisoning. Arch. Pathol., 24, 560–598.

Strichartz, G. R. (1984). Structural determinations of the affinity of saxitoxin for neuronal sodium channels: Electrophysiological studies on frog peripheral nerve. Journal of General Physiology, 84(August 1984), 281–305. https://doi.org/10.1085/JGP.84.2.281

Velzeboer, R. M. A., Baker, P. D., Rositano, J., Heresztyn, T., Codd, G. A., & Raggett, S. L. (2000). Geographical patterns of occurrence and composition of saxitoxins in the cyanobacterial genus Anabaena (Nostocales, Cyanophyta) in Australia. Phycologia, 39(5), 395–407. https://doi.org/10.2216/i0031-8884-39-5-395.1

Vo Duy, S., Munoz, G., Dinh, Q. T., Zhang, Y., Simon, D. F., & Sauvé, S. (2022). Fast screening of saxitoxin, neosaxitoxin, and decarbamoyl analogues in fresh and brackish surface waters by on-line enrichment coupled to HILIC-HRMS. Talanta, 241. https://doi.org/10.1016/j.talanta.2022.123267

Xu, X. min, Huang, B. fen, Xu, J. jiao, Cai, Z. xuan, Zhang, J., Chen, Q., & Han, J. L. (2018). Fast and quantitative determination of saxitoxin and neosaxitoxin in urine by ultra performance liquid chromatography-triple quadrupole mass spectrometry based on the cleanup of solid phase extraction with hydrophilic interaction mechanism. Journal of Chromatography B: Analytical Technologies in the Biomedical and Life Sciences, 1072 (November 2017), 267–272. https://doi.org/10.1016/j.jchromb.2017.11.032

APPENDIX

Figures

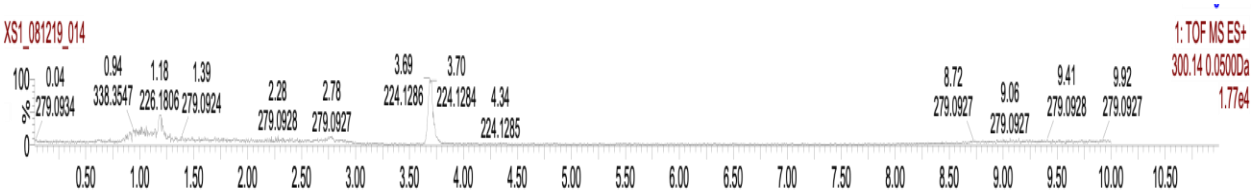

Figure 2-7: Representative chromatogram of STX

Tables

Table 2-2: F-test performed on the SPE recovery data for Day 2 between Genpure water samples and tap water samples.

F-Test Two-Sample for Variances		
	Variable 1	*Variable 2*
Mean	0.64239477	0.69610993
Variance	0.00080168	0.00507715
Observations	3	3
df	2	2
F	0.15789912	
P(F<=f) one-tail	0.13636691	
F Critical one-tail	0.02564103	

Table 2-3: t-test performed on SPE recovery data for Day 2 between Genpure water samples and tap water samples.

t-Test: Two-Sample Assuming Unequal Variances		
	Variable 1	*Variable 2*
Mean	0.64239477	0.69610993
Variance	0.00080168	0.00507715
Observations	3	3
Hypothesized Mean Difference	0	
df	3	
t Stat	-1.2134227	
P(T<=t) one-tail	0.15589499	
t Critical one-tail	2.35336343	
P(T<=t) two-tail	0.31178999	
t Critical two-tail	3.18244631	

CHAPTER 3 : Development Of An Inexpensive, Rapid Method To Measure Nitrates In Freshwater To Enhance Student Learning

ABSTRACT

An inquiry-based learning approach was employed in a STEM teaching laboratory at Michigan State University to engage students in an activity that not only introduced an innovative nitrate detection technique but also addressed one of the negative impacts of climate change, i.e., the eutrophication of water bodies. The adverse effects of eutrophication on public health due to the presence of cyanotoxins make it crucial to monitor the trophic state of water bodies, which can be assessed by measuring the nitrate and phosphate concentrations. We developed a rapid method to measure nitrate concentrations in freshwater samples using a Hanna Instrument checker, which was designed to measure nitrate levels in seawater. We identified the sample matrix that would maximize the accuracy of the checker instrument for freshwater samples and validated the analytical method via ion chromatography. Students gained knowledge of other aspects of laboratory procedures, such as sample collection, sample storage, and material compatibility, which are often ignored during conventional teaching practices.

INTRODUCTION

Inquiry-Based Learning

In 2020, the engineering accreditation board, ABET, published a revised set of student learning outcomes. *Outcome 6* states that at the time of graduation, engineering students are to have an "ability to design, develop and conduct appropriate experimentation, analyze and interpret data, and use engineering judgment to draw conclusions" (ABET 2022). In addition, the Environmental Engineering Program Criteria states that the curriculum is to include "hands-on laboratory experiments, and analysis and interpretation of the resulting data in more than one

major environmental engineering focus area, e.g., air, water, land, environmental health" (ABET 2022). As a result, the undergraduate environmental engineering laboratory course at Michigan State University was redesigned to be learner-centered, knowledge-centered, community-centered, and assessment-centered. The laboratory exercise described herein is the second of five laboratory experiments, designed to facilitate student learning and guide students toward the final laboratory exercise, where they design and conduct an experiment.

Traditionally, many undergraduate laboratory courses in STEM use a "cookbook" approach, where students are provided a recipe for the experiment and are expected to answer a limited set of questions. This is not surprising, as the development and implementation of inquiry-based laboratory exercises require considerable time and effort along with guidance and oversight by the instructor (Christian, Hershock, and Melville 2019). However, inquiry-based learning enhances student learning (Beck, Butler, and Silva 2014; Flora and Cooper 2005), improves the ability of students to design experiments and analyze data (Myers and Burgess 2003), and promotes higher order thinking skills (Madhuri, Kantamreddi, and Prakash Goteti 2012). An adaptation of the inquiry-based flowchart as described by Madhuri et al (Madhuri, Kantamreddi, and Prakash Goteti 2012) is put into context with the learning objectives of our study, linked to concepts aligned with Bloom's taxonomy (Armstrong 2010) (Figure 3-1).

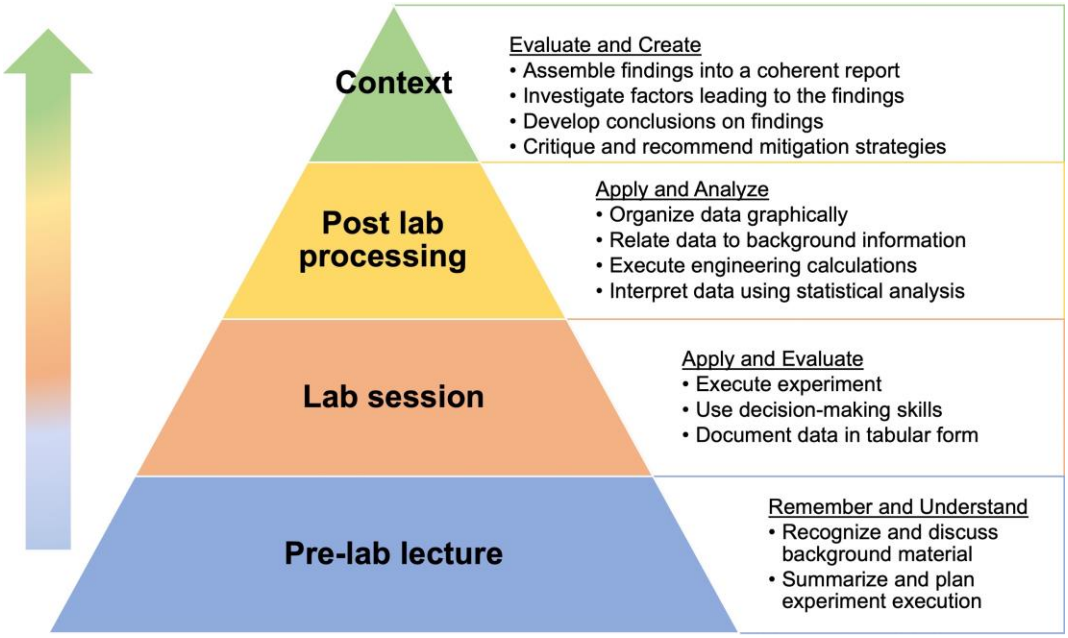

Figure 3-1*:* Inquiry-based flowchart representing the learning objectives of this lab and compared to the levels of Bloom's taxonomy.

Learning Objectives

For each of the five laboratory exercises, students were expected to engage with a challenging problem, investigate the phenomena or causes of the problem, explain their results obtained in the laboratory, apply their knowledge to develop a solution, and reflect on their knowledge and proposed solution. For example, in the first laboratory exercise, students were expected to develop a set of questions related to the red water issues in the campus tap water, use their knowledge from the prerequisite causes to investigate the causes of red water, develop a sampling plan for the collection of the tap water, test for relevant analytes, analyze the data using the Langelier Saturation Index, and apply this information to develop a solution to the red water problems on campus. Toward this goal, students attended a pre-lab lecture that provided the foundational information for the laboratory exercise. Following the lecture, the students were expected to review the material provided, refine the relevant set of questions, and plan the experiment's execution.

As mentioned above, this laboratory experiment was designed for an undergraduate teaching laboratory in the field of environmental engineering; however, it is also appropriate for chemistry, biology, limnology, and general environmental science laboratories. A pre-lab lecture provided background information on the trophic state of ecosystems, along with the experimental procedures for the measurement of nitrates and phosphates. Using the results collected in the laboratory, along with the data provided by the instructor, students wrote a memorandum to the local environmental commission documenting their study. In the memorandum, students were expected to comment on the spatial variability of the data, discuss the potential sources of nutrient runoff, propose mitigation strategies to prevent algae blooms and overcome eutrophication, and develop a more extensive monitoring plan for the site that would provide more conclusive information regarding water quality. In all laboratory exercises, students were expected to conduct data analysis using the appropriate statistical methods and provide a discussion of their interpretation of the data. In the final laboratory exercise, students were expected to develop the methodology to model chlorine decay as a function of time and pH, determine the first order rate constant for chlorine decay, and then use the data to design a dechlorination basin that meets specified criteria. The uncertainty in the rate constant was to be incorporated into the design. Students were also expected to build on knowledge from previous coursework to relate their experimental results to the impact of wastewater discharge into water bodies. A detailed description of the learning objectives is provided in Table 3-1. The rubrics used to assess mastery of the learning objectives were designed to be aligned with ABET Student Outcomes and the learning objectives.

Students at the undergraduate level at Michigan State University were asked to perform this laboratory experiment in groups of two or three. Measurements required for this experiment were

conducted within the laboratory session, i.e., one 3-hour session per week. To make the most of the time allotted for this laboratory experiment, samples were collected by the instructor and TA and provided to the students. Detailed information on sampling procedures (e.g., sample containers, storage, location, date/time, depth of the sample, and weather) were also provided to the students along with a pre-laboratory lecture on developing sampling plans and sample collection, storage, and material compatibility.

Table 3-1: Learning objectives of the laboratory experiment.

Category	Learning Objective
Laboratory techniques	1. Collect the following data for the environmental samples provided: a. Measure pH, conductivity, and temperature of samples using the probes supplied. b. Follow the instructions in the test kit for colorimetric measurement of phosphate. 2. Add salt to samples to modify background electrolyte concentration. 3. Follow the instructions in the test kit for colorimetric measurement of nitrate. 4. Properly document the data.
Data Analysis	1. Report data in the appropriate graphical and tabular form while also including a map of the sampling locations. 2. Perform statistical analysis which includes determination of mean, standard deviation, and confidence interval.
Interpretation of results	1. Based on the data collected, comment on the trophic level of water. 2. Discuss potential sources of nutrients, including land use patterns, based on the sampling locations. 3. Discuss potential mitigation strategies. 4. Discuss spatial variability of results, develop a more comprehensive sampling plan, and recommend more accurate methods of assessing the trophic level of water bodies.

Background

Eutrophication is a natural phenomenon that is caused by an increase in the nutrient content of a water body. The consequences of climate change, i.e., an increase in water temperatures and stratification, along with increased nutrient runoff, have led to an expansion of eutrophication events, which can have a serious detrimental impact on aquatic and human life. Eutrophication in freshwaters, most often characterized by the presence of algae blooms, is a result of the excessive availability of nitrogen and phosphorus. Hence, nitrogen and phosphorus are reliable indicators used to determine the level of pollution and the trophic state of a water body (Figure 3-2).

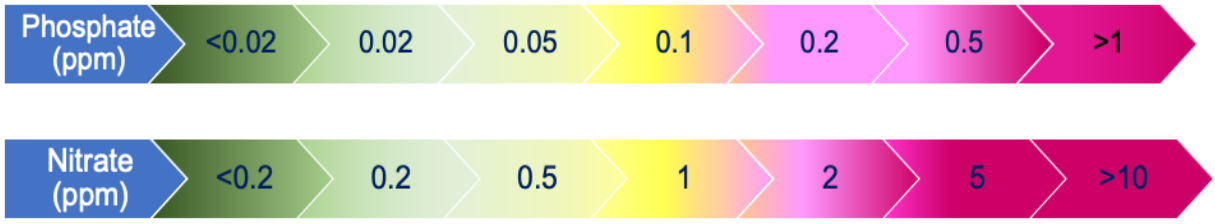

Nutrient	No evidence of pollution	Some evidence of nutrient pollution	High levels of pollution	Very high levels of pollution
Phosphate	< 0.02 – 0.05 ppm	0.05 – 0.1 ppm	0.1 – 0.5 ppm	0.5 - > 1 ppm
Nitrate	< 0.2 – 0.5 ppm	0.5 – 1 ppm	1 – 2 ppm	2 - > 10+ ppm

Figure 3-2*:* Nitrogen and phosphorus as indicators of eutrophication in a water body (adapted from (Briggs et al. 2016)).

Harmful algae blooms (HABs) are not only detrimental to aquatic ecosystems, but the organisms that cause HABs release cyanotoxins, which can be fatal to humans, fish, and other organisms upon ingestion, inhalation, or exposure via dermal contact (Harold W. Walker 2014). Nitrogen, primarily resulting from agricultural activities and industrial runoff, is one of the limiting nutrients in the formation of harmful algae blooms (Lewis, Wurtsbaugh, and Paerl 2011). Consequently, the detection of nitrates in freshwaters is a useful technique to analyze the risk of

harmful algae blooms (Cremona et al. 2021; V. H. Smith 1982; Downing, Watson, and McCauley 2011).

Ion chromatography is one of the most accurate methods used to measure nitrates. However, it requires users to be skilled and experienced in using ion chromatography. Other reliable detection methods include electrochemical detection, UV-vis spectrometry, and high-performance liquid chromatography (Alahi and Mukhopadhyay 2018; Moorcroft, Davis, and Compton 2001; Singh et al. 2019). However, most of these methods are unsuitable for measuring aqueous concentrations of nitrates in the field, in many undergraduate laboratories, and by citizen scientists.

Colorimetry is an easy-to-use technique to detect nitrates in water (Shinn 1941) without the use of expensive equipment and can be implemented into microfluidic devices or portable test kits that allow for the field measurement of nitrates (Charbaji et al. 2021; Hwang et al. 2013; Y. Cheng et al. 2021; Murray et al. 2017; Sargazi and Kaykhaii 2020). The chemistry of the colorimetric method for the detection of nitrate concentrations involves the reduction of nitrate to nitrite followed by detection using the diazotization method proposed by Griess (Slough and Wang 2010). Cadmium, zinc, nitrate reductase, vanadium (III), and hydrazine sulfate are among the reducing agents that have been employed for the reduction of nitrate to nitrite in the colorimetric method (Charbaji et al. 2021; Moorcroft, Davis, and Compton 2001). The high efficiency (> 90%) of cadmium for the reduction of nitrate to nitrite makes it a popular choice among nitrate test kits developed for natural waters (Murray et al. 2017). However, the toxic properties of cadmium limit the use of these test kits in undergraduate laboratories and in field test kits where the safe disposal of spent cadmium is challenging. Zinc is a popular alternative to cadmium that provides accurate results in various water matrices (Ellis et al. 2011; Murray et al.

2017) and is suitable for use in portable test kits since it is neither toxic nor is its disposal regulated.

This study utilizes the Hanna Instrument nitrate test kit that reduces the nitrate to nitrite using zinc. See equation (3.1) for details on the reaction.

$$NO_3^- + Zn_{(s)} + 2H^+ \rightarrow NO_2^- + Zn^{2+} + H_2O \quad (3.1)$$

The nitrite then reacts with the Griess reagent, an aromatic aniline compound (e.g., sulfanilic acid), to form a diazonium salt. This salt results in the formation of an azo dye which is a pinkish-violet color, through a coupling reaction with N-(1-naphthyl) ethylenediamine (NED) (Slough and Wang 2010) (see Figure 3-3). The color generated can be measured using a spectrophotometer at a wavelength of 543 nm (Patton and Kryskalla 2011; Sargazi and Kaykhaii 2020; Giovannoni et al. 1997).

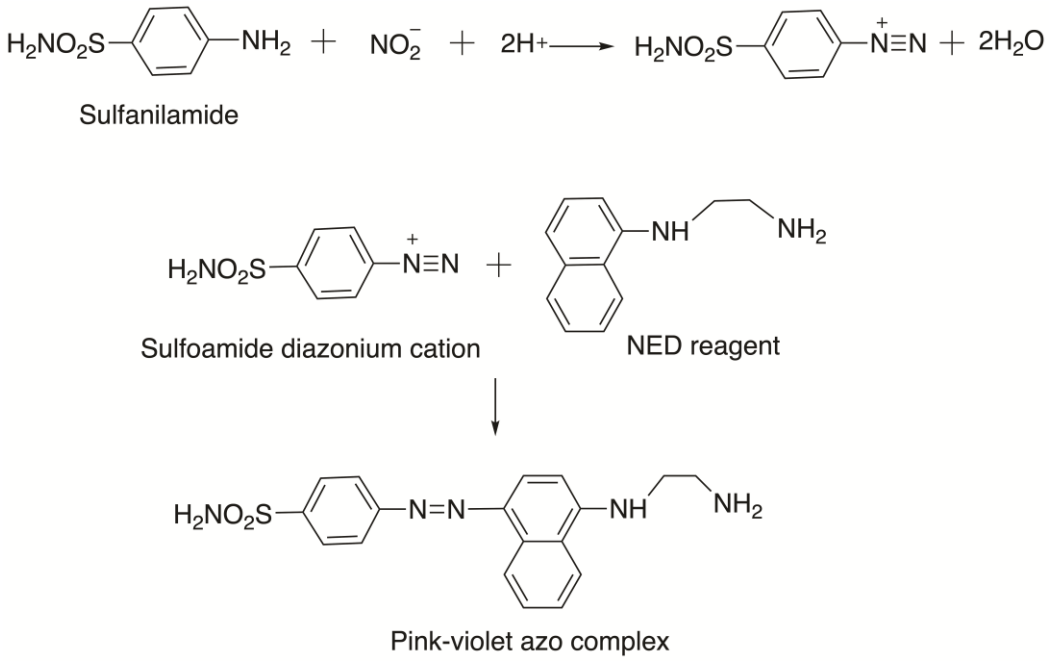

Figure 3-3: Reaction of nitrite with Griess reagent to form a pinkish-violet azo dye (Tsikas 2007).

The test kit is supplied with a colorimeter that uses a fixed wavelength of 525 nm LED and a silicon photodetector to provide a digital reading of concentration based on Beer's Law and a stored calibration curve. The Hanna Instrument test method, which was low-cost, rapid, and easy to use, was successfully modified and used by undergraduate students to quantify nitrate levels in freshwater samples. Table 3-2 provides a comparison of some of the popular nitrate test kits available on the market.

Table 3-2: Cost Comparison of Commercial Nitrate Test Kits for Freshwaters.

Type of nitrate measurement kit	**Price/kit**	**No. of tests/kit**	**Price/ test**	**Shelf life**	**Detection range** $ppm\ as\ NO_3^-$	**Specific notes**
Hanna Instrument HI781 (current study)	$59.95	25	$2.40	4 years	$0 - 5.0$	Supplied with a portable colorimeter that provides accurate nitrate measurements
Hach test kit TNT835	$62.71	25	$2.50	< 2 years	$1 - 60$	Requires the use of a visible spectrophotometer (~$430 - $6,000) and cannot be used in the field
LaMotte Tablet test kit 3354-01	$69.30	50	$1.39	Not specified	$0 - 66$	Uses color comparator against specific concentration range, which limits the accuracy

Table 3-2 (cont'd)

API test kit	$12.25	90	$0.14	Not specified	$\mathbf{0-160}$	Reads concentrations as $\boldsymbol{NO_3^-}$. Also, concentrations are 0, 5, 10, 20, 40, 80, and 160 ppm, which are not relevant for most natural waters.
Hanna Instrument HI3874	$41	100	$0.41	Not specified	$0-220$	Uses cadmium reduction, which is hazardous, and color comparator, which can be inaccurate
Hach test kit NI-11	$123	100	$1.23	Not specified	$0-176$	Uses cadmium reduction, which is hazardous

EXPERIMENTAL

Materials & Reagents

Saltwater nitrate low-range ($0.00-5.00\ ppm$) checker® HC (HI781) and additional reagents (HI781-25) were purchased from Hanna Instruments (Woonsocket, RI). Step-by-step instructions from the manufacturer of the checker are provided on the product information webpage ("Https://Www.Hannainst.Com/Marine-Nitrate-Checker-Hi781.Html" 2022). The nitrate standard (Cat # 5307-16), 1000 ppm concentration, was purchased from RICCA Chemical Company (Arlington, TX). Stock solutions were prepared by performing serial dilutions of the 1000 ppm standard. High-purity deionized water (ultrapure water) with a resistivity of 18 MΩ · cm was used to prepare stocks and laboratory-fortified blanks. Instant Ocean®, an aquarium salt mix, was purchased from Instant Ocean® (Blacksburg, VA). Sodium chloride (CAS 7647-14-5),

purchased from ChemPure Brand Chemicals® (Plymouth, MI), was used as a comparative salt to Instant Ocean®. The Instant Ocean® salt mixture contains no detectable nitrate or nitrite(Holder, Conmy, and Venosa 2015). Sodium bicarbonate (CAS 144-55-8) and sodium carbonate (CAS 497-19-8) were purchased from Fisher Chemical (Pittsburgh, PA) for preparing the eluent for the IC. Environmental samples were collected from six locations in Meridian Township and Lansing, Michigan in amber glass bottles and were stored at < 10℃ until analysis.

Instrumentation

The absorbances of the resulting solutions were measured at 543 nm using the Spectronic Genesys 5 spectrophotometer and 1.0 cm path length cuvettes. IC measurements of nitrates were conducted on the Dionex series 2000i/SP Ion Chromatograph connected to an Alcott 728 autosampler. The analytical and guard columns used were Dionex IonPac™ AS4A-SC ($4 \times 250\ mm$) and Dionex IonPac™ AG4A-SC ($4 \times 50\ mm$), respectively. The eluent contained sodium bicarbonate 1.7 mM and sodium carbonate 1.6 mM. Its flow rate through the column was 1 mL/min. The retention time of the nitrate ion was 3.2 minutes for a total run time of 10 minutes.

Methods

Optimization of the salt concentration to create a saltwater matrix: This study was performed to ensure that the addition of salt into the sample did not interfere with the color development. Solutions containing nitrate at a concentration of 2.5 mg/L and salt concentrations ranging from $0 - 40{,}000\ mg/L$ were prepared. The instructions ("Https://Www.Hannainst.Com/Marine-Nitrate-Checker-Hi781.Html" 2022) provided with the Hanna Instrument kit (see Figure 3-4) were followed as written. However, instead of reading the nitrate measurement using the colorimeter provided with the kit, the absorbance at 543 nm was measured using a

spectrophotometer at 1 min time intervals from the point the last reagent was completely mixed into the solution until the absorbance of the dye stabilized.

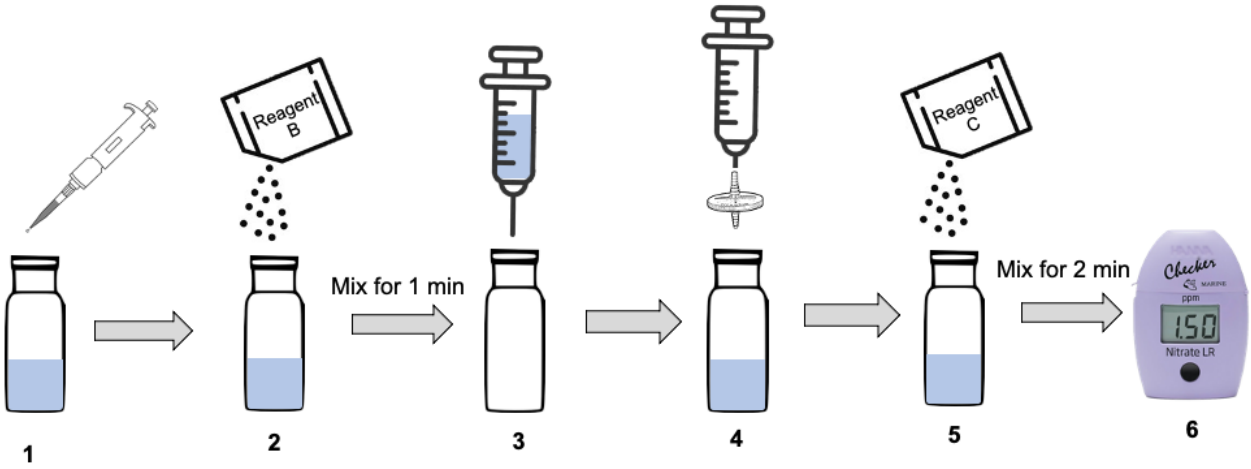

Figure 3-4: Schematic diagram of the stepwise procedure for nitrate determination using Hanna Instrument marine nitrate checker (HI781) following the addition of Instant Ocean® at a concentration of 35,000 mg/L; 1 – add 4 mL of reagent A (2-3% ammonium hydroxide) to 7 mL of sample; 2 – add contents of reagent B packet (EDTA tetrasodium salt (50-70%) and zinc powder, stabilized (30-50%)) and mix well for 1 min; 3 – draw 10 mL of solution using a syringe; 4 – filter contents of syringe through the filter provided in the kit into another vial; 5 – add the content of reagent C packet (potassium disulfate (50-100%)) into the filtrate and mix well for 2 min; after 8 min, measure the nitrate concentration using the checker instrument. It should be noted that the SDSs provided by Hanna Instrument did not contain a complete listing of all reagents nor do their product information sheets provide a description of the purpose of each of the chemicals provided in the reagent packets.

Comparison of the standard curve obtained by adding Instant Ocean® vs sodium chloride:

Using the results from the optimization of salt concentrations, a salt concentration to be added into the samples was determined based on conditions yielding the highest absorbance after 9 minutes of color development. As such, 35,000 mg/L was selected as the optimal salt concentration. Hence, solutions used to create the standard curve contained 35,000 mg/L salt concentration and nitrate concentrations ranging from $0 - 5\ mg/L$. Measurements were taken using the checker as well as by measuring the absorbance of the resulting dye using a spectrophotometer.

Testing precision of the method using Instant Ocean® and sodium chloride: The nitrate concentration (2.5 mg/L) was determined in triplicate to determine the method precision. Salt concentrations of $10{,}000\ mg/L$, $30{,}000\ mg/L$, and $40{,}000\ mg/L$ were used. The stepwise procedure provided with the Hanna Instrument kit was followed, after which measurements were taken using the checker as well as by measuring the absorbance of the resulting dye at 543 nm using a spectrophotometer.

Investigation of Method Detection Limit (MDL): To investigate the MDL, Instant Ocean was used as the salt. A stock containing $0.25\ mg/L$ nitrate concentration and $35{,}000\ mg/L$ salt concentration was prepared. Measurement of nitrate using the Hanna Instrument kit was performed 8 times. The MDL was calculated following the procedure reported by the EPA(U.S. EPA 2016).

Comparison of Hanna Instrument nitrate checker with Ion Chromatograph (IC): The accuracy of the method developed to measure nitrates using the Hanna Instrument checker was compared with the nitrate measurements obtained using an IC. Samples were spiked with known concentrations of nitrate and were measured by IC and Hanna Instrument checker.

Hazards and safety precautions: Before the start of the activity, students should be made aware of laboratory safety procedures in their respective laboratories. Proper ventilation is essential and students should be required to wear to wear protective gloves, eye protection, and appropriate clothing while conducting the experiments described in this study. Ammonium hydroxide in reagent A of the kit is corrosive and can cause eye damage and skin irritation. The EDTA tetrasodium salt (reagent B) is harmful if swallowed or inhaled and can cause serious eye damage. Potassium disulfate (reagent C) is toxic, if inhaled, and can cause severe burns and eye damage. The activities of this study should be conducted under the supervision of trained

personnel. Where students are to gather their own samples, instructors should consult with their institution's safety officers to mitigate against hazards including drowning, insect bites, and contact with poisonous plants and animals.

Application of Detection Method on Freshwater Samples

To verify the usability of the developed method, the method was applied to measure nitrate concentrations in freshwater samples. These experiments were performed by the first co-author. Freshwater samples were collected by the first co-author from the six locations in Meridian Township and Lansing from September – November 2021. During collection, the pH, temperature, and conductivity of the samples were recorded. pH and temperature were measured with the HI98108 pocket pH tester by Hanna Instruments, which allows for both pH and temperature measurements to be taken simultaneously. The pH readings have a resolution of 0.01 units and an accuracy of ± 0.10 units. Calibration was done by a 2-point calibration at pH 4.0 and pH 7.0. Conductivity was measured with the HI98393 DiST3 EC tester by Hanna Instruments, which can be used for waters having a conductivity less than 2000 $\mu S/cm$. Nitrate measurements using the Hanna Instrument checker were performed within 48 hours of sample collection. Samples were preserved at $< 10℃$ until measurement. Instant Ocean® was added to the freshwater samples at a concentration of $35{,}000\ mg/L$ prior to analysis. A standard curve was created by spiking known concentrations of nitrate into one of the samples to confirm the linear range of detection of the Hanna Instrument checker in freshwater samples.

Student Engagement

In the pre-lecture, the instructor provided students with background information along with details regarding the sampling and laboratory procedures. During the morning of the afternoon laboratory sessions, samples were collected from Lake Lansing and Tacoma Hills Lagoon

located in Meridian Township, Michigan, at three distinct locations in each of the two bodies of water. The pH, conductivity, and temperature of the samples were measured on-site. The samples were spiked with 35,000 mg/L of Instant Ocean® prior to the start of the laboratory session. The students measured the nitrate and phosphorus concentrations in the laboratory, along with pH, temperature, and conductivity. Photographs and maps of the sampling events were provided to the students, from which students were asked to make observations on the color of water, presence/absence of aquatic organisms, algae, or plants, and locate possible nearby sources of pollution, such as surface water runoff from fertilized lawns, stormwater runoff from roads, animal feces. Students were asked to conduct triplicate analyses on any one set of samples to determine the mean, standard deviation, and confidence interval. For assessment, on the basis of the data collected, students were asked to discuss the trophic state of water, the potential sources of pollution and their mitigation strategies, and the spatial variability of the results. In addition, students were asked to propose a sampling plan that would better assess the trophic state of water and help address the above-mentioned points.

RESULTS & DISCUSSION

Method Validation

The concentration of salt required to create an optimal response: As mentioned previously, the results of optimizing the salt concentrations were used to determine the concentration of the salts required to create a saltwater matrix with the best response using the Hanna Instrument checker. The highest absorbance reading, which was obtained at the 9-minute time interval, was selected as a criterion for the determination of optimal salt concentration. The resulting profiles of different salt concentrations were similar (see Figure 3-13); however, the peak absorbance values differed as shown in Figure 3-5.

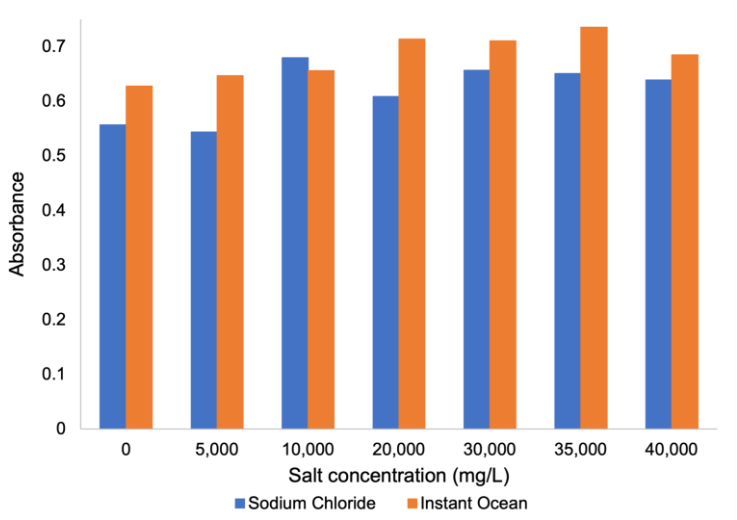

Figure 3-5*:* Absorbance after 9 mins obtained using solutions containing nitrate at a concentration of 2.5 mg/L and varying concentrations of the salts: Instant Ocean® and sodium chloride. Data were collected by the first co-author.

The addition of Instant Ocean® at increasing concentrations resulted in an increase in the absorbance measured at 543 nm, whereas the absorbance has a weak relationship with the sodium chloride concentration (Figure 3-13). To further confirm the significance of the differences in peak absorbances across the different salt concentrations, a t-test was performed. The results of the t-test for Instant Ocean® comparing the peak absorbance from $0 - 10{,}000\ mg/L$ vs $20{,}000 - 40{,}000\ mg/L$, implied that the difference in the mean values was significant at a 95% confidence interval ($p = 0.004$). Conversely, for sodium chloride, the difference was not significant ($p = 0.4$). Instant Ocean® at a concentration of 35,000 mg/L was chosen as it was closest to the salt concentration in seawater (KESTER et al. 1967).

Standard Curve: The accuracy of nitrate measurement was compared based on the regression value of the standard curves generated by using the two salts. The overall fit of the data to a linear model was better for samples analyzed in the saltwater matrix formulated using Instant Ocean® (($R^2 = 0.98$) as shown in Figure 3-6A) than for samples analyzed with sodium chloride

as the background electrolyte (((($R^2 = 0.92$) as shown in Figure 3-6B). Although the slope of the sodium chloride standard curve is also >0.9, indicating a strong positive relationship between the checker reading and the nitrate concentration, the variability represented by the standard deviation of the slope at a 95% confidence interval is ~2.5 times greater for the sodium chloride samples than that of the Instant Ocean® (see Table 3-5). This further confirms the appropriateness of Instant Ocean® as the saltwater matrix. The standard curve plots of absorbance vs nitrate concentrations for the salts are given in Figure 3-15.

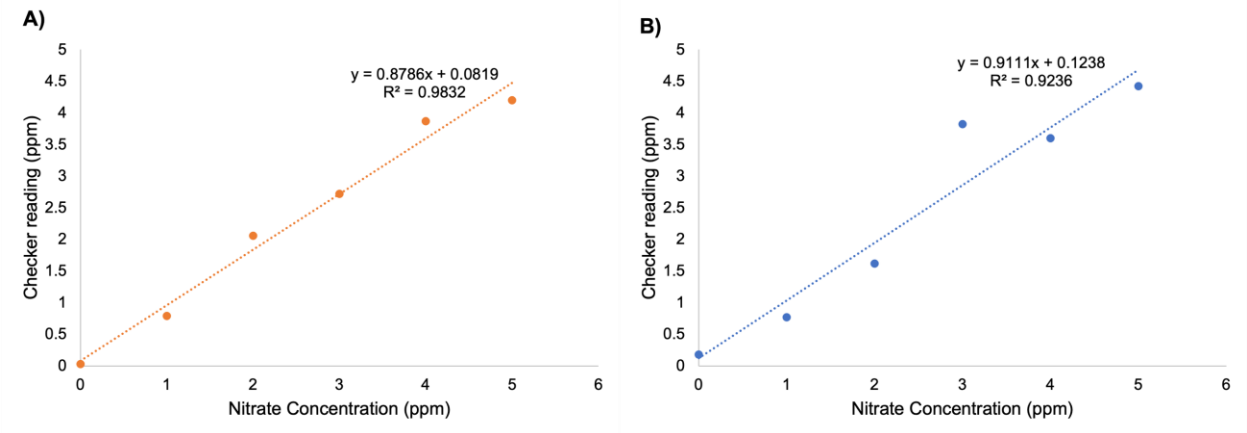

Figure 3-6: Standard curves obtained for the checker reading vs nitrate concentration using A) Instant Ocean® and B) sodium chloride.

The precision of the method developed: The precision data for different concentrations of Instant Ocean® and sodium chloride are depicted in Figure 3-7. The addition of Instant Ocean® at a concentration of 30,000 mg/L into the matrix resulted in a mean nitrate concentration closest to the spiked value, i.e., 2.5 mg/L. A comparison of the chosen salt concentration, i.e., 35,000 mg/L Instant Ocean® versus the other salt concentrations in Figure 3-7 is shown in Figure 3-16. However, for sodium chloride, the lowest salt concentration provided results closest to the spiked value with no clear distinction in the precision of data at the different concentrations.

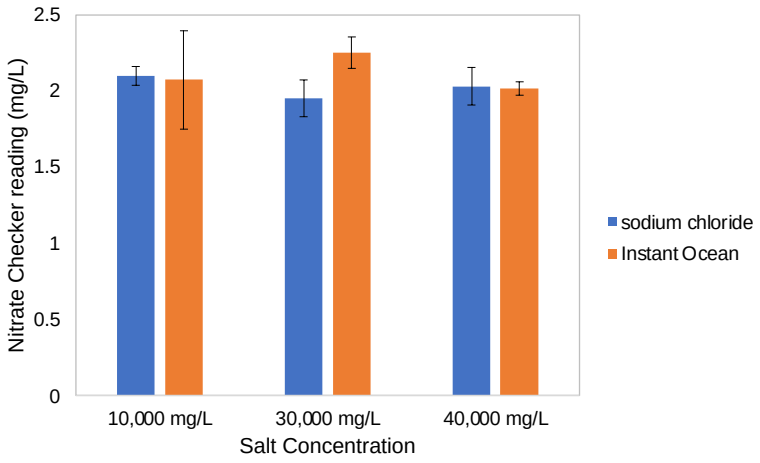

Figure 3-7: Bar chart representing the mean of replicate samples ($n = 3$) spiked with nitrate at a concentration of 2.5 mg/L and different salt concentrations. The standard deviation is shown using the error bars.

In the presence of sodium chloride, the highest absorbance was observed at $10{,}000\ mg/L$ during the salt optimization study as well as the precision study (see Figure 3-5 and Figure 3-7).

Method Detection Limit (MDL): The MDL was determined using equation 3.2:

$$MDL_s = t_{n-1,1-\alpha=0.99} \times S_s \tag{3.2}$$

where: $t_{n-1,1-\alpha=0.99}$ represents the Student's t-value appropriate for a single-tailed 99th percentile t statistic and a standard deviation estimate with n-1 degrees of freedom; S_s is the sample standard deviation of replicate spiked sample analyses (mg/L).

The MDL was calculated according to the EPA method[30] as $0.18\ mg/L$, with a relative standard deviation of 26.6%.. The concentration of nitrate spiked into the sample was $0.25\ mg/L$ with a salt concentration of $35{,}000\ mg/L$ and 8 such replicates were measured which provided a standard deviation of $0.060\ mg/L$. The Student's t-value used was 2.998.

Verification of accuracy of Hanna Instrument checker by comparing with Ion Chromatograph (IC): Ultrapure water samples were spiked with known concentrations of nitrate and were analyzed by IC as well as the Hanna Instrument checker. However, the linear range of the IC was

limited to $0.16\ mg/L - 2.5\ mg/L$, resulting in a limited range for comparison of the detection methods. A plot representing the data collected using Hanna Instrument as well as IC is shown in Figure 3-8. The accuracy of the data is portrayed by comparison against a 1:1 regression line.

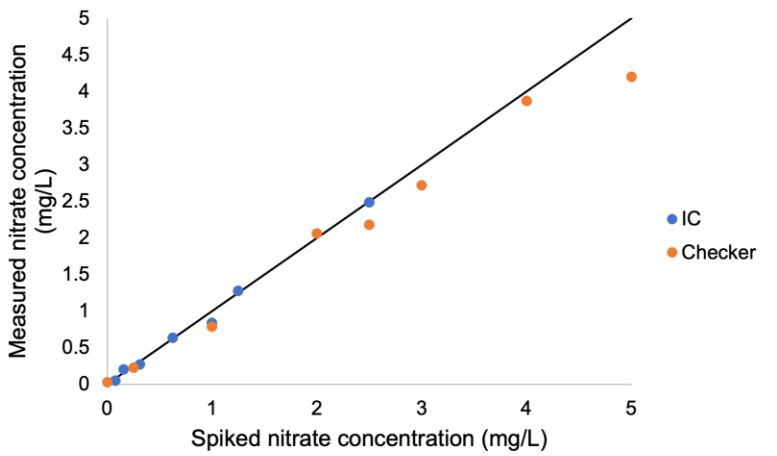

Figure 3-8: Representation of the accuracy of data collected by Hanna Instrument checker and IC against the solid black line which is a 1:1 relationship between the measured and spiked nitrate concentrations. Slope of checker nitrate data = 0.88 ± 0.11 and slope of IC nitrate data = 0.99 ± 0.09.

Application of the Developed Method to Freshwater Samples

The method using the Hanna Instrument checker was employed for the detection of nitrate concentrations in six freshwater locations. The measured nitrate concentrations of the freshwater samples are presented in Table 3-3. UV_{254nm} absorbance was measured to assess the presence of naturally occurring organic matter (NOM) and general water quality (see Table 3-3). A standard curve using the Hawk Island Pond sample was prepared by spike additions and analyzed using the Hanna Instrument checker. The resulting standard curve is shown in Figure 3-9. The freshwater matrix did not affect the linearity of the standard curve as demonstrated by the regression value R^2 of 0.99. However, a higher relative standard deviation was observed for samples with high NOM, thus affecting the precision of the modified method with the Hanna Instrument checker. The influence of NOM on precision would also be a problem with seawater

samples. As a result, further studies should be conducted to determine an approach to eliminating the influence of NOM. The accuracy of the method developed when compared against the IC was confirmed as the data points were located close to the linear regression line for most concentrations.

Table 3-3: Nitrate data for the freshwater samples collected by the co-author in Lansing and Meridian Charter Township region in mid-Michigan.

Location	**Nitrate measurement**			**pH**	**Conductivity of sample at the collection point ($\mu S/cm$)**	**Temperature of the sample at the collection point ($^{\circ}C$)**	**UV_{254} (A/cm)**
	Mean (mg/L)	Standard deviation	Relative Standard Deviation				
Cornell woods retention pond	0.31	0.05	16%	7.98	170	8.7	0.219
Nemoke Trail Drain	0.30	0.15	51%	7.84	609	8	0.861
Hawk Island Pond	0.08	0.05	59%	8.42	470	11.7	0.104
Lake Lansing South dock	0.47	0.05	11%	8.45	328	7.7	0.148
Tacoma Hills Lagoon	4.29	0.95	22%	8.55	610	12.5	0.158
Powell Road wetland	0.06	0.04	66%	7.78	525	12.6	0.416

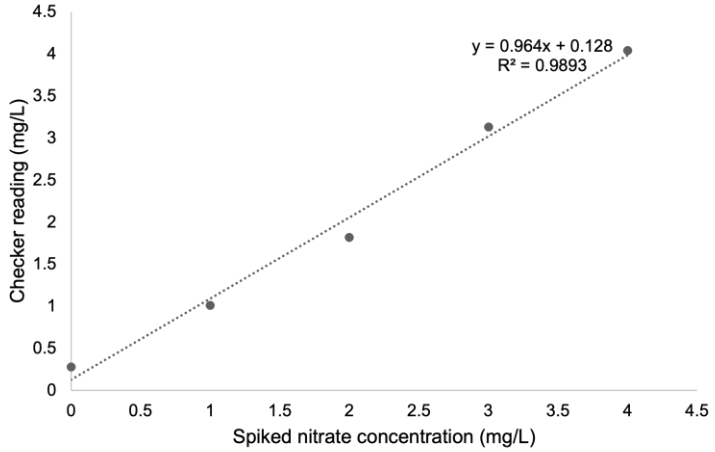

Figure 3-9: Standard curve using Hawk Island Pond sample. Instant Ocean saltwater mix was added to samples at a concentration of 35,000 mg/L before analysis.

The Hanna Instrument checker has the following advantages over IC:

a) the linear range of detection is greater for the checker as compared to the IC instrument that was used, hence eliminating the need for dilution of samples to fall into a limited detection range;

b) accurate nitrate measurements from environmental samples were possible using the checker, however, the IC produced peaks of all the major anions present in the sample, resulting in peak overlap, which ultimately affected the accuracy of the nitrate measurements;

c) nitrate measurements can be easily performed in the field using the checker with the only modification of adding the appropriate mass of Instant Ocean® in the sample bottles before collecting samples to achieve a background salt concentration of $35{,}000\ mg/L$.

d) the checker instrument is low-cost as it does not require high maintenance costs that are associated with the IC.

Use of the Developed Method by Students

The nitrate data obtained by the students for the samples collected are summarized in Figure 3-10. There was a total of 12 groups of students who reported data, six for each set of locations.

While the students analyzing the Lake Lansing samples were able to achieve reproducible results, that was not the case for the groups analyzing the Tacoma Hill Lagoon samples. The reason for this is unclear as there were no apparent differences in their data for pH and temperature. The UV-254 absorbance for the Tacoma Hills Lagoon sample was 0.158 vs that of Lake Lansing was 0.148, suggesting similar organic matter contents in the samples. However, it should be noted that one team obtained values much lower than the other five teams evaluating Tacoma Hill Lagoon water. The mean, standard deviation, and relative standard deviation of the replicate samples measured by individual groups are represented in Table 3-6.

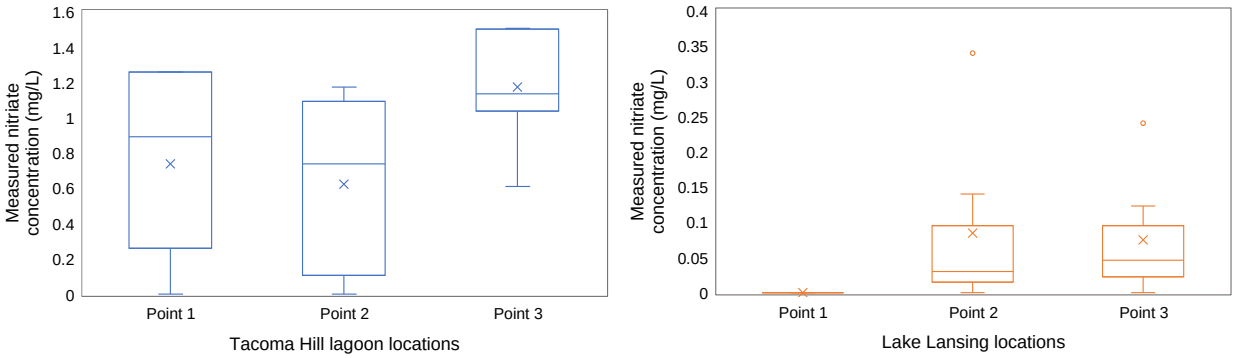

Figure 3-10: Summary of nitrate data collected by students using the Hanna Instrument checker for the 2 locations - Tacoma Hills lagoon and Lake Lansing at different points in the water body. The “x” represents the mean value of the data set and the line within the box indicates the median value of the dataset.

ASSESSMENT OF LEARNING OUTCOMES

Analytic rubrics were developed by the departmental undergraduate curriculum committee and the ABET program coordinator and used for assessment in both civil and environmental engineering programs. A rubric was created for each of the ABET Student Outcomes and used to provide feedback about the strengths and weaknesses of student performance. Elements were chosen to align with the ABET student outcomes. Sub-elements were selected to align with the performance criteria specific to the learning objectives of each of the assignments to be assessed. The scales were determined to align with conventional grading practices (A=4.0 B=3.0 (3.25 or

80%), C=2.0 (2.8 or 70%), D=1.0 (2.4 or 60%) and E=0.0 (0%). A score of E was typically reserved for complete failure to address the sub-element. The weightings were chosen by the individual instructor to reflect their sense of the relative importance of each sub-element. Guidance on the achievement designations was provided. A score of A corresponds to "Exceeds expectations", B and C to "Meets Expectations", D to "Needs Improvement", and E to "Did not meet criteria". This approach allowed instructors to use the rubrics for both ABET assessment and grading and aimed to ensure consistency across courses.

Mastery of ABET Student Outcome 6 ("an ability to develop and conduct appropriate experimentation, analyze and interpret data, and use engineering judgment to draw conclusions") was assessed using this laboratory assignment using the rubric that is provided in Table 3-7. The elements used were *Operates Equipment and Executes Experiment*, *Analyzes Data*, *Interprets Data*, and *Uses Engineering Judgment to Draw Conclusions*. The first part of the Student Outcome, "*Designs appropriate experimentation*" was not assessed in this laboratory exercise. For the most part, equal weighting was assigned to each of the sub-elements. The team scores for each of the elements are presented graphically in Figure 3-11. Not surprisingly, the level of attainment of the elements was greater for the first two elements, which simply required students to follow the instructions provided. The mean scores on the last two elements, both of which required a higher level of thinking, were 3.5±0.5 (CoV (coefficient of variance) of 15%) and 3.7±0.3 (CoV of 9%). The scores of 86.7% of the student teams met or exceeded expectations for the element, *Interprets Results*. The scores of 100% of the student teams met or exceeded the other three elements, demonstrating that the learning outcomes were met.

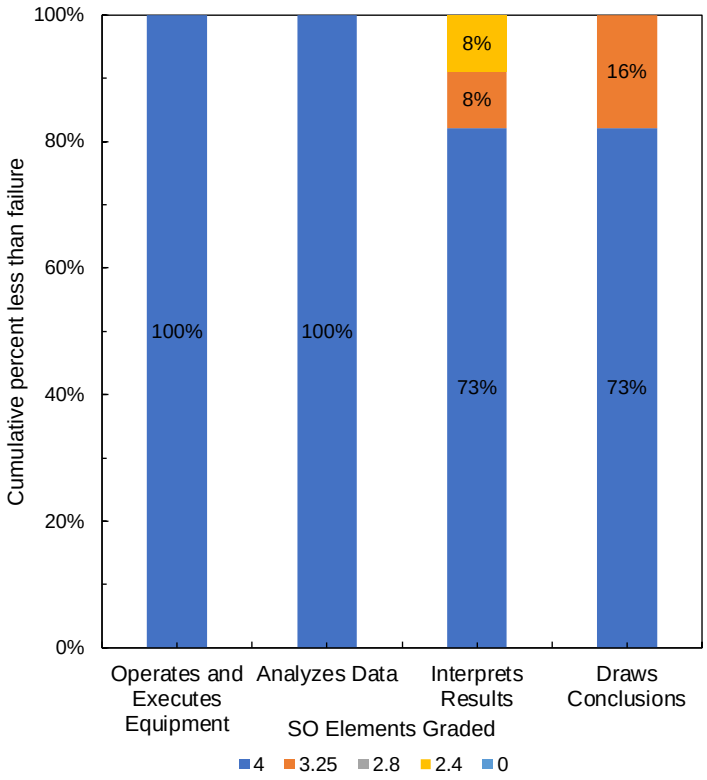

Figure 3-11: Frequency Plot demonstrating the results from the rubric assessment.

ASSESSMENT OF STUDENT ENGAGEMENT

Student engagement was assessed by asking the students to reflect upon (1) their mastery of the course learning objectives and (2) the questions (a) what type of course assignments were the most thought-provoking/educational for you and (b) how did you grow as an environmental engineering student during this course? The survey asking students to reflect on the course learning objectives was conducted in the last week of the semester by the departmental curriculum committee and results were not available to the instructor until after grades were submitted. The reflective questions were administered in the last week of the semester as part of the course and as with all other participation questions, full credit was given irrespective of the answer.

The course was taught with an online/remote lecture on Mondays during which time the instructor presented the laboratory experiment along with background information. Students were then expected to review the material along with pre-recorded videos demonstrating the use of the equipment needed for the associated laboratory exercise. Attendance at the online lectures typically exceeded 90% of those enrolled. Lectures were recorded so students could return to watch the videos if desired. Laboratory exercises were conducted in groups of two to three and designed to ensure that each student participated in hands-on activities.

As shown in Table 3-4, the students who responded (n=11 of 37) uniformly ranked their mastery of the learning outcomes as high (on a 4-point scale). No student ranked their mastery at less than a 3 (B-level). Not surprisingly, the lowest rankings were for those activities that involved synthesis and analysis of the data generated.

All but five students responded to the self-reflection in the last of the weekly participation questions. The responses were uniformly positive, and several students commented that they became more interested in environmental engineering as a result of the course. One student commented that what they "loved about this class is that unlike labs where we were to just follow a recipe, in this class we actually had to think through the procedure and had to use our own judgment, which I feel is very important". Another student commented that they "had never gone to a lab where we were expected to know so much background information to conduct the lab, which I actually very much enjoyed and felt was extremely beneficial".

Table 3-4: Self-assessment of Course Learning Objectives.

Course Learning objectives	**Mean**	**Std Dev.**
Explain and demonstrate the use of safe laboratory practices	3.82	0.40
Explain and implement basic laboratory techniques used in environmental engineering	4	0
Be able to prepare sampling plans for air, surface water, groundwater, and soils characterization, remediation, and post-remediation monitoring of site-specific environmental projects	3.91	0.30
Be able to assess status and trends for critical environmental parameters and indicators using monitoring techniques and data sets	3.73	0.47
Be able to assess compliance with relevant federal, state, and local regulations using statistically valid sampling data.	3.91	0.30
Be able to communicate data effectively to a range of audiences	4	0
Be able to develop and conduct appropriate experimentation given a set of goals and objectives	4	0
Be able to analyze and interpret data and use engineering judgment to make appropriate recommendations	4	0

CONCLUSION

There is a pressing need to educate students on the harmful consequences of climate change. Harmful algae blooms (HABs) in lakes, rivers, and other drinking water sources are caused by the presence of excess nutrients and are only fostered by the increase in water temperatures, one of the many effects of climate change. The development of questions by the students, student-lead research, application of laboratory tools to real-world problems, and critical thinking skills are all elements of an inquiry-based laboratory. Hence, the monitoring of nitrates, an important factor in detecting water pollution, must not only be accessible to students but should be incorporated into an inquiry-based teaching laboratory that would enhance the ability of students to understand the problem and act on it.

Through this study, we were able to develop a method that can be easily executed by students in an inquiry-based teaching laboratory. The successful fulfillment of learning outcomes also depicts the ability of students to apply this data to discuss one of the consequences of climate change and make decisions about mitigating pollution that directly affects public health in a community.

In addition, the method was employed on freshwater samples to measure nitrate concentrations, and the standard curve prepared using the collected freshwater sample further confirmed the suitability of using this method for measuring nitrate concentrations in freshwater samples.

REFERENCES

ABET. (2022). Criterion 3: Student Outcomes - #6. https://www.abet.org/wp-content/uploads/2021/02/E001-21-22-EAC-Criteria.pdf

Alahi, M. E. E., & Mukhopadhyay, S. C. (2018). Detection methods of nitrate in water: A review. Sensors and Actuators, A: Physical, 280, 210–221. https://doi.org/10.1016/j.sna.2018.07.026

Armstrong, P. (2010). Bloom's Taxonomy. Vanderbuilt University Center for Teaching. https://cft.vanderbilt.edu/guides-sub-pages/blooms-taxonomy/

Beck, C., Butler, A., & Silva, K. B. da. (2014). Promoting Inquiry-Based Teaching in Laboratory Courses: Are we Meeting the Grade? CBE-Life Sciences Education, 13, 444–452.

Briggs, J., McGoff, E., Ewald, N., Williams, P., Dunn, F., & Nicolet, P. (2016). Clean Water for Wildlife Technical Manual: Evaluating PackTest nitrate and phosphate test kits to find clean water and assess the extent of nutrient pollution. Freshwater Habit Trust. https://freshwaterhabitats.org.uk/wp-content/uploads/2015/10/CWfWTechnicalDocumentFINAL.pdf

Charbaji, A., Heidari-Bafroui, H., Rahmani, N., Anagnostopoulos, C., & Faghri, M. (2021). Colorimetric determination of nitrate after reduction to nitrite in a Paper-based Dip Strip. Chemistry Proceedings, 5(9). https://doi.org/https://doi.org/10.3390/CSAC2021-10459

Cheng, Y., Yang, R. M. H., Alejandro, F. M., Li, F., Balavandy, S. K., Wang, L., Breadmore, M., Doyle, R., & Naidu, R. (2021). Current applications of colourimetric microfluidic devices (smart phone based) for soil nutrient determination. Smartphone-Based Detection Devices, 103–128. https://doi.org/10.1016/b978-0-12-823696-3.00010-6

Christian, S. J., Hershock, C., & Melville, M. C. (2019). Guided inquiry-based lab activities improve students' recall and application of material properties compared to structured inquiry. ASEE Annual Conference and Exposition, Conference Proceedings. https://doi.org/10.18260/1-2--32881

Cremona, F., Öglü, B., McCarthy, M. J., Newell, S. E., Nõges, P., & Nõges, T. (2021). Nitrate as a predictor of cyanobacteria biomass in eutrophic lakes in a climate change context. Science of the Total Environment, xxxx, 151807. https://doi.org/10.1016/j.scitotenv.2021.151807

Downing, J. A., Watson, S. B., & McCauley, E. (2011). Predicting Cyanobacteria dominance in lakes. Canadian Journal of Fisheries and Aquatic Sciences, 58(10), 1905–1908. https://doi.org/10.1139/f01-143

Ellis, P. S., Shabani, A. M. H., Gentle, B. S., & McKelvie, I. D. (2011). Field measurement of nitrate in marine and estuarine waters with a flow analysis system utilizing on-line zinc reduction. Talanta, 84(1), 98–103. https://doi.org/10.1016/j.talanta.2010.12.028

Flora, J. R. V., & Cooper, A. T. (2005). Incorporating inquiry-based laboratory experiment in undergraduate environmental engineering laboratory. Journal of Professional Issues in Engineering Education and Practice, 131(1), 19–25. https://doi.org/10.1061/(ASCE)1052-3928(2005)131:1(19)

Giovannoni, G., Land, J. M., Keir, G., Thompson, E. J., & Heales, S. J. R. (1997). Adaptation of the nitrate reductase and Griess reaction methods for the measurement of serum nitrate plus nitrite levels. Annals of Clinical Biochemistry, 34, 193–198.

Harold W. Walker. (2014). Chapter 3: Toxin Properties, Toxicity, and Health Effects. In Harmful Algae Blooms in Drinking Water: Removal of Cyanobacterial Cells and Toxins: Vol. 1st Edition (pp. 27–46).

Holder, E., Conmy, R., & Venosa, A. (2015). Comparative Laboratory-Scale Testing of Dispersant Effectiveness of 23 Crude Oils Using Four Different Testing Protocols*. Journal of Environmental Protection, 06, 628–639. https://doi.org/10.4236/jep.2015.66057

https://www.hannainst.com/marine-nitrate-checker-hi781.html. (2022, August 24).

Hwang, H., Kim, Y., Cho, J., Lee, J. Y., Choi, M. S., & Cho, Y. K. (2013). Lab-on-a-disc for simultaneous determination of nutrients in water. Analytical Chemistry, 85(5), 2954–2960. https://doi.org/10.1021/ac3036734

KESTER, D. R., DUEDALL, I. W., CONNORS, D. N., & PYTKOWICZ, R. M. (1967). Preparation of artificial seawater. Limnology and Oceanography, 12(1), 176–179. https://doi.org/10.4319/lo.1967.12.1.0176

Lewis, W. M., Wurtsbaugh, W. A., & Paerl, H. W. (2011). Rationale for control of anthropogenic nitrogen and phosphorus to reduce eutrophication of inland waters. Environmental Science and Technology, 45(24), 10300–10305. https://doi.org/10.1021/es202401p

Madhuri, G. V., Kantamreddi, V. S. S. N., & Prakash Goteti, L. N. S. (2012). Promoting higher order thinking skills using inquiry-based learning. European Journal of Engineering Education, 37(2), 117–123. https://doi.org/10.1080/03043797.2012.661701

Moorcroft, M. J., Davis, J., & Compton, R. G. (2001). Detection and determination of nitrate and nitrite: A Review. Talanta, 54, 785–803.

Murray, E., Nesterenko, E. P., McCaul, M., Morrin, A., Diamond, D., & Moore, B. (2017). A colorimetric method for use within portable test kits for nitrate determination in various water matrices. Analytical Methods, 9(4), 680–687. https://doi.org/10.1039/c6ay03190k

Myers, M. J., & Burgess, A. B. (2003). Inquiry-based Laboratory course Improves Students' Ability to Design Experiments and Interpret data. Advances in Physiology Educated, 27, 26–33.

Patton, C. J., & Kryskalla, J. R. (2011). Chapter 8: Colorimetric Determination of Nitrate Plus Nitrite in Water by Enzymatic Reduction , Automated Discrete Analyzer Methods. In U.S.

Geological Survey Techniques and Methods, Book 5 (pp. 1–34). https://pubs.usgs.gov/tm/05b08/contents/TM5-B8.pdf

Sargazi, M., & Kaykhaii, M. (2020). Application of a smartphone based spectrophotometer for rapid in-field determination of nitrite and chlorine in environmental water samples. Spectrochimica Acta - Part A: Molecular and Biomolecular Spectroscopy, 227, 117672. https://doi.org/10.1016/j.saa.2019.117672

Shinn, M. B. (1941). Colorimetric Method for Determination of Nitrite. Industrial and Engineering Chemistry - Analytical Edition, 13(1), 33–35. https://doi.org/10.1021/i560089a010

Singh, P., Singh, M. K., Beg, Y. R., & Nishad, G. R. (2019). A review on spectroscopic methods for determination of nitrite and nitrate in environmental samples. Talanta, 191(August 2018), 364–381. https://doi.org/10.1016/j.talanta.2018.08.028

Slough, G., & Wang, Z. (2010). Griess Diazotization. In Comprehensive Organic Name Reactions and reagents. Wiley.

Smith, V. H. (1982). The nitrogen and phosphorus dependence of algal biomass in lakes: An empirical and theoretical analysis. Limnology and Oceanography, 27(6), 1101–1111. https://doi.org/10.4319/lo.1982.27.6.1101

Tsikas, D. (2007). Analysis of nitrite and nitrate in biological fluids by assays based on the Griess reaction: Appraisal of the Griess reaction in the L-arginine/nitric oxide area of research. Journal of Chromatography B: Analytical Technologies in the Biomedical and Life Sciences, 851, 51–70. https://doi.org/10.1016/j.jchromb.2006.07.054

U.S. EPA. (2016). Definition and procedure for the determination of the method detection limit—Revision 2. In EPA 821-R-16-006. https://www.epa.gov/sites/default/files/2016-12/documents/mdl-procedure_rev2_12-13-2016.pdf

APPENDIX

Figures

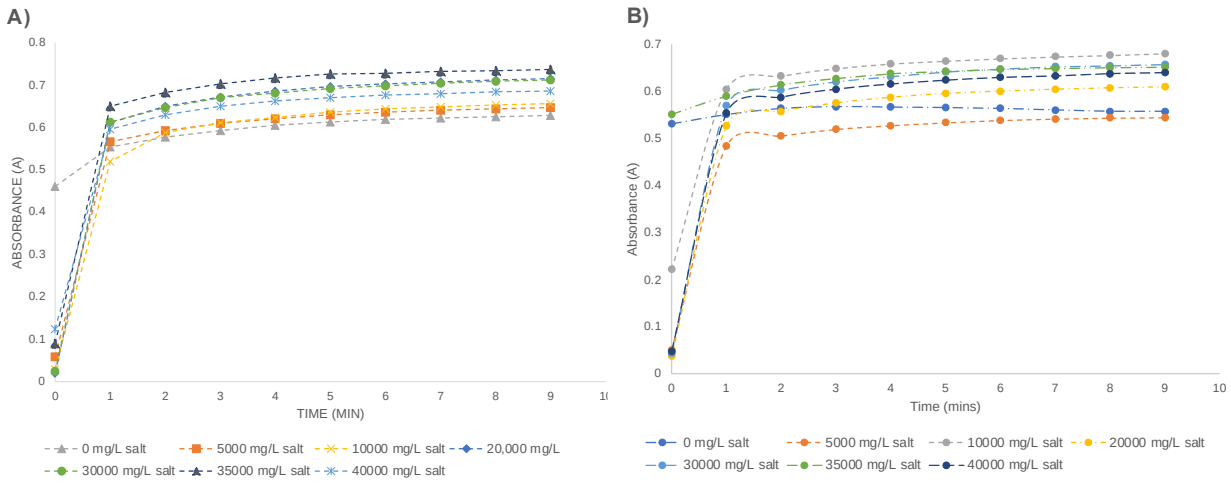

Figure 3-12: Kinetic profile of absorbance measured per 1 minute time interval after complete mixing of last reagent until the absorbance was stabilized A) Salt used was Instant Ocean®; B) salt used was sodium chloride; concentration of nitrate was 2.5 mg/L in all samples.

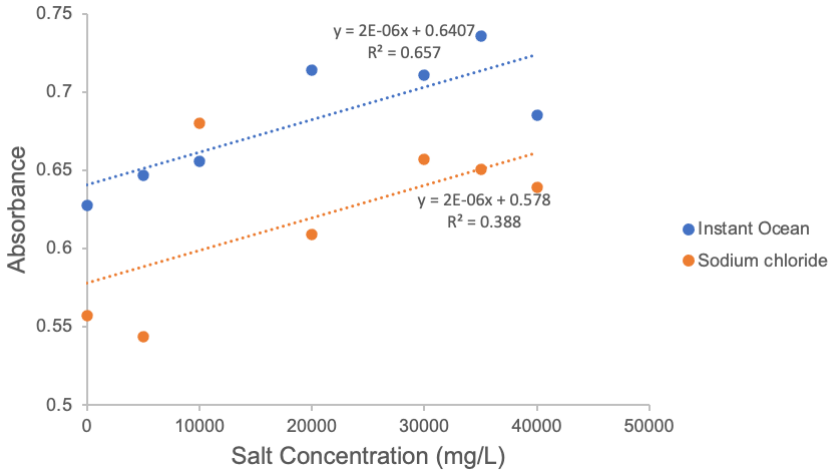

Figure 3-13: Comparison of the absorbance measured at 543 nm after 9 minutes with the increase in salt concentrations of Instant Ocean and Sodium chloride, both containing nitrate at a concentration of 2.5 mg/L.

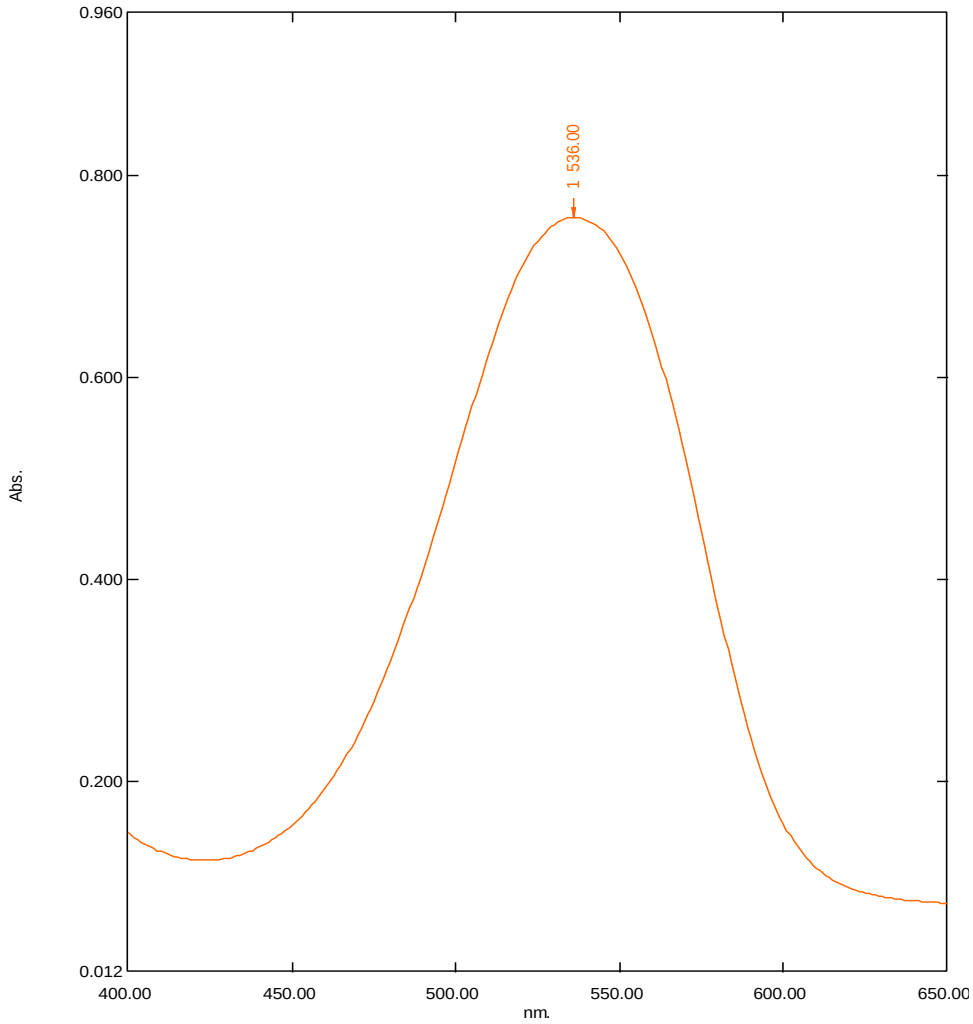

Figure 3-14: Absorption spectrum of pink-violet azo dye generated after following the stepwise procedure provided in the Hanna Instrument Low Range Marine Nitrate checker kit. Nitrate concentration = 2.5 mg/L and Instant Ocean concentration = 35,000 mg/L.

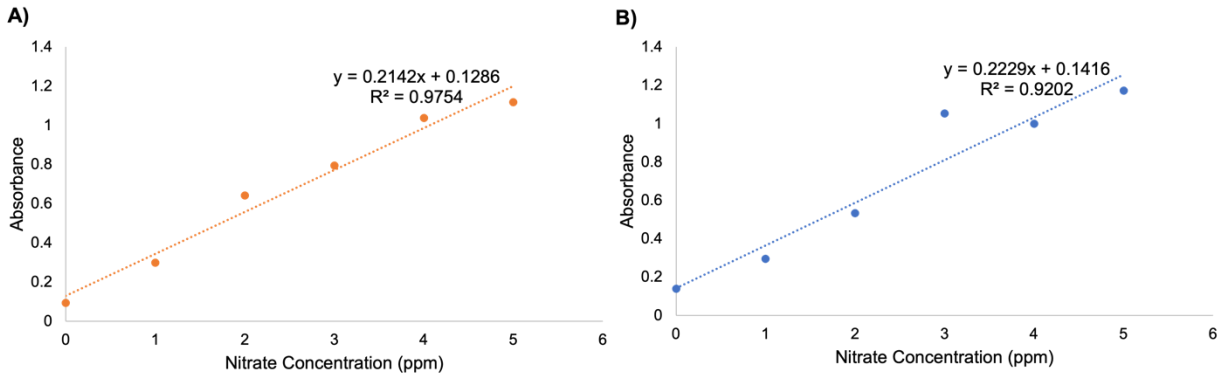

Figure 3-15: Standard curves using absorbance measurement vs nitrate concentrations for A) Instant Ocean and B) Sodium chloride.

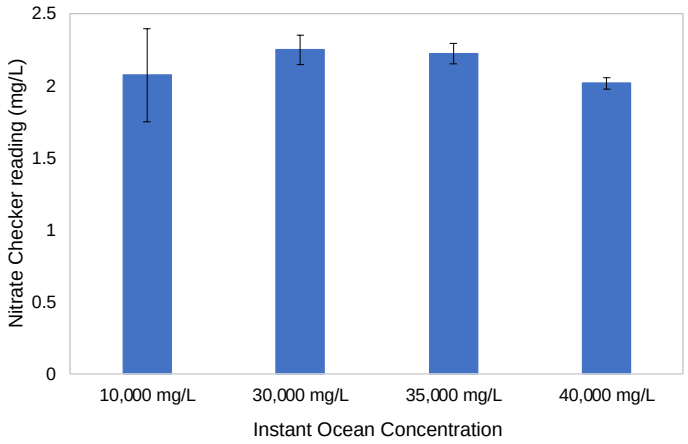

Figure 3-16: Bar chart representing mean of replicate samples ($n = 3$) spiked with nitrate at a concentration of 2.5 mg/L with different Instant Ocean® concentrations. The standard deviation is shown using error bars.

Tables

Table 3-5: Comparison of the slopes of standard curve obtained by using Instant Ocean® and sodium chloride at 95% confidence interval.

Salt	**Mean slope**	**Standard deviation**
Instant Ocean	0.878	0.160
Sodium Chloride	0.911	0.364

Table 3-6: Mean and standard deviation data of the samples that were measured in triplicate by different groups of students.

Location	**Group #**	**Sub-location**	**Mean concentration (mg/L)**	**Standard deviation**	**Relative Standard Deviation**	**Temperature (℃)**	**pH**	**Conductivity ($\mu S/cm$)**
Tacoma Hills Lagoon	1	Point 1	0.74	0.195	26%	21.2	7.82	564
	2	Point 2	1.177	0.362	31%	21.2	8.1	790
	3	Point 3	1.51	0.135	9%	21.6	7.89	575
	4	Point 3	1.083	0.015	1%	19.4	8.6	563
	5	Point 2	1.06	0.02	2%	21.3	8.6	257
	6	Point 2	0.147	0.189	129%	21.1	8.51	658
Lake Lansing	1	Point 3	0.047	0.042	89%	20	8.76	330
	2	Point 3	0.023	0.032	138%	20	8.8	471
	3	Point 3	0.067	0.115	173%	19.8	8.58	331
	4	Point 3	0.123	0.110	89%	20.3	8.69	394
	5	Point 3	0.24	0.157	65%	19.7	8.28	338
	6	Point 1	0	0	0%	20.3	8.68	323

Table 3-7: Rubric that was used to assess mastery of ABET Student Outcome 6 during this laboratory assignment.

	E	D	C	B	A	Weighting	Score
OPERATES EQUIPMENT AND EXECUTES EXPERIMENT							
Operates equipment and conducts experiment safely						1.5	
Follows design of experimental plan						1.5	
Uses data and sufficient replication as required						1	
Documents data as required						1.5	
Uses appropriate methods to collect data						1	
ANALYZES DATA							
Data reported in appropriate tabular and graphical form, including a map						1.5	
Statistical analysis performed as required, including determination of 95% CI of replicate samples						1.5	
INTERPRETS DATA							
Discussion of sampling plan						1.5	
Discussion of trophic level of water						1.5	
Discussion of potential sources of nutrients, including land use patterns						1.5	
Discussion of potential mitigation strategies						1.5	
Discussion of spatial variability of results and recommendations regarding more accurately and precisely assessing the trophic level						1.5	
USES JUDGMENT TO DRAW CONCLUSIONS							
Uses the data analysis as the basis for thoughtful judgments						1.5	
Draws correct conclusions from the analysis						1.5	

CHAPTER 4 : Development Of A Screening Technique For The Production Of Radicals During Persulfate/Peroxide Oxidation Activated By Ferrous Ions Using Methylene Blue

ABSTRACT

Oxidation by metal activated persulfate and peroxide produces sulfate radicals ($SO_4^{\bullet -}$) and hydroxyl radicals ($^{\bullet}OH$), powerful oxidants that can be used for the destruction of a wide range of pollutants in water and wastewater. In this study, methylene blue dye was used as an indicator to determine the reaction kinetics and identify the radicals produced during oxidation by persulfate, which was added in the form of monopersulfate, and peroxide in the presence of ferrous ions. There was a positive linear relation between the monopersulfate concentration and the degradation of methylene blue in the absence of ferrous ions at pH 3, 5, and 7. In the absence of ferrous ions, peroxide had little to no effect on the degradation of methylene blue. Fe^{2+}/monopersulfate and Fe^{2+}/peroxide systems at a ratio of 0.5:1 resulted in the rapid degradation (< 20 mins) of methylene blue. Humic acid, at a concentration as high as $20\ mg/L$, did not affect the degradation kinetics in both systems. Bicarbonate inhibited the Fe^{2+}/peroxide reaction; however, in the Fe^{2+}/monopersulfate system, the scavenging effect of bicarbonate was inhibited at higher concentrations, i.e., $< 100\ mM$. The dominant radical species in Fe^{2+}/monopersulfate system was identified as the $SO_4^{\bullet -}$ using ethanol and *tert*-butyl alcohol as probes. This screening method was validated by employing the same oxidation conditions for the degradation of microcystin-LR. Similar reaction kinetics were observed between microcystin-LR and monopersulfate. Fe^{2+}/monopersulfate and Fe^{2+}/peroxide reactions resulted in the rapid degradation of microcystin-LR. Humic acid and bicarbonate had a similar effect on the microcystin-LR degradation. $SO_4^{\bullet -}$ was again identified as the dominant radical species in degradation of microcystin-LR in the Fe^{2+}/monopersulfate system.

INTRODUCTION

Hydroxyl radicals (•OH), with a standard reduction potential of $2.80\ V$ (Oh, Dong, and Lim 2016), and sulfate radicals ($SO_4^{\bullet -}$), with a standard reduction potential of $2.60\ V$ (Oh, Dong, and Lim 2016), are strong oxidants that are capable of oxidizing a wide range of organic compounds, which makes them very useful in water and wastewater treatment (Guerra-Rodríguez et al. 2018; Rivas 2022; Xia et al. 2020; Amor et al. 2021; Deng and Zhao 2015). The use of •OH for the removal of contaminants in water treatment has been studied extensively. Processes that generate •OH include the Fenton process as described in equations 4.1 – 4.6 (Anipsitakis & Dionysiou, 2004; Song et al., 2019), ozone/peroxide, UV/ozone, UV/peroxide (Deng and Zhao 2015; Glaze, Kang, and Chapin 1987; Andreozzi et al. 1999).

$$Fe^{2+} + H_2O_2 \rightarrow Fe^{3+} + {}^{\bullet}OH + HO^- \quad (4.1)$$

$$Fe^{3+} + H_2O_2 \rightarrow Fe^{2+} + {}^{\bullet}HO_2 + H^+ \quad (4.2)$$

$$H_2O_2 + {}^{\bullet}OH \rightarrow H_2O + {}^{\bullet}HO_2 \quad (4.3)$$

$${}^{\bullet}HO_2 \rightarrow O_2^{\bullet -} + H^+ \quad (4.4)$$

$$Fe^{2+} + {}^{\bullet}HO_2 + H^+ \rightarrow Fe^{3+} + H_2O_2 \quad (4.5)$$

$$Fe^{2+} + {}^{\bullet}OH \rightarrow Fe^{3+} + HO^- \quad (4.6)$$

Similarly, as peroxide is predominantly used in hydroxy radical-based AOPs, either monopersulfate (HSO_5^-) or persulfate ($S_2O_8^{2-}$) is activated for the production of $SO_4^{\bullet -}$. Physical (e.g., thermal activation, UV, or ultrasound) or chemical (e.g., use of transition metal ions, alkaline activation, or use of carbon-based materials) methods are used to activate HSO_5^- and $S_2O_8^{2-}$ to produce $SO_4^{\bullet -}$ (Xia et al. 2020). The activation of HSO_5^- by ferrous ions for the generation of $SO_4^{\bullet -}$ is shown in equation 4.7 (Rastogi, Al-Abed, and Dionysiou 2009). Equations 4.8 – 4.12 are other side reactions that occur in the system (Ghanbari and Moradi 2017).

$$Fe^{2+} + HSO_5^- \rightarrow Fe^{3+} + SO_4^{\bullet -} + OH^- \quad (4.7)$$

$$Fe^{3+} + HSO_5^- \rightarrow Fe^{2+} + SO_5^{\bullet -} + H^+ \quad (4.8)$$

$$Fe^{2+} + SO_4^{\bullet -} \rightarrow Fe^{3+} + SO_4^{2-} \quad (4.9)$$

$$HSO_5^- + SO_4^{\bullet -} \rightarrow SO_4^{2-} + SO_5^{\bullet -} + H^+ \quad (4.10)$$

$$HSO_5^- + H_2O \rightarrow SO_4^{2-} + 2^{\bullet}OH + H^+ \quad (4.11)$$

$$SO_5^{\bullet -} + 2H_2O \rightarrow SO_4^{2-} + 3^{\bullet}OH + H^+ \quad (4.12)$$

The detection of $^{\bullet}$OH and $SO_4^{\bullet -}$ is critical to understanding the kinetics and mechanisms of these reactions. Electron spin resonance (ESR), later developed to electron paramagnetic resonance (EPR), is commonly used for quantifying the formation of $^{\bullet}$OH and $SO_4^{\bullet -}$ (Burgos Castillo Rutely et al. 2018; Cashman et al. 2019). However, this method is expensive, requires specialized equipment, and is labour intensive. Where $^{\bullet}$OH and $SO_4^{\bullet -}$ can co-exist, such as with sulfate-based advanced oxidation processes, this method is not capable of directly identifying the dominant reactive species that degrades the analyte (Wang and Wang 2020). Gas chromatography (GC) and high-performance liquid chromatography (HPLC) can also be used to detect radicals but require the use of chemical probes, such as benzoic acid, 1-propanol, atrazine, and nitrobenzene (Yang et al. 2015; Lindsey and Tarr 2000; Liang and Su 2009). These probe compounds are specific to the reaction in question (Wang and Wang 2020) and their measurement requires specific and expensive analytical equipment, along with operator skill. Qualitative methods such as colorimetric tests using reagent dyes (e.g., aniline and benzidine) were one of the early methods employed for the detection of persulfate (Clark and Tso 1949). The decolourization of Alcian blue in a buffered solution turned the qualitative method into a quantitative analysis for determination of persulfate (E. Villegas, Y. Pomeranz, and J. A. Shellenberger 1963). Other quantitative methods used for the determination of persulfate include

reductometric methods such as iodometric and ferrometric methods (Kolthoff and Carr 1953), polarographic methods (Amin 1981; I. M. Kolthoff and R. Woods 1966), and spectrophotometric methods (Paul M Shiundu, Adrian P. Wade, and Jonnalagadda 1990). A modification of the iodometric titration method (Kolthoff and Stenger 1947) was used for the spectrophotometric determination of persulfate, which was quantified through the absorbance change of iodine generated from the reaction of persulfate and potassium iodide in the presence of sodium bicarbonate (Liang et al. 2008). To overcome the complexity and time-consuming nature of the above methods, an alternate method using the decolorization of azo dyes (i.e., rhodamine B, methylene blue, methyl violet, and orange II) was developed for the determination of persulfate (Ding et al. 2011). The decolorization of the dyes was found to be linear in relation to the concentration of persulfate. While Ding et al. (2011) used Fe^{2+} to activate the persulfate reaction, Zhao et al. (2015) used microwaves for its activation and measured the depletion of the absorbance of methylene blue to quantify the persulfate concentration. Another unique procedure was developed that could qualitatively indicate the presence of $^{\bullet}OH$ through rapid and distinct bleaching of methylene blue on a paper test strip (Satoh, Trosko, and Masten 2007). The described state of literature inspired the current study which uses methylene blue as a screening technique to predict the fate of recalcitrant chemicals in catalytic oxidation reactions using monopersulfate and peroxide, which can be applied to water treatment.

Microcystins are a class of cyanotoxins with more than 80 variants, one of which is microcystin-LR (Figure 4-1). This variant is the most commonly found cyanotoxin and one of the most potent (H W Walker 2014). The provisional lifetime drinking-water guideline is 1 $\mu g/L$ for microcystin-LR (MC-LR) based on the liver toxicity caused by it in humans with long-term

exposure (World Health Organization 2020). These microcystins are produced by numerous species of cyanobacteria, which are found to exist in harmful algal blooms (HABs).

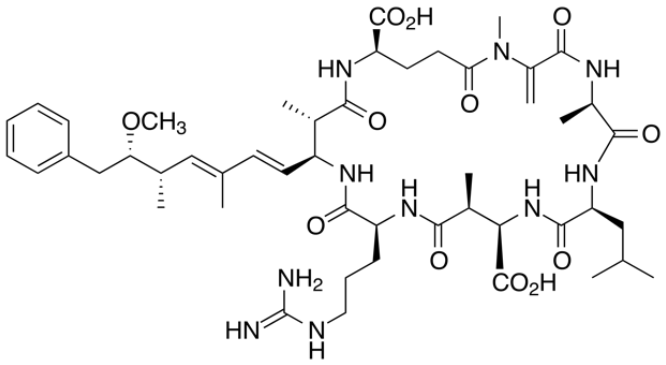

Figure 4-1: Structure of MC-LR.

The formation of HABs in freshwaters is a concern for drinking water treatment plant operators. Although conventional water treatment processes are effective at removing these cyanobacteria, cyanotoxins are challenging to remove using conventional treatment methods (Szlag et al. 2015; Westrick et al. 2010). The cyclic peptide structure of microcystins causes the toxin to be very stable. •OH acts by attacking the conjugated diene bond of the Adda side chain through electrophilic addition followed by oxidation, the benzene ring through electrophilic substitution and further oxidation, and the methoxy groups of the Adda side chain through hydrogen abstraction (W. Song et al. 2009; Y. Liu et al. 2016) resulting in the loss of toxicity of the compound. Hence, several studies have been conducted that employ •OH produced via advanced oxidation processes (AOPs) for the degradation of cyanotoxins (Schneider and Bláha 2020; Jasim et al. 2020; Loganathan 2016; He 2014; al Momani, Smith, and Gamal El-Din 2008). Recently, studies have investigated the degradation of MC-LR by $SO_4^{\bullet -}$ (Maria G. Antoniou, de la Cruz, and Dionysiou 2010; M. G. Antoniou et al. 2018; Maria G. Antoniou, de La Cruz, and Dionysiou 2010; S. Zhou et al. 2018; J. Zhou et al. 2020) due to the higher selectivity of $SO_4^{\bullet -}$ than •OH to react with organic compounds possessing unsaturated bond and aromatic

constituents (Neta et al. 1977). The following were the pathways identified for degradation of MC-LR by $SO_4^{\bullet -}$: (i) multiple hydroxylation of the benzene ring of Adda amino acid, (ii) simultaneous hydroxylation of the aromatic ring and the diene bonds, (iii) oxidative cleavage of the Adda amino acid chain, and (iv) simultaneous oxidation of the unsaturated carbon bonds, i.e., Adda and Mdha (Maria G. Antoniou, de La Cruz, and Dionysiou 2010).

While it is possible to conduct a kinetic study to investigate the production of $^{\bullet}OH$ and $SO_4^{\bullet -}$, which are formed independently of the degradation reaction of cyanotoxins, there exist several limitations that make the process challenging and tedious; (i) cyanotoxin standards are expensive and available in small quantities, (ii) the radicals in samples taken to perform kinetic analysis need to be quenched, (iii) extensive sample preparation needs to be performed before measuring the cyanotoxins, and (iv) the methods used to measure cyanotoxins (e.g., ELISA and LC/MS/MS) are expensive and require skill and expertise.

Given the increased demand for the use of $^{\bullet}OH$ and $SO_4^{\bullet -}$-based processes in water treatment, the development of rapid and low-cost methods that can detect the radical species is necessary. For rapid and reliable identification of radicals governing the reaction, methylene blue was used as the target compound in this study, whose absorbance was measured to evaluate the kinetics of degradation, which was further validated by using MC-LR. The goal of this study is to provide a screening tool using methylene blue which could be applied to catalytic oxidation reactions to predict the degradation of recalcitrant target analytes.

METHODS

Materials & Instrumentation

Oxoneâ, monopersulfate compound ($KHSO_5 \cdot 0.5KHSO_4 \cdot 0.5K_2SO_4$) (CAS# 70693-62-8; Sigma-Aldrich Inc., St. Louis, Missouri, USA) and hydrogen peroxide solution, 50 wt. % in water,

stabilized (CAS# 7722-84-1; Sigma-Aldrich Inc., St. Louis, Missouri, USA) were used as the oxidants in this study. Methylene blue hydrate, ≥ 95% (CAS# 122965-43-9; Sigma-Aldrich Inc., St. Louis, Missouri, USA) was used as a screening agent to determine the kinetics of the reactions. Hydrochloric acid 36.5 – 38.0%, GR ACS (CAS# 7647-01-0; Supelcoâ, Bellefonte, Pennsylvania, USA) was used to regulate the pH of the solution. Ferrous chloride (CAS# 13478-10-9; Avantor Performance Materials, Inc., Center Valley, Pennsylvania, USA) was used as the iron salt and manganese chloride, tetrahydrate, ACS reagent, ≥ 98% (CAS# 13446-34-9; Sigma-Aldrich Inc., St. Louis, Missouri, USA) was used as the manganese salt to provide metal ions serving as the catalyst in the reaction. Sodium bicarbonate (CAS# 144-55-8; Fisher Scientific, Fair Lawn, New Jersey, USA) and Suwannee River humic acid (IHSS) were used as scavengers to investigate their effect on the reaction. Ethanol absolute, 200 proof (CAS#64-17-5) and *tert*-butyl alcohol (TBA), ≥ 99.3% (CAS# 75-65-0; Sigma-Aldrich Inc., St. Louis, Missouri, USA) were used to quench the radicals in the reaction to determine the dominant radical species in the reaction. Sodium thiosulfate pentahydrate (CAS#10102-17-7; Fisher Scientific, Fair Lawn, New Jersey, USA) and phenol (CAS#108-95-2; Mallinckrodt Pharmaceuticals, St. Louis, Missouri, USA) were investigated to quench the oxidation reaction. High-purity deionized water (ultrapure water) with a resistivity of 18 $M\Omega \cdot cm$ was used to prepare stocks and laboratory-fortified blanks.

The absorbance of methylene blue was determined using a Shimadzu (UV-2600) UV-Vis Spectrophotometer using 1.0 cm cuvettes and at a wavelength of 664 nm, the peak absorbance (Figure 4-15). The pH of the solutions was measured using a Thermo Scientificä Orion Starä A211 Benchtop pH Meter. The meter was calibrated using Orion™ pH buffers of 4, 7, and 10 purchased from Thermo Scientific (Waltham, Massachusetts, USA).

MC-LR, $\geq 95\%$ purity (CAS# 101043-37-2; Cayman Chemical Co., Ann Arbor, Michigan, USA) was used as the target compound to verify the kinetics determined using the methylene blue. Abraxisâ microcystins/nodularins (ADDA) enzyme-linked immunosorbent assays (ELISA) kits (part #520011OH), purchased from Eurofins Abraxis Inc. (Warminster, Pennsylvania, USA), were used for detection of MC-LR. The ELx808ä Absorbance plate reader (BioTek Instruments, Inc), equipped with Gen5 Reader control software version 2.09 was used to read absorbance from the ELISA plate for measurement of microcystins. The measured ELISA data were analyzed using GainDataâ (Arigo Biolaboratories, https://www.arigobio.com/elisa-analysis). The stocks of each compound were prepared and stored as follows: (i) $1\ mM$ methylene blue was prepared once at the start of the study and stored at room temperature wrapped in aluminium foil, (ii) $10\ mg/L$ MC-LR was prepared once a week and stored at -20℃, (iii) $100\ mM$ monopersulfate and (iv) $100\ mM$ peroxide were prepared once a week and stored at room temperature, (v) $50\ mM$ ferrous chloride was freshly prepared for each experiment, (vi) $500\ mM$ sodium bicarbonate, and (v) $200\ mg/L$ humic acid were prepared at the start of the study and stored at room temperature. Ethanol, TBA, and phenol were used in their commercially available forms to be added to samples at the required concentrations.

Methylene Blue experiments

The degradation kinetics of methylene blue were determined by measuring the absorbance of methylene blue at different time intervals during its reaction with the oxidants: monopersulfate and hydrogen peroxide, with and without the addition of ferrous salt, bicarbonate, humic acid, ethanol, and TBA. The effect of pH on the degradation of methylene blue was assessed at pH levels of ~3, ~5, and ~7 by the addition of hydrochloric acid. The addition of ferrous chloride further decreased the pH in some experiments but to eliminate any possibility of precipitation or

quenching, no base was added to regulate the pH values. The use of a buffer was avoided to eliminate any possibility of quenching of radical species.

Experiments were conducted in glass vials at room temperature (21 ℃) and the reaction kinetics were determined for each condition in triplicate. The sample volume for each condition was $10\ mL$. To measure absorbance, samples were drawn at specific times and transferred to a 1.0 cm cuvette.

MC-LR experiments

The kinetic results obtained from methylene blue degradation were used as a basis for developing an experimental plan to verify the kinetics for the degradation of MC-LR. Hence, the following conditions were tested to validate the methylene blue screening technique: (i) monopersulfate at low and high concentrations, (ii) ferrous chloride as a catalyst in the oxidation reaction with monopersulfate and peroxide, (iii) presence of humic acid, (iv) presence of bicarbonate, and (v) presence of probe compounds like ethanol and TBA for radical identification.

Unlike methylene blue, MC-LR cannot be detected in real-time and hence, it was crucial to identify a compound that would instantly quench the reaction between MC-LR and the oxidants prior to detection using Abraxis ELISA test kits. Ethanol, phenol, and sodium thiosulfate were compared as quenching agents. The pH was not regulated for these experiments to avoid interferences in reactions as the buffering chemicals can act as radical scavengers. Due to addition of ferrous chloride, the pH was generally around pH 5, except when bicarbonate was added as a scavenger.

A stock of $10\ mg/L$ MC-LR in Milli-Q water was used for preparing standards and samples. Sample volume for MC-LR experiments was 20 mL. 1 mL sample was drawn into a separate,

pre-loaded vial with sodium thiosulfate, at specified times. Only one trial per condition was performed due to limited availability of ELISA test kits. Samples were diluted 20-fold such that the resulting concentration would fall within the detection range of the ELISA test kits. All standards (i.e., $0\ \mu g/L, 0.15\ \mu g/L, 0.4\ \mu g/L, 1\ \mu g/L, 2\ \mu g/L$ and $5\ \mu g/L$) and samples were run in duplicate using the ELISA test.

RESULTS & DISCUSSION

Methylene Blue

Reaction of monopersulfate and peroxide with methylene blue: Prior to addition of the metal catalyst, the reaction between the oxidant (concentrations = $1 mM, 2\ mM, 4\ mM$, and $8\ mM$) and methylene blue (concentration = $0.01\ mM$) was investigated, which showed that the methylene blue degraded in the presence of monopersulfate (Figure 4-2); however, peroxide did not result in any decoloration of methylene blue at pH levels of 2.93 and 5.67 (Figure 4-3), which is consistent with the results obtained by Song et al. (2019) in which negligible degradation ($<$ 2%) of triphenyl phosphate was observed in the presence of peroxide alone.

The reaction of monopersulfate with methylene blue was shown to occur according to first-order kinetics over the range of monopersulfate concentrations used (see Figure 4-16). The rate of the reaction of methylene blue increased linearly with increasing monopersulfate concentration as shown in Figure 4. The reaction rate was greatest at pH 6.72 as compared to that at pH 3.03 and pH 4.86.

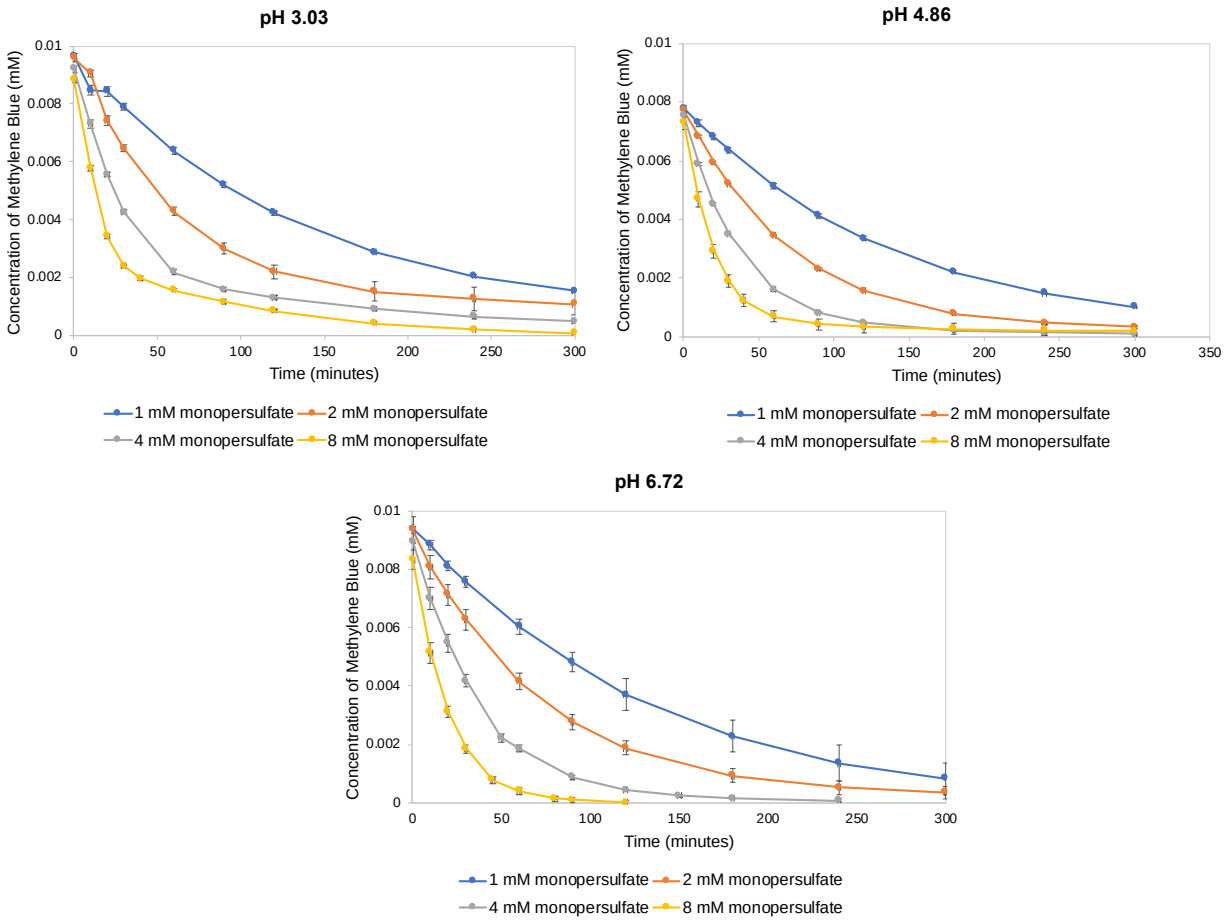

Figure 4-2: Degradation of Methylene blue (0.01 mM) at different pH values in the presence of monopersulfate at concentrations ranging from 1 mM to 8 mM. Error bars represent SD for 3 replicates.

The only possible explanation for the degradation of methylene blue by monopersulfate alone is the production of radical species. Tan et al. (2018) demonstrated that $^{\bullet}OH$ is produced in the monopersulfate system without the presence of any catalyst of activation compound, likely due to the hydrolysis of monopersulfate via reactions 4.13 and 4.14.

$$HSO_5^- + H_2O \rightarrow H_2O_2 + HSO_4^- \quad (4.13)$$

$$H_2O_2 \rightarrow 2^{\bullet}OH \quad (4.14)$$

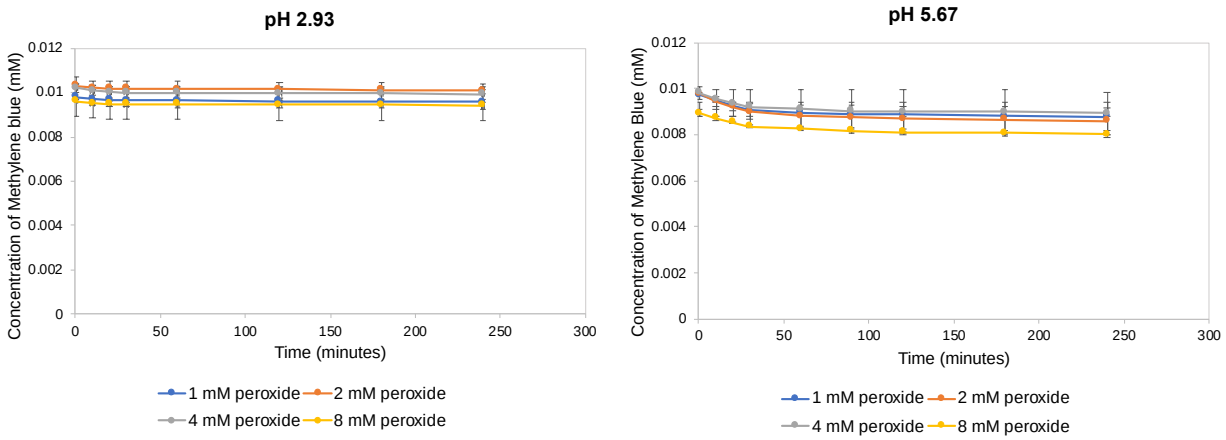

Figure 4-3: The effect of varying peroxide concentrations (1 mM – 8 mM) on the degradation of methylene blue (0.01 mM) at different pH values. Error bars represent SD for 3 replicates.

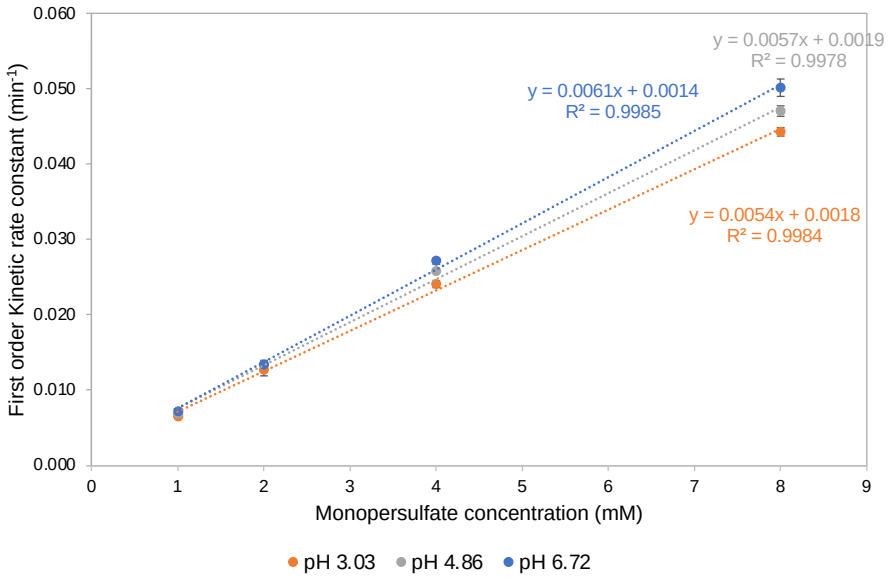

Figure 4-4: The relationship between first order reaction rate constants and monopersulfate concentration for pH 3.03, 4.86, and 6.72. Data points represent the mean and error bars show the standard deviation (n=3).

Fe^{2+}/monopersulfate and Fe^{2+}/peroxide reactions with methylene blue: The effect of a metal catalyst on the degradation of methylene blue was investigated using $MnCl_2 \cdot 4H_2O$ and $FeCl_2$ salts. The reaction kinetics were compared at metal ion to oxidant molar ratios of 1:1 and 0.5:1 (see Figure 4-5). Rapid degradation was observed when iron was used as the metal catalyst. Complete degradation of methylene blue (0.02 mM) occurred within 30 minutes at pH 3 with 0.5

mM $FeCl_2$ and 1 mM monopersulfate. However, when manganese was used as the metal catalyst, only 31% degradation occurred after 60 minutes. Upon increasing the concentrations of manganese chloride and monopersulfate to 4 mM, resulting in a 1:1 ratio, the efficiency of degradation increased to 65% after 60 minutes.

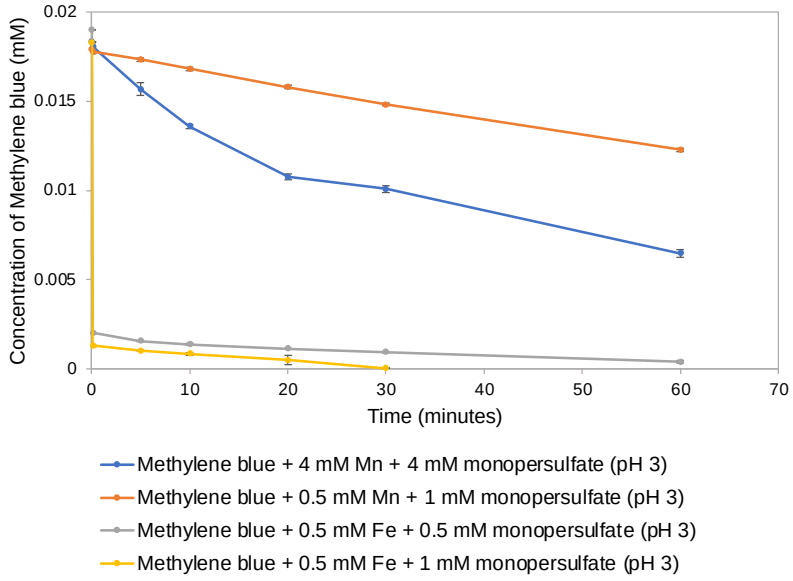

Figure 4-5: Comparison of metal catalysts (Iron and Manganese) for the degradation of methylene blue (0.02 mM) by monopersulfate at pH 3. Data points represent the mean and error bars represent the standard deviation for each condition (n=3).

Since methylene blue was effectively oxidized in the presence of 0.5 mM $FeCl_2$ and 1 mM monopersulfate, 0.5 mM Fe and 1 mM oxidant (i.e., monopersulfate and peroxide) were used to study the methylene blue degradation kinetics at pH 3, 4.8, and 5.2. While higher pH resulted in a comparatively faster degradation of methylene blue with monopersulfate as the oxidant (Figure 4-6A), pH had little effect on the degradation by peroxide (Figure 4-6B). This observed effect of pH is consistent with previous studies, one in which the degradation of Orange II by Fe^{2+}/monopersulfate was highest at pH 7 and lowest at pH 1 (Tan et al. 2018). At lower pH, Fe^{2+} exists as a complex $(Fe^{2+}(H_2O))^{2+}$ that reacts slowly with monopersulfate, hence reducing the amount of $^{\bullet}OH$ in solution, which reduces the degradation efficiency (Tan et al. 2018).

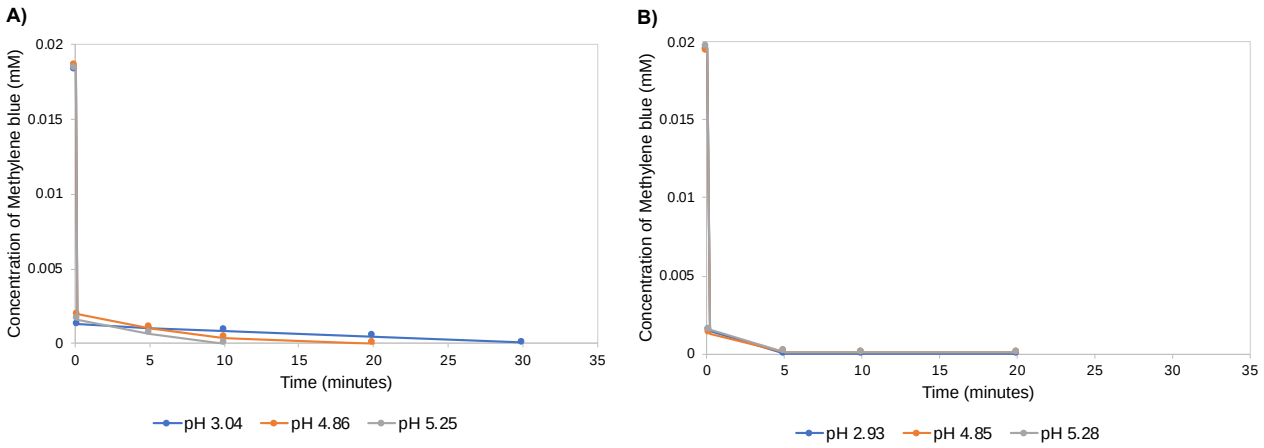

Figure 4-6: Comparison of methylene blue degradation at pH 3, 4.8, and 5.2 by A) monopersulfate (1mM) and B) peroxide (1 mM); Methylene blue starting concentration = 0.02 mM, Fe = 0.5 mM.

Effect of humic acid on Fe^{2+}/monopersulfate and Fe^{2+}/peroxide reactions with methylene blue:

The addition of humic acid at concentrations ranging from 5 mg/L to 20 mg/L did not have a significant effect on the degradation kinetics of methylene blue by both monopersulfate and peroxide (Figure 4-7).

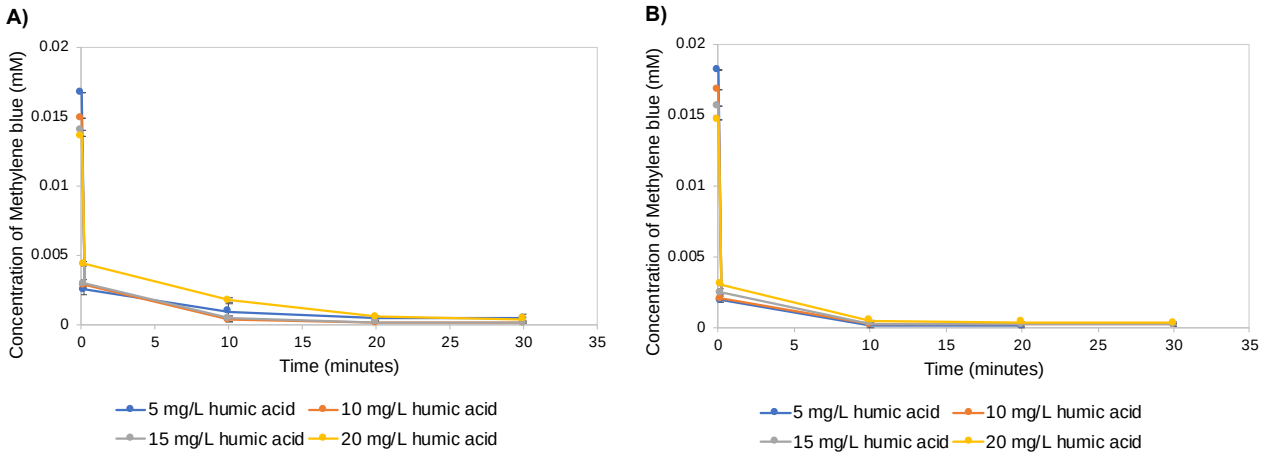

Figure 4-7: Effect of humic acid (5 mg/L - 20 mg/L) on the degradation of methylene blue (0.02 mM) by A) monopersulfate and B) peroxide.

Scavenging effect of bicarbonate on Fe^{2+}/monopersulfate and Fe^{2+}/peroxide reactions with methylene blue: Bicarbonate (HCO_3^-) (5 mM – 200 mM) was used to investigate the scavenging

of radicals produced during the catalytic oxidation of methylene blue. The pH was adjusted to 7 using hydrochloric acid for all experiments where bicarbonate was added. When monopersulfate was used as the oxidant, the presence of $5\ mM$ HCO_3^- reduced the rate of methylene blue reaction, resulting in 96% degradation within 60 minutes. Increasing the HCO_3^- concentration to $25 - 100\ mM$ further slowed the degradation, resulting in $\sim 78\%$ degradation after 4 hours. However, as the HCO_3^- concentration was further increased beyond $100\ mM$, the rate of the reaction increased, resulting in 97% degradation after 4 hours in the presence of $200\ mM$ HCO_3^- (Figure 4-8A). The first-order reaction kinetics for degradation of methylene blue by monopersulfate in the presence of HCO_3^- at different concentrations are depicted in Figure 4-9. It is well known that HCO_3^- is an efficient scavenger of $SO_4^{\bullet -}$**,** which upon reaction, results in the formation of the lesser reactive bicarbonate radical ($HCO_3^{\bullet}$) as shown in equation 4.15 (Liang, Wang, and Mohanty 2006; Fan et al. 2015)**.**

$$SO_4^{\bullet -} + HCO_3^- \rightarrow SO_4^{2-} + HCO_3^{\bullet}\ ;\ k = 1.6 \times 10^6 M^{-1}s^{-1} \qquad (4.15)$$

The redox potential of $HCO_3^{\bullet}$ is $\sim 1.65\ V$ at pH 7 (Liang, Wang, and Mohanty 2006), which is less than that of $SO_4^{\bullet -}$ (i.e., $2.60\ V$). This explains the reduced degradation efficiency of methylene blue in the presence of HCO_3^- as compared to in its absence.

On the contrary, with peroxide as the oxidant, there was very little to almost no degradation of methylene blue, implying that the $^{\bullet}OH$ are effectively quenched by HCO_3^- (Figure 4-8B) which leads to the formation of the carbonate radical ($CO_3^{\bullet -}$) through the reaction depicted in equation 4.16 (Fan et al. 2015).

$$^{\bullet}OH + HCO_3^- \rightarrow CO_3^{\bullet -} + H_2O\ ;\ k = 8.5 \times 10^6 M^{-1}s^{-1} \qquad (4.16)$$

$CO_3^{\bullet -}$ is considerably less reactive, with a redox potential of $1.57\ V$ as compared to the $2.80\ V$ redox potential of $^{\bullet}OH$, and is also more selective (Patra, Mizrahi, and Meyerstein 2020). A

study showed that Fenton's reaction at neutral pH in the presence of HCO_3^-, produces $CO_3^{\bullet -}$ as the active oxidizing product, and not •OH (Illés et al. 2019). The considerable inhibition of methylene blue degradation with peroxide as the oxidant in the presence of HCO_3^-, can be explained by two factors: (i) HCO_3^- outcompetes methylene blue for •OH and (ii) the $CO_3^{\bullet -}$ produced (equation 4.16) does not selectively react with methylene blue.

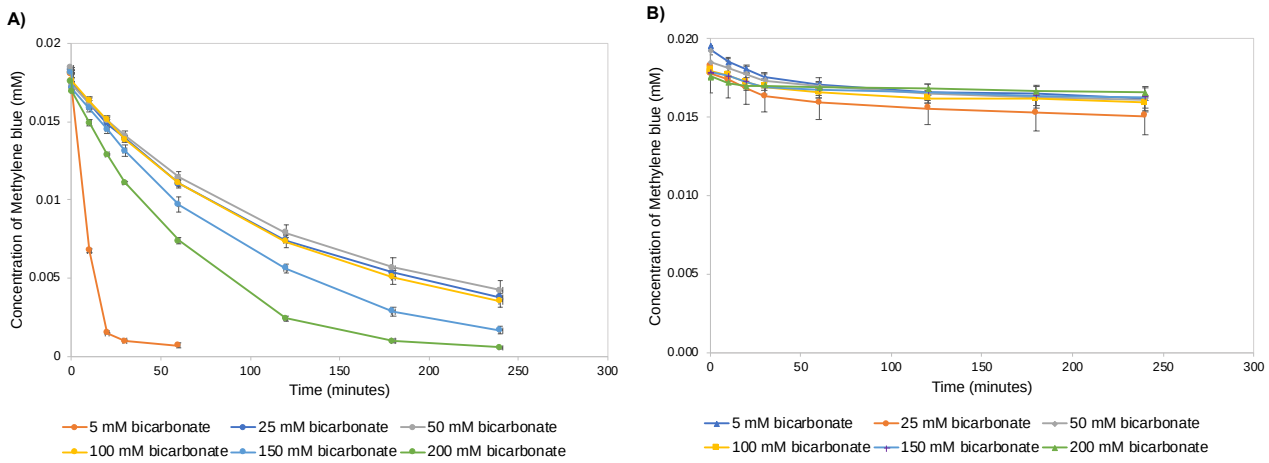

Figure 4-8: Comparison of degradation of methylene blue (0.02 mM) in the presence of HCO_3^- (5 mM - 200 mM) by A) monopersulfate (1 mM) and B) peroxide (1 mM), in the presence of Fe (0.5 mM); pH ~7 for all conditions. Error bars represent the standard deviation for 3 replicates.

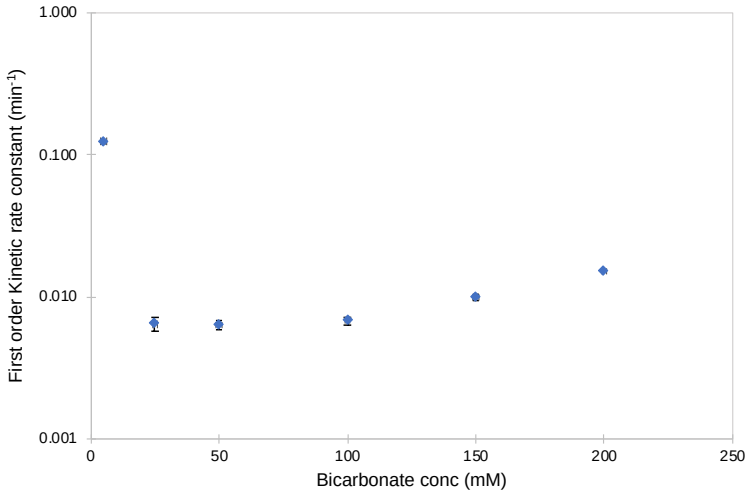

Figure 4-9: First order reaction kinetics of degradation of methylene blue (0.02 mM) by monopersulfate (1 mM) at pH 7 in the presence of Fe (0.5 mM) and HCO_3^- at concentrations ranging from 5 mM to 200 mM. Error bars represent standard deviation of the slopes obtained across 3 replicates.

Effect of probe compounds on methylene blue degradation for radical identification: Ethanol and TBA, at concentrations of $500\ mM$, were used as probes to indicate the dominant radical species during oxidation by monopersulfate and peroxide. Table 4-1 provides details of the rate constants along with the scavenging capacities of ethanol and TBA. The scavenging capacities show that ethanol has a high scavenging capacity for both $^{\bullet}OH$ and $SO_4^{\bullet-}$, whereas TBA has a low scavenging capacity for $SO_4^{\bullet-}$ but is a good scavenger of $^{\bullet}OH$. This difference in the two probes is essential to identify the dominant radical species during oxidation by monopersulfate and peroxide.

Table 4-1: Second-order rate constant and scavenging capacity of 500 mM ethanol and TBA (Ghanbari and Moradi 2017).

	Rate constant ($M^{-1}s^{-1}$)	**Scavenging capacity (s^{-1})**
Ethanol (500 mM)		
$^{\bullet}OH$	$(1.2 - 2.8) \times 10^9$	1.40×10^9
$SO_4^{\bullet-}$	$(1.6 - 7.7) \times 10^7$	2.50×10^7
TBA (500 mM)		
$^{\bullet}OH$	$(3.8 - 7.6) \times 10^8$	2.85×10^8
$SO_4^{\bullet-}$	$(4.0 - 9.1) \times 10^5$	3.25×10^5

$SO_4^{\bullet-}$ is the dominant radical species when monopersulfate is used as the oxidant (Xiao et al. 2018; Ghanbari and Moradi 2017)**.** The results shown in Figure 4-10A are consistent with this, as the addition of ethanol significantly inhibited the degradation of methylene blue, whereas TBA was only able to slow down the reaction without inhibiting it completely. When peroxide is used as the oxidant, $SO_4^{\bullet-}$ is not produced; only $^{\bullet}OH$ is generated during this oxidation reaction. Hence as shown in Figure 4-10B, the degradation of methylene blue by peroxide was similarly inhibited by both ethanol and TBA.

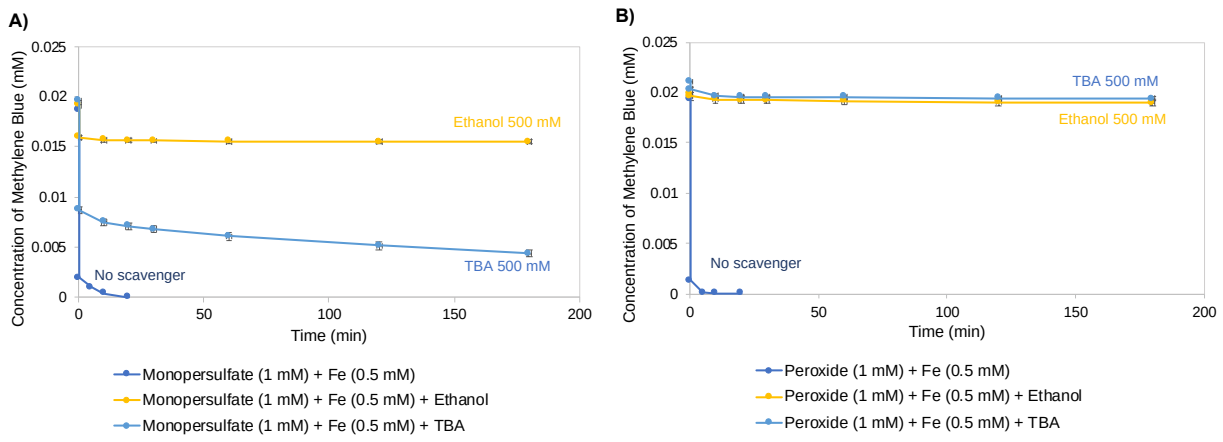

Figure 4-10: Comparison of the degradation of methylene blue by A) monopersulfate (1 mM) and B) peroxide (1 mM) in the presence of ethanol and TBA.

MC-LR

Identification of proper quenching agent to inhibit reaction with MC-LR: As mentioned earlier, the reaction of MC-LR and the oxidants cannot be measured in real-time. Hence it required the use of a quenching agent than can completely stop the reaction to allow for sample storage and analysis. Ethanol and phenol at concentrations of $500\ mM$, and sodium thiosulfate at a concentration of $12\ g/L$, were tested to quench the reaction between monopersulfate. The initial concentrations of monopersulfate and MC-LR were $1\ mM$ and $50\ \mu g/L$ respectively. The choice of ethanol and phenol were based on their high second-order rate constants for the reactions with $^{\bullet}OH$ and $SO_4^{\bullet-}$. The second order rate constants of phenol with $^{\bullet}OH$ and $SO_4^{\bullet-}$ are $6.6 \times 10^9\ M^{-1}s^{-1}$ and $8.8 \times 10^9\ M^{-1}s^{-1}$, respectively. The rate constants for the reactions with ethanol are provided in Table 1 (Ghanbari and Moradi 2017). Sodium thiosulfate was used in a previous study as a quenching agent for the oxidation reaction between permanganate and microcystin-LA (Szlag et al. 2019). Since the ELISA kit limits the presence of alcohols to less than 5%, the samples with ethanol and phenol were dried and reconstituted in water to eliminate any interferences in analysis. Sodium thiosulfate at a concentration of $12\ g/L$ successfully

quenched the reaction between MC-LR and monopersulfate. Ethanol and phenol did not effectively quench the reaction as the concentration of MC-LR was observed to decrease rapidly within 10 minutes of reaction (Figure 4-11).

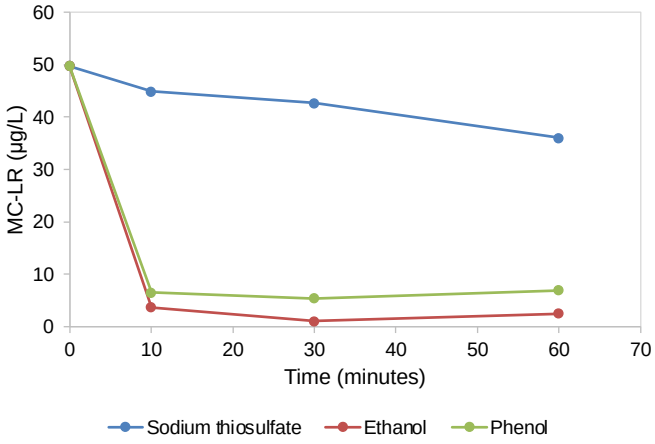

Figure 4-11: Comparison of quenching reagents: Ethanol (500 mM), phenol (500 mM), and sodium thiosulfate (12 g/L) for the reaction between MC-LR (50 $\mu g/L$) and monopersulfate (1 mM).

Reaction with monopersulfate and effect of Fe^{2+} on monopersulfate and peroxide reactions:

Based on results obtained with methylene blue degradation, it was expected that MC-LR would not be degraded by peroxide. This is consistent with the findings of Gajdek et al. (2001) and Al al Momani et al. (2008) who demonstrated that the presence of peroxide in the absence of ferrous ions had no effect on the degradation of MC-LR. Hence, the oxidation of MC-LR by peroxide was not studied. The reaction with monopersulfate followed similar kinetics as seen with methylene blue, wherein the kinetic rate constant for the reaction with 8 mM monopersulfate was significantly higher than that with 1 mM monopersulfate. Figure 4-12 presents the first-order reaction kinetics for the degradation of MC-LR by monopersulfate at the two concentrations studied.

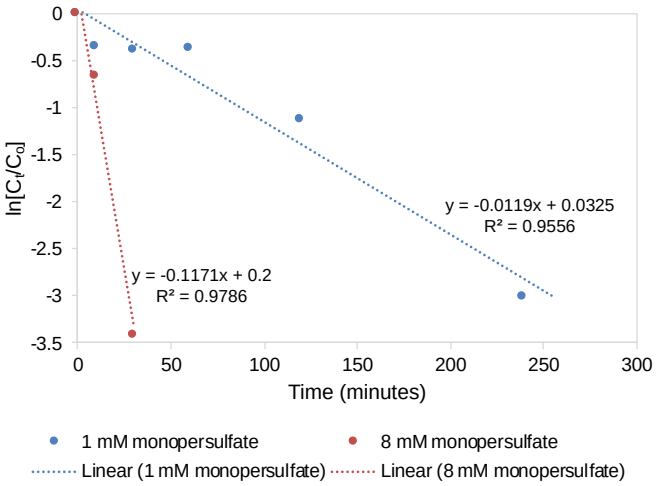

Figure 4-12: First order reaction kinetics for degradation of MC-LR by monopersulfate at 1 mM and 8 mM concentrations.

The reaction of Fe^{2+}/monopersulfate and Fe^{2+}/peroxide with MC-LR was rapid, mirroring the methylene blue reaction. After the first 10 minutes of reaction, the MC-LR concentration was below the detection limit of the ELISA kit, i.e., 0.1 $\mu g/L$, implying $> 99\%$ degradation within 10 minutes of reaction.

Effect of bicarbonate and humic acid on Fe^{2+}/monopersulfate and Fe^{2+}/peroxide reactions with MC-LR: Two concentrations of HCO_3^-: 5 mM and 50 mM, and only one concentration of humic acid: 5 mg/L were used to study the degradation of microcysin-LR. The results of the reactions of Fe^{2+}/monopersulfate and Fe^{2+}/peroxide with methylene blue in the presence of HCO_3^- and humic acid suggest that HCO_3^- was effective at quenching $^{\bullet}OH$ during the Fe^{2+}/peroxide reaction whereas HCO_3^- promoted the degradation of methylene blue during Fe^{2+}/monopersulfate reaction.

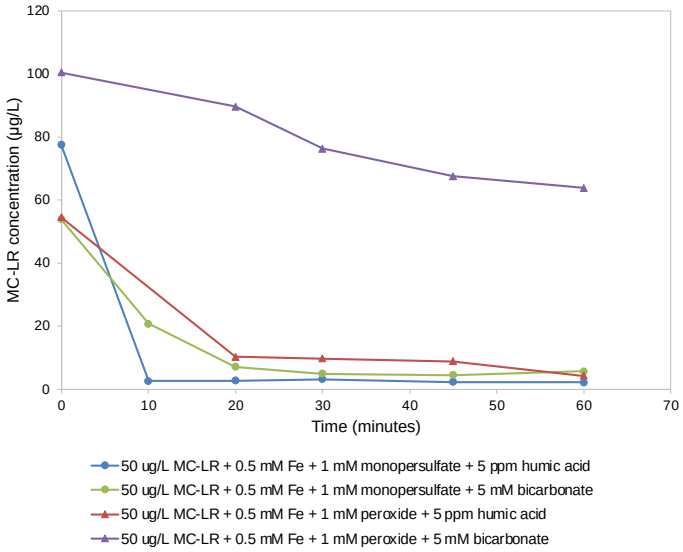

Figure 4-13: Degradation of MC-LR by Fe^{2+}/monopersulfate and Fe^{2+}/peroxide in the presence of HCO_3^- and humic acid.

As seen in Figure 4-13, humic acid slowed the reaction kinetics in the case of both oxidants, resulting in $>$ 90% degradation in 60 minutes, which is expected as the carboxyl and hydroxyl groups in humic acid readily react with $^{\bullet}OH$ and $SO_4^{\bullet -}$ (Feng et al. 2017; Q. Song et al. 2019). HCO_3^- had a similar effect in the presence of monopersulfate but was able to quench the $^{\bullet}OH$ leading to the considerable inhibition of the peroxide reaction. Thus, for these conditions, the reaction kinetics were consistent with that observed for methylene blue.

Verifying radical formation in Fe^{2+}/monopersulfate and Fe^{2+}/peroxide reactions with MC-LR using probe chemicals: The results shown in Figure 4-14, are comparable to the degradation of methylene blue by Fe^{2+}/monopersulfate and Fe^{2+}/peroxide in the presence of probe compounds, i.e., ethanol and TBA. The high scavenging capacity of ethanol and TBA for $^{\bullet}OH$ (as shown in Table 4-1) results in effective quenching of the Fe^{2+}/peroxide reaction with MC-LR. The greater degradation of MC-LR in the Fe^{2+}/monopersulfate system in the presence of TBA implies the

presence of $SO_4^{\bullet -}$ which are not scavenged as effectively by TBA as compared to ethanol. Another factor leading to the higher degradation rate seen in MC-LR experiments in presence of ethanol and TBA is the high second-order rate constant, i.e., $2.1 \times 10^{10}\ M^{-1}s^{-1}$ (W. Song et al. 2009; Y. Liu et al. 2016) for MC-LR with •OH. Considering the initial concentration of MC-LR in the system is $50\ \mu g/L$ or $0.05\ \mu M$, the scavenging capacity of MC-LR towards •OH is computed to be $1.05 \times 10^3\ s^{-1}$.

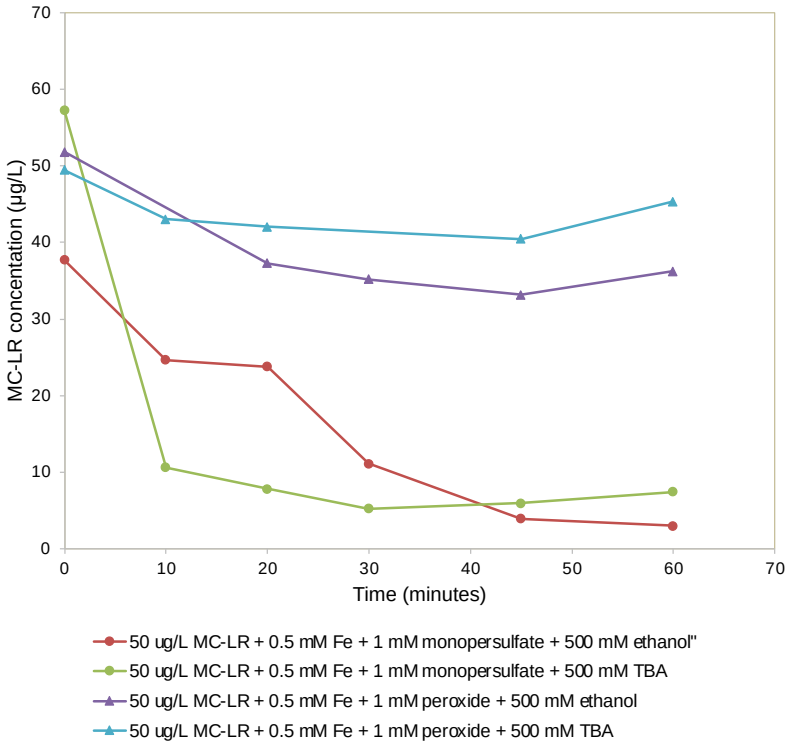

Figure 4-14: Effect of probe chemicals: Ethanol and TBA on the degradation of MC-LR by Fe^{2+}/monopersulfate and Fe^{2+}/peroxide.

CONCLUSION

This study demonstrated that methylene blue can be used as a screening tool for identifying the reaction kinetics and radicals produced during oxidation by Fe^{2+}/monopersulfate and

Fe^{2+}/peroxide, which can be applied to recalcitrant chemicals in water treatment, which was validated using MC-LR. Monopersulfate produces $^{\bullet}OH$ without any activation and was hence able to degrade methylene blue and MC-LR by itself, whereas peroxide, in the absence of metal ions, has no effect on degradation. Low concentrations of Fe^{2+}/monopersulfate and Fe^{2+}/peroxide, i.e., 0.5 mM $FeCl_2$ and 1 mM oxidant, were sufficient to completely degrade methylene blue and MC-LR in under 20 minutes, independent of the pH. The presence of HCO_3^- quenched the radicals produced in the Fe^{2+}/peroxide system but was shown to promote the reaction in Fe^{2+}/monopersulfate system. Humic acid did not alter the reaction kinetics in both systems. The use of probe chemicals, i.e., ethanol and TBA, indicated $SO_4^{\bullet -}$ as the dominant oxidative species in the Fe^{2+}/monopersulfate system and $^{\bullet}OH$ in the Fe^{2+}/peroxide system.

REFERENCES

al Momani, F., Smith, D. W., & Gamal El-Din, M. (2008). Degradation of cyanobacteria toxin by advanced oxidation processes. Journal of Hazardous Materials, 150(2), 238–249. https://doi.org/10.1016/j.jhazmat.2007.04.087

Amin, D. (1981). Indirect Amplification Method for Determining Peroxydisulphate by Alternating-current Polarography. Analyst, 106(1268), 1217–1221.

Amor, C., Fernandes, J. R., Lucas, M. S., & Peres, J. A. (2021). Hydroxyl and sulfate radical advanced oxidation processes: Application to an agro-industrial wastewater. Environmental Technology and Innovation, 21. https://doi.org/10.1016/j.eti.2020.101183

Andreozzi, R., Caprio, V., Insola, A., & Marotta, R. (1999). Advanced oxidation processes (AOP) for water purification and recovery. Catalysis Today, 53(1), 51–59. https://doi.org/10.1016/S0920-5861(99)00102-9

Anipsitakis, G. P., & Dionysiou, D. D. (2004). Radical generation by the interaction of transition metals with common oxidants. Environmental Science and Technology, 38(13), 3705–3712. https://doi.org/10.1021/es035121o

Antoniou, M. G., Boraei, I., Solakidou, M., Deligiannakis, Y., Abhishek, M., Lawton, L. A., & Edwards, C. (2018). Enhancing photocatalytic degradation of the cyanotoxin microcystin-LR with the addition of sulfate-radical generating oxidants. Journal of Hazardous Materials, 360, 461–470. https://doi.org/10.1016/j.jhazmat.2018.07.111

Antoniou, M. G., de la Cruz, A. A., & Dionysiou, D. D. (2010). Degradation of microcystin-LR using sulfate radicals generated through photolysis, thermolysis and e- transfer mechanisms. Applied Catalysis B: Environmental, 96(3–4), 290–298. https://doi.org/10.1016/j.apcatb.2010.02.013

Antoniou, M. G., de La Cruz, A. A., & Dionysiou, D. D. (2010). Intermediates and reaction pathways from the degradation of microcystin-LR with sulfate radicals. Environmental Science and Technology, 44(19), 7238–7244. https://doi.org/10.1021/es1000243

Burgos Castillo Rutely, C., Fontmorin, J. M., Tang Walter, Z., Xochitl, D. B., & Mika, S. (2018). Towards reliable quantification of hydroxyl radicals in the Fenton reaction using chemical probes. RSC Advances, 8(10), 5321–5330. https://doi.org/10.1039/c7ra13209c

Cashman, M. A., Kirschenbaum, L., Holowachuk, J., & Boving, T. B. (2019). Identification of hydroxyl and sulfate free radicals involved the reaction of 1,4-dioxane with peroxone activated persulfate oxidant. Journal of Hazardous Materials, 380. https://doi.org/10.1016/j.jhazmat.2019.120875

Clark, G. L., & Tso, T.-C. (1949). Detection of Persulfate in Acid Solution. Analytical Chemistry, 21(7), 874–875. https://pubs.acs.org/sharingguidelines

Deng, Y., & Zhao, R. (2015). Advanced Oxidation Processes (AOPs) in Wastewater Treatment. Current Pollution Reports, 1(3), 167–176. https://doi.org/10.1007/s40726-015-0015-z

Ding, Y., Zhu, L., Yan, J., Xiang, Q., & Tang, H. (2011). Spectrophotometric determination of persulfate by oxidative decolorization of azo dyes for wastewater treatment. Journal of Environmental Monitoring, 13(11), 3057–3063. https://doi.org/10.1039/c1em10454c

E. Villegas, Y. Pomeranz, & J. A. Shellenberger. (1963). Colorimetric Determination of Persulfate with Alcian Blue. Analytical Chimic Acta, 29, 145–148.

Fan, Y., Ji, Y., Kong, D., Lu, J., & Zhou, Q. (2015). Kinetic and mechanistic investigations of the degradation of sulfamethazine in heat-activated persulfate oxidation process. Journal of Hazardous Materials, 300, 39–47. https://doi.org/10.1016/j.jhazmat.2015.06.058

Feng, Y., Song, Q., Lv, W., & Liu, G. (2017). Degradation of ketoprofen by sulfate radical-based advanced oxidation processes: Kinetics, mechanisms, and effects of natural water matrices. Chemosphere, 189, 643–651. https://doi.org/10.1016/j.chemosphere.2017.09.109

Gajdek, P., Lechowski, Z., Bochnia, T., & Kępczyński, M. (2001). Decomposition of microcystin-LR by Fenton oxidation. Toxicon, 39, 1575–1578. www.elsevier.com/locate/toxicon

Ghanbari, F., & Moradi, M. (2017). Application of peroxymonosulfate and its activation methods for degradation of environmental organic pollutants: Review. Chemical Engineering Journal, 310, 41–62. https://doi.org/10.1016/j.cej.2016.10.064

Glaze, W. H., Kang, J.-W., & Chapin, D. H. (1987). The Chemistry of Water Treatment Processes involving Ozone, Hydrogen Peroxide and UV Radiation. Ozone Science & Engineering, 9, 335–352.

Guerra-Rodríguez, S., Rodríguez, E., Singh, D. N., & Rodríguez-Chueca, J. (2018). Assessment of sulfate radical-based advanced oxidation processes for water and wastewater treatment: A review. In Water (Switzerland) (Vol. 10, Issue 12). MDPI AG. https://doi.org/10.3390/w10121828

He, X. (2014). Kinetic and Mechanistic Studies on the Removal of Cyanotoxins and Antibiotics with Hydroxyl and Sulfate Radical Based Advanced Oxidation Processes. ProQuest Dissertations and Theses, 244. http://sfx.scholarsportal.info/guelph/docview/1619352727?accountid=11233%5Cnhttp://sfx.scholarsportal.info/guelph?url_ver=Z39.88-2004&rft_val_fmt=info:ofi/fmt:kev:mtx:dissertation&genre=dissertations+%26+theses&sid=ProQ:ProQuest+Dissertations+%26+Theses+A

I. M. Kolthoff, & R. Woods. (1966). Polarographic Kinetic Currents in Mixtures of Persulfate and Copper(II) in Chloride Medium. Journal of the American Chemical Society, 88(7), 1371–1375.

Illés, E., Mizrahi, A., Marks, V., & Meyerstein, D. (2019). Carbonate-radical-anions, and not hydroxyl radicals, are the products of the Fenton reaction in neutral solutions containing

bicarbonate. Free Radical Biology and Medicine, 131, 1–6. https://doi.org/10.1016/j.freeradbiomed.2018.11.015

Jasim, S. Y., Uslu, M., Seth, R., & Biswas, N. (2020). Removal of Cyanotoxins in Detroit River Water Using Ozone-Based Advanced Oxidation Processes. Ozone: Science and Engineering, 42(5), 461–468. https://doi.org/10.1080/01919512.2020.1793731

Kolthoff, I. M., & Carr, E. M. (1953). Volumetric Determination of Persulfate in the Presence of Organic Substances. J., Anal. Chem, 25(2), 298–301. https://pubs.acs.org/sharingguidelines

Kolthoff, I. M., & Stenger, V. A. (1947). Vol. 2: Titration Methods: Acid-base, Precipitation, and Complex-formation Reactions. Interscience.

Liang, C., Huang, C. F., Mohanty, N., & Kurakalva, R. M. (2008). A rapid spectrophotometric determination of persulfate anion in ISCO. Chemosphere, 73(9), 1540–1543. https://doi.org/10.1016/j.chemosphere.2008.08.043

Liang, C., & Su, H. W. (2009). Identification of sulfate and hydroxyl radicals in thermally activated persulfate. Industrial and Engineering Chemistry Research, 48(11), 5558–5562. https://doi.org/10.1021/ie9002848

Liang, C., Wang, Z. S., & Mohanty, N. (2006). Influences of carbonate and chloride ions on persulfate oxidation of trichloroethylene at 20 °C. Science of the Total Environment, 370(2–3), 271–277. https://doi.org/10.1016/j.scitotenv.2006.08.028

Lindsey, M. E., & Tarr, M. A. (2000). Quantitation of hydroxyl radical during Fenton oxidation following a single addition of iron and peroxide. Chemosphere, 41, 409–417.

Liu, Y., Ren, J., Wang, X., & Fan, Z. (2016). Mechanism and reaction pathways for microcystin-LR degradation through UV/H2O2 treatment. PLoS ONE, 11(6). https://doi.org/10.1371/journal.pone.0156236

Loganathan, K. (2016). Ozone-based advanced oxidation processes for the removal of harmful algal bloom (HAB) toxins: a review. Desalination and Water Treatment, 59(November), 65–71. https://doi.org/10.5004/dwt.2016.0346

Neta, P., Madhavan, V., Zemel, H., & Fessenden, R. W. (1977). Rate Constants and Mechanism of Reaction of SO4· with Aromatic Compounds. Journal of the American Chemical Society, 99, 163–164. https://pubs.acs.org/sharingguidelines

Oh, W. Da, Dong, Z., & Lim, T. T. (2016). Generation of sulfate radical through heterogeneous catalysis for organic contaminants removal: Current development, challenges and prospects. Applied Catalysis B: Environmental, 194, 169–201. https://doi.org/10.1016/j.apcatb.2016.04.003

Patra, S. G., Mizrahi, A., & Meyerstein, D. (2020). The Role of Carbonate in Catalytic Oxidations. Accounts of Chemical Research, 53(10), 2189–2200. https://doi.org/10.1021/acs.accounts.0c00344

Paul M Shiundu, Adrian P. Wade, & Jonnalagadda, S. B. (1990). Spectrophotometric determination of peroxydisulphate with o-dianisidine by flow injection. Can. J. Chem, 68, 1750–1756.

Rastogi, A., Al-Abed, S. R., & Dionysiou, D. D. (2009). Sulfate radical-based ferrous-peroxymonosulfate oxidative system for PCBs degradation in aqueous and sediment systems. Applied Catalysis B: Environmental, 85(3–4), 171–179. https://doi.org/10.1016/j.apcatb.2008.07.010

Rivas, F. J. (2022). Monopersulfate in water treatment: Kinetics. Journal of Hazardous Materials, 430. https://doi.org/10.1016/j.jhazmat.2022.128383

Satoh, A. Y., Trosko, J. E., & Masten, S. J. (2007). Methylene blue dye test for rapid qualitative detection of hydroxyl radicals formed in a Fenton's reaction aqueous solution. Environmental Science and Technology, 41(8), 2881–2887. https://doi.org/10.1021/es0617800

Schneider, M., & Bláha, L. (2020). Advanced oxidation processes for the removal of cyanobacterial toxins from drinking water. Environmental Sciences Europe, 32(1). https://doi.org/10.1186/s12302-020-00371-0

Song, Q., Feng, Y., Liu, G., & Lv, W. (2019). Degradation of the flame retardant triphenyl phosphate by ferrous ion-activated hydrogen peroxide and persulfate: Kinetics, pathways, and mechanisms. Chemical Engineering Journal, 361, 929–936. https://doi.org/10.1016/j.cej.2018.12.140

Song, W., Xu, T., Cooper, W. J., Dionysiou, D. D., de La Cruz, A. A., & O'Shea, K. E. (2009). Radiolysis studies on the destruction of microcystin-LR in aqueous solution by hydroxyl radicals. Environmental Science and Technology, 43(5), 1487–1492. https://doi.org/10.1021/es802282n

Szlag, D. C., Sinclair, J. L., Southwell, B., & Westrick, J. A. (2015). Cyanobacteria and cyanotoxins occurrence and removal from five high-risk conventional treatment drinking water plants. Toxins, 7(6), 2198–2220. https://doi.org/10.3390/toxins7062198

Szlag, D. C., Spies, B., Szlag, R. G., & Westrick, J. A. (2019). Permanganate Oxidation of Microcystin-LA: Kinetics, Quantification, and Implications for Effective Drinking Water Treatment. Journal of Toxicology, 2019. https://doi.org/10.1155/2019/3231473

Tan, C., Dong, Y., Shi, L., Chen, Q., Yang, S., Liu, X., Ling, J., He, X., & Fu, D. (2018). Degradation of Orange II in ferrous activated peroxymonosulfate system: Efficiency, situ EPR spin trapping and degradation pathway study. Journal of the Taiwan Institute of Chemical Engineers, 83, 74–81. https://doi.org/10.1016/j.jtice.2017.11.014

Walker, H. W. (2014). Harmful Algae Blooms in Drinking Water: Removal of Cyanobacterial Cells and Toxins. CRC Press. https://books.google.com/books?id=gUQrBgAAQBAJ

Wang, J., & Wang, S. (2020). Reactive species in advanced oxidation processes: Formation, identification and reaction mechanism. Chemical Engineering Journal, 401. https://doi.org/10.1016/j.cej.2020.126158

Westrick, J. A., Szlag, D. C., Southwell, B. J., & Sinclair, J. (2010). A review of cyanobacteria and cyanotoxins removal/inactivation in drinking water treatment. Analytical and Bioanalytical Chemistry, 397(5), 1705–1714. https://doi.org/10.1007/s00216-010-3709-5

World Health Organization. (2020). Cyanobacterial toxins: microcystins. Background document for development of WHO Guidelines for drinking-water quality and Guidelines for safe recreational water environments. http://apps.who.int/bookorders.

Xia, X., Zhu, F., Li, J., Yang, H., Wei, L., Li, Q., Jiang, J., Zhang, G., & Zhao, Q. (2020). A Review Study on Sulfate-Radical-Based Advanced Oxidation Processes for Domestic/Industrial Wastewater Treatment: Degradation, Efficiency, and Mechanism. Frontiers in Chemistry, 8. https://doi.org/10.3389/fchem.2020.592056

Xiao, R., Luo, Z., Wei, Z., Luo, S., Spinney, R., Yang, W., & Dionysiou, D. D. (2018). Activation of peroxymonosulfate/persulfate by nanomaterials for sulfate radical-based advanced oxidation technologies. Current Opinion in Chemical Engineering, 19, 51–58. https://doi.org/10.1016/j.coche.2017.12.005

Yang, Y., Jiang, J., Lu, X., Ma, J., & Liu, Y. (2015). Production of Sulfate Radical and Hydroxyl Radical by Reaction of Ozone with Peroxymonosulfate: A Novel Advanced Oxidation Process. Environmental Science and Technology, 49(12), 73307339. https://doi.org/10.1021/es506362e

Zhao, L., Yang, S., Wang, L., Shi, C., Huo, M., & Li, Y. (2015). Rapid and simple spectrophotometric determination of persulfate in water by microwave assisted decolorization of Methylene Blue. Journal of Environmental Sciences (China), 31, 235–239. https://doi.org/10.1016/j.jes.2014.09.036

Zhou, J., Liu, J., Zhao, Z., Peng, W., Cui, F., & Liang, Z. (2020). Microcystis aeruginosa-laden water treatment using peroxymonosulfate enhanced Fe(II) coagulation: Performance and the role of in situ formed Fe3O4. Chemical Engineering Journal, 382. https://doi.org/10.1016/j.cej.2019.123012

Zhou, S., Yu, Y., Zhang, W., Meng, X., Luo, J., Deng, L., Shi, Z., & Crittenden, J. (2018). Oxidation of Microcystin-LR via Activation of Peroxymonosulfate Using Ascorbic Acid: Kinetic Modeling and Toxicity Assessment. Environmental Science and Technology, 52(7), 4305–4312. https://doi.org/10.1021/acs.est.7b06560

APPENDIX

Figures

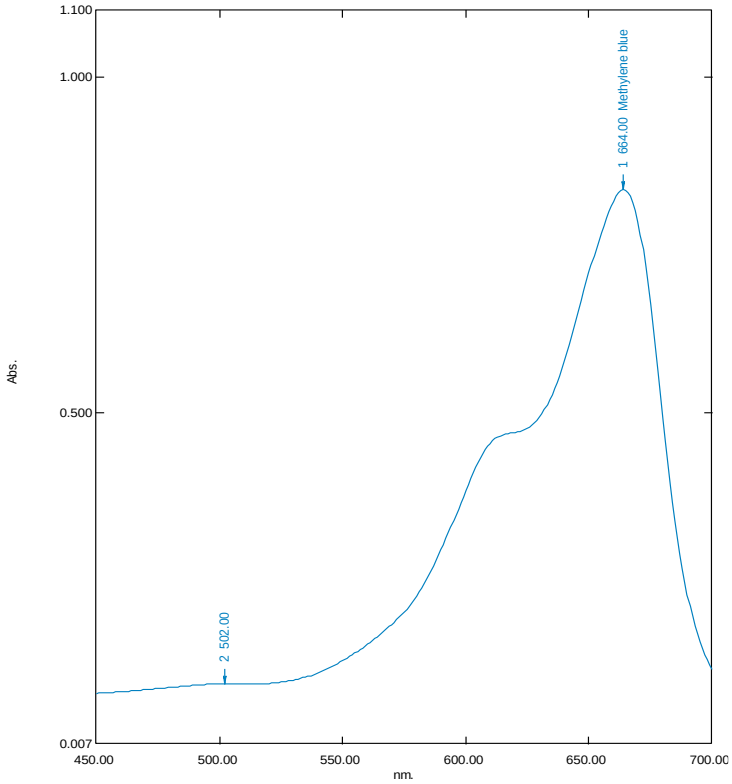

Figure 4-15: Absorbance of methylene blue at a concentration of 0.01 mM.

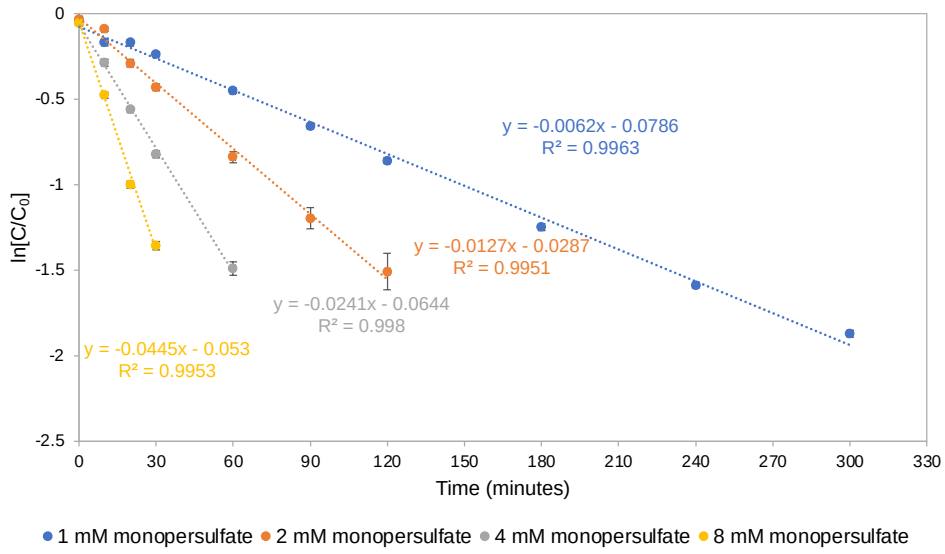

Figure 4-16: First-order reaction kinetics of degradation of methylene blue by monopersulfate at different concentrations.

CHAPTER 5 : Screening Of Iron Coated Ceramic Membrane Filtration Combined With Persulfate Oxidation Using Methylene Blue

ABSTRACT

Persulfate-based advanced oxidation produces sulfate radicals that are strong oxidants of many organic compounds. This increases the demand of persulfate-based advanced oxidation in water treatment. Membrane filtration is commonly used in water treatment but comes with the drawback of membrane fouling which increases operational costs. The use of catalytic membranes has proven to reduce fouling, along with producing higher quality of permeate. Hence, in this study, monopersulfate was applied to an iron oxide coated ceramic membrane to investigate the removal of methylene blue, which was used a radical probe. The removal of methylene blue by monopersulfate assisted membrane filtration was compared in iron-coated and uncoated ceramic membranes. The results of this study indicate that the iron oxide coating on the ceramic membrane did not activate monopersulfate. However, when ferrous chloride was present in solution, rapid degradation of methylene blue was observed, implying that colloidal ferrous ions are required for activation of monopersulfate.

INTRODUCTION

Membrane processes, which include nanofiltration, microfiltration, ultrafiltration, and reverse osmosis, are becoming increasingly popular in water and wastewater treatment due to their high operational stability, greater removal efficiency of wide range of contaminants, and ease-of-operation (Peters 2010). However, a major drawback involved with membrane processes is the fouling of membranes, which results from the accumulation of natural organic matter (NOM) on the surface of membranes after a period of operation (Erhayem and Sohn 2014; Zhu et al. 2018). This fouling results in reduced permeate quality and flux. Methods to combat fouling include

membrane replacement and cleaning, which require large quantities of chemicals, resulting in higher operational costs (Li et al. 2021).

On the other hand, advanced oxidation processes (AOP) such as Fenton oxidation, sulfate radical based oxidation, and catalytic wet oxidation, are capable of oxidizing a wide range of organic compounds due to the production of hydroxyl and sulfate radicals (Amor et al. 2021; Deng and Zhao 2015). Some of the advanced oxidation processes require the use of metal catalysts which can only be recovered from the heterogeneous reaction using centrifugation or filtration, which in turn require additional energy and cost (Li et al. 2021).

The combination of membrane filtration with catalytic oxidation helps combat the shortcomings of the two processes when used individually. The transformation of traditional membranes into catalytic membranes is shown to drastically reduce membrane fouling while increasing permeate quality (Yu et al. 2022; Li et al. 2021; Alpatova, Davies, and Masten 2013) and can also successfully reuse the metal catalyst embedded on the membrane.

Catalytic membranes can be classified into the following categories: metal-based, carbon-based, polymer-based, and ceramic-based (Yu et al. 2022). There are several ways of preparation of catalytic membranes, which include dip coating, spin coating, casting, layer-by-layer assembly, surface grafting, etc., which determine their properties such as rejection of contaminants, selectivity, pollutant degradation, and antifouling ability (Qing et al. 2020). Ceramic membranes exhibit higher mechanical, thermal, and chemical stability in addition to higher fouling resistance as compared to other polymeric membranes (Freeman and Shorney-Darby 2011). The evolution of catalytic ceramic membranes and their implementation in hybrid membrane-AOP systems is provided in a literature review by Li et al. (2020). The generation of hydroxyl radicals, via decomposition of ozone by metal oxides coated on ceramic membranes, exhibited higher

removal of dissolved organic carbon (DOC) along with the disinfection and ozonation by-products (Karnik et al. 2007; Karnik et al. 2005; Karnik et al. 2005).

The combination of Fenton's reaction and membrane filtration is cumbersome because Fenton's reaction required acidic pH (pH < 3) to prevent iron precipitation and since the reaction is exothermic and creates oxygen, it can result in the formation of bubbles within the membrane system, which in turn can cause pressure buildup, creating unsafe conditions. Hence, sulfate radical based oxidation is preferred over Fenton's reaction for integration into catalytic membrane filtration. Ferrous ion activated persulfate has been used as a pre-treatment to ultrafiltration using ceramic membranes, which reduces the fouling of the membranes caused by NOM (Liu et al. 2018; Cheng et al. 2018; 2017; Li et al. 2020). Bao et al. (2018) investigated the activation of peroxymonosulfate (PMS) by $CoFe_2O_4$ impregnated Al_2O_3 ceramic membrane, which was found to completely degrade sulfamethoxazole in just 90 seconds of contact time. In another study, the integration of $CuFe_2O_4$ with ceramic membrane, activated by PMS, was shown to enhance the removal of humic acid while reducing the irreversible fouling resistance (Y. Zhao et al. 2020). The innovative integration of MnO_2, with Al_2O_3 ceramic membranes exhibited effective degradation of 4-hydroxylbenzoic acid, which was induced by sulfate radicals generated via PMS activation (Wu et al. 2019). Selective pollutant removal was achieved by cobalt-doped ceramic membrane filtration in the presence of PMS, wherein the primary reactive species during the oxidative filtration process were identified as surface-complexed PMS (H. Xu et al. 2022).

In this work, the effectiveness of iron oxide coated ceramic membranes is evaluated for the oxidative removal of methylene blue dye in the presence of PMS. The removal is compared to filtration with uncoated ceramic membranes.

METHODS

Materials & Instrumentation

Tubular ceramic membranes (CéRAM, TAMI, North America, St. Laurent, Québec, Canada) with the combination of alumina, zirconia, and titania as the support layer were used in this study. The membrane consisted of 7 channels and had an outer diameter of 1.0 cm with a total length of 25 cm. The molecular weight cutoff of the membrane was 5 kDa. For this study, the membrane was used as is, i.e., supplied by the manufacturer, and coated with iron oxide. Colloidal iron oxide particles were coated on the membrane in a layer-by-layer technique as described by Karnik et al. (2005a). The membrane was supported in a stainless steel filter holder. The membrane system consisted of Teflon tubing and stainless steel or Teflon joints and valves. Two stainless steel pressure vessels, that were pressurized used nitrogen, were used for supplying samples into the system. Cole-Parmer (Vernon Hills, Illinois, USA) 75211-50 Gear Pump Drive Console was used to regulate continuous flow through the membrane system. Oxone®, PMS compound ($KHSO_5 \cdot 0.5KHSO_4 \cdot 0.5K_2SO_4$) (CAS# 70693-62-8; Sigma-Aldrich Inc., St. Louis, Missouri, USA) was used as the oxidant in this study. Methylene blue hydrate, ≥ 95% (CAS# 122965-43-9; Sigma-Aldrich Inc., St. Louis, Missouri, USA) was used as a screening agent to determine the kinetics of the reactions. Ferrous chloride (CAS# 13478-10-9; Avantor Performance Materials, Inc., Center Valley, Pennsylvania, USA) was used as the iron salt in solution. Sodium chloride, 99.0%, ACS grade (CAS# 7647-14-5; ChemPure Chemicals, Westland, Michigan, USA) was used to increase the conductivity of solution and the conductivity was measured using HI98393 DiST3 EC tester (Hanna® Instruments, Woonsocket, Rhode Island, USA). The water used in this study was high-purity deionized water (ultrapure water) with a resistivity of 18 $M\Omega \cdot cm$.

The absorbance of methylene blue was determined using a Shimadzu (UV-2600) UV-Vis Spectrophotometer using 1.0 cm cuvettes and at a wavelength of 664 nm, the peak absorbance. The pH of the solutions was measured using a Thermo Scientificä Orion Starä A211 Benchtop pH Meter. The meter was calibrated using Orion™ pH buffers of 4, 7, and 10 purchased from Thermo Scientific (Waltham, Massachusetts, USA).

Experimental Setup

The system included 2 pressure vessels that were connected to the crossflow system as shown in Figure 5-1. A valve connected to the membrane was used to switch the flow from the pressure vessels. Since sample could only be drawn from one pressure vessel at a time, sample containing the analyte was placed in one vessel while the oxidant or water, when performing control experiments, was placed in the other vessel. The transmembrane pressure (TMP) was controlled by changing the nitrogen gas pressure that was applied to the pressure vessels. The flow rate through the membrane was estimated by measuring the volume of the permeate and time.

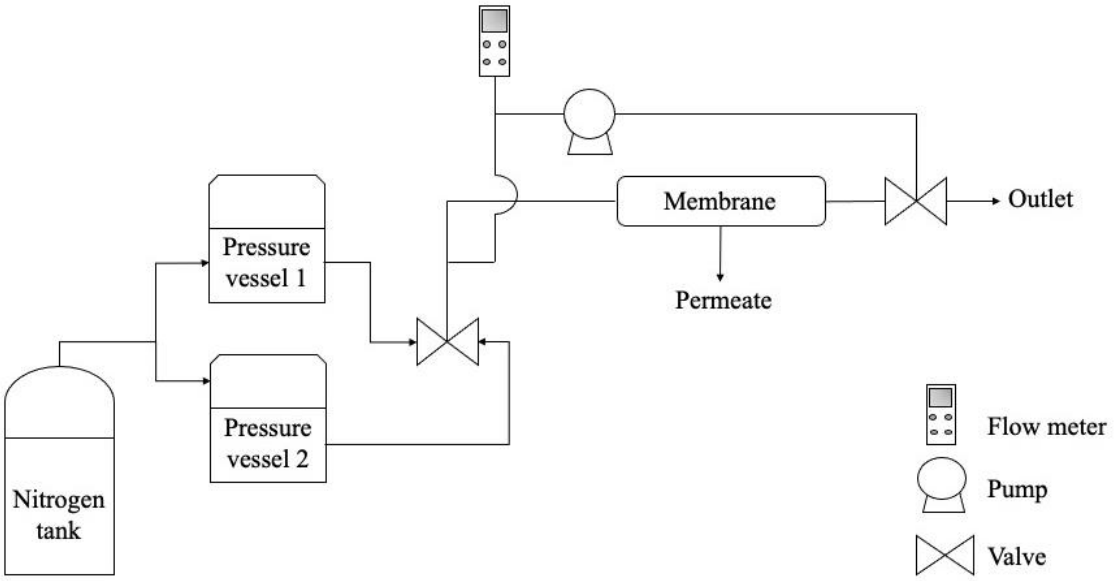

Figure 5-1: Schematic representation of the ceramic membrane filtration system.

RESULTS & DISCUSSION

Steady State estimation

Steady state measurements were performed initially on the uncoated ceramic membrane using a solution of sodium chloride (NaCl) with a concentration of $1\ g/L$. This salt was selected as it does not adsorb on the ceramic membrane. The conductivity of the $1\ g/L$ NaCl solution was measured to be $1715\ \mu S/cm$. The time taken to reach steady state was estimated by measuring the conductivity of the permeate at regular intervals until it matched the conductivity of the feed, i.e., $1715\ \mu S/cm$. The steady state time was also confirmed by measuring the decline of conductivity, by flushing the membrane with water, until it reached 0. With the combined results of 3 trials, the time to reach steady state was estimated to be 60 minutes. A representative trial is shown in Figure 5-2.

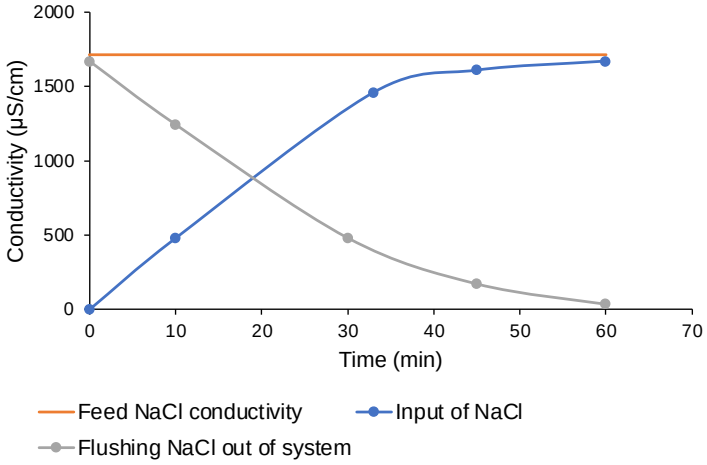

Figure 5-2: Graph representing the conductivity data from a steady state trial experiment for uncoated ceramic membrane using NaCl.

The volume of sample in the crossflow system was determined by modelling the conservation of mass equation as shown in equation 5.1, which on integration leads to the form represented in equation 5.2.

$$V\frac{dC}{dt} = C_{in}Q - C_{out}Q \tag{5.1}$$

$$C_t = C_{in}\left\{1 - exp\left[-\left(\frac{Q}{V}\right)t\right]\right\} + C_o exp\left[-\left(\frac{Q}{V}\right)t\right] \quad (5.2)$$

With an average from 3 trials, the estimated volume in the crossflow system with the uncoated ceramic membrane was $112.2 \pm 5.38\ mL$. Pressure was maintained at $\sim 40\ psi$ and the average flow rate within the trials was $5.61 \pm 0.22\ mL/min$.

The estimated volume was also validated by running methylene blue through the system. The average volume resulting from 2 trials using methylene blue was $110.5 \pm 0.49\ mL$. A representative trial is shown in Figure 5-3. The flow rate maintained at $5.82 \pm 0.39\ mL/min$ by regulating the pressure at $\sim 40\ psi$. The time taken to reach steady state with methylene blue in the sample was around 80 minutes, which is slightly longer than that observed using NaCl.

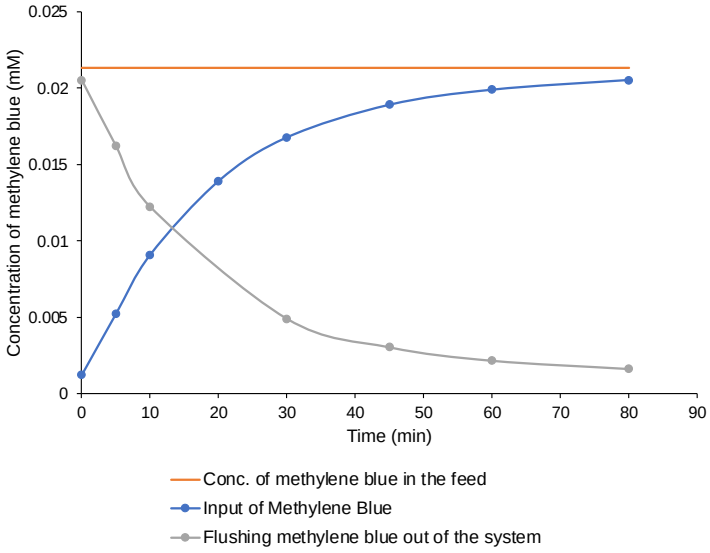

Figure 5-3: The trend observed for the concentration of methylene blue while being input and flushed out of the membrane system, while using uncoated membrane.

A similar check was also performed on iron oxide coated ceramic membrane. The estimated volume from 2 trials was $106.0 \pm 12.0\ mL$. The flow rate for the same was $11.63 \pm 0.59\ mL/min$ with the pressure regulated at $\sim 20\ psi$. A graph of the representative trial is shown in Figure 5-4.

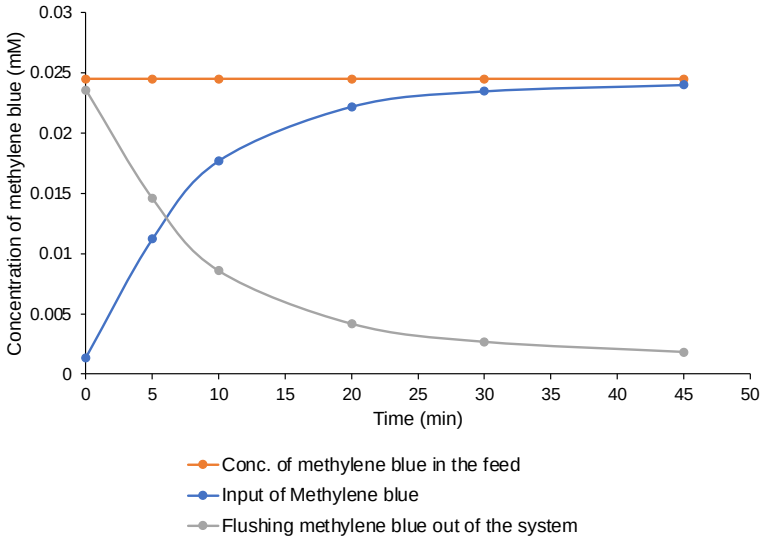

Figure 5-4: The trend observed for the concentration of methylene blue while being input and flushed out of the membrane system, while using iron coated membrane.

Effect of PMS on Methylene Blue removal

To investigate the effect of monopersulfate in the uncoated membrane system, the methylene blue was first allowed to reach steady state within the system, after which, the flow was switched to solution containing PMS. Two concentrations of PMS were investigated: 1 mM and 8 mM. However, as seen in Figure 5-5, the effect of monopersulfate was negligible. This can be explained by the fact that PMS requires time to reach steady state, which means that the concentration of PMS that is in contact with methylene blue at the start of the flush is low. The rise in concentration of PMS was estimated using equation 5.2 and is depicted in Figure 5-6.

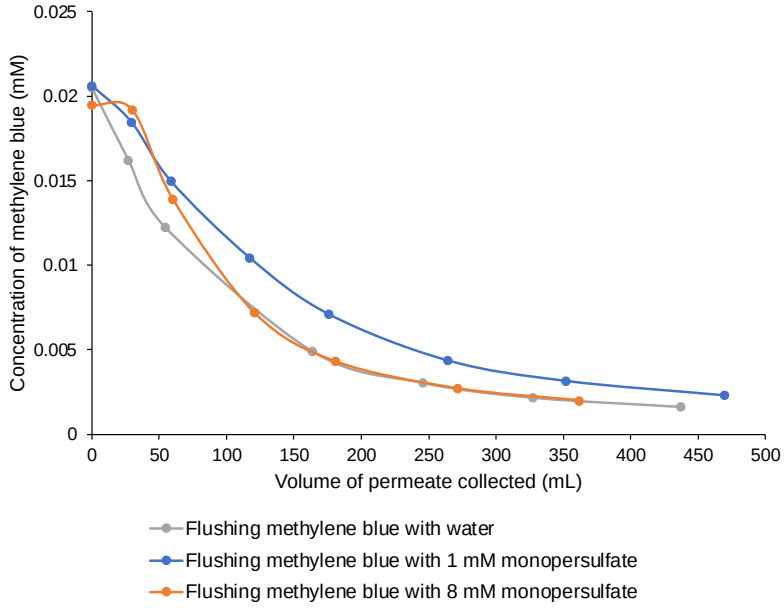

Figure 5-5: Comparison of decrease in concentration of methylene blue when flushed with water versus different concentrations of PMS.

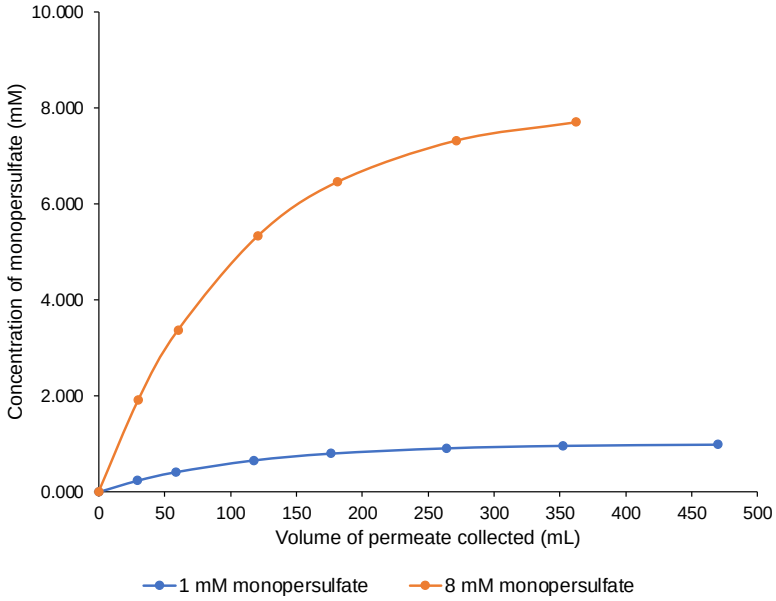

Figure 5-6: The increase in concentration of PMS when supplied at different concentrations into the system based on conservation of mass theory.

In the system with the iron coated membrane, the PMS was supplied to the system and allowed to reach steady state prior to injecting methylene blue. As shown in Figure 5-6, the presence of

PMS in the system, delayed the increase in concentration of methylene blue, indicating initial degradation within the system.

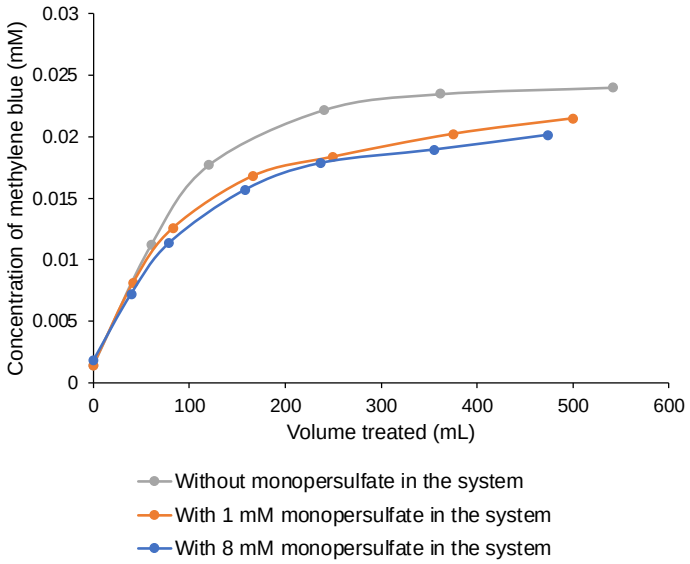

Figure 5-7: Comparison of the rise in concentration of methylene blue in the iron coated membrane system with and without the presence of PMS at different concentrations.

However, the presence of iron oxide coated on the membrane did not seem to have any effect on the degradation of methylene blue. As seen in the previous study, PMS is capable of degrading methylene blue without the presence of any catalyst, which is seen in Figure 5-7. Using the area under the curves without PMS and with 8 mM PMS as shown in Figure 5-7, the degradation of methylene blue with 8 mM PMS in the system was estimated to be ~30% higher than without PMS in the system.

To distinguish between the reaction of PMS activated by iron versus not, $FeCl_2$ at a concentration of $0.25\ mM$ was added in solution with methylene blue and the pH was adjusted to 3.22, such that any precipitation of iron in the system would be avoided. As seen in Figure 5-8, the rise in concentration of methylene blue is considerably hindered at the start due to presence of PMS in the system. This proves that the iron oxide coated on the membrane played no role in activation of PMS to produce sulfate radicals. By estimating the area under the curves without

PMS and with FeCl2 and PMS in the system, the degradation of methylene blue in the presence of FeCl2 and PMS was ~23% higher than without either present in the system.

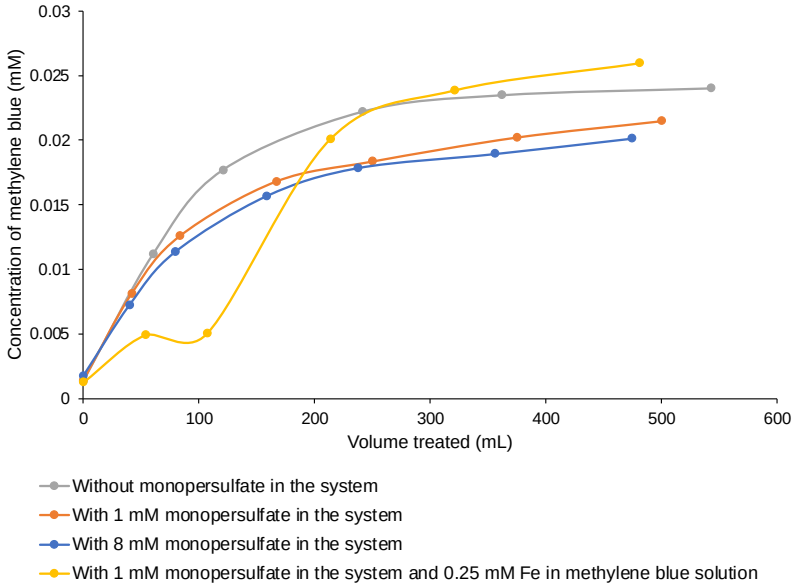

Figure 5-8: Comparing the rise of methylene blue concentration with $FeCl_2$ in solution and presence of PMS in the system to the absence of iron particles and PMS.

To confirm that the coated membrane had no effect in activation of PMS, a control study was performed in which methylene blue was prepared with PMS in solution. A sample was drawn and placed on benchtop and the decline of concentration of this sample was compared to the sample that was passed through the membrane. As shown in Figure 5-9, the change in absorbance over time is similar in both the samples, hence confirming that the iron oxide coating on the membrane had no effect in activation of PMS.

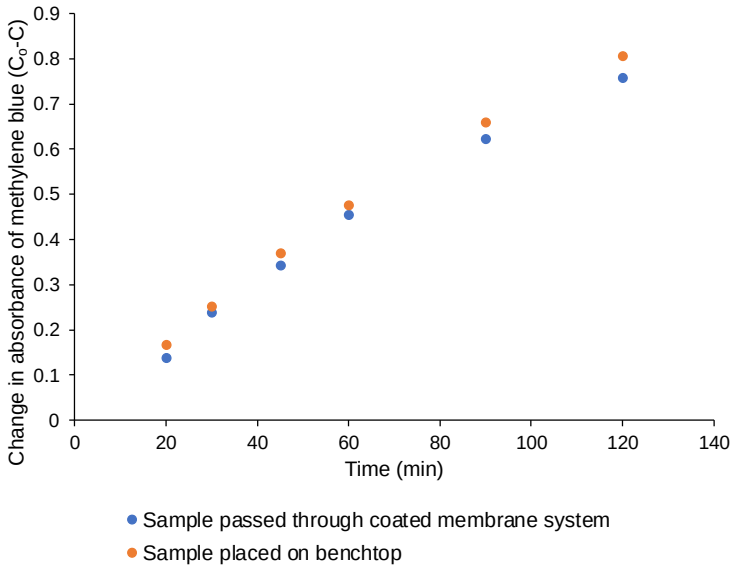

Figure 5-9: Comparison in the change in absorbance of methylene blue with 1 mM PMS in solution, when passed through the coated membrane system versus when placed on benchtop.

CONCLUSION

The experiments conducted in this study prove that PMS cannot be activated by single metal coated ceramic membrane and requires colloidal iron to be present in solution for a rapid degradation reaction. Methylene blue served as a screening analyte which allowed for rapid measurement of permeate. A major limitation in this study was the inability to simultaneously inject the oxidant with the sample into the membrane system. An additional flow meter would be required to make this change, which was unavailable during the course of this study. As seen in previous studies, persulfate has potential to be used as a pretreatment for membrane filtration to reduce membrane fouling, but additional work needs to be performed to demonstrate the activation of persulfate by a single metal coated ceramic membrane surface.

REFERENCES

Alpatova, A. L., Davies, S. H., & Masten, S. J. (2013). Hybrid ozonation-ceramic membrane filtration of surface waters: The effect of water characteristics on permeate flux and the removal of DBP precursors, dicloxacillin and ceftazidime. Separation and Purification Technology, 107, 179–186. https://doi.org/10.1016/j.seppur.2013.01.013

Amor, C., Fernandes, J. R., Lucas, M. S., & Peres, J. A. (2021). Hydroxyl and sulfate radical advanced oxidation processes: Application to an agro-industrial wastewater. Environmental Technology and Innovation, 21. https://doi.org/10.1016/j.eti.2020.101183

Bao, Y., Lim, T. T., Wang, R., Webster, R. D., & Hu, X. (2018). Urea-assisted one-step synthesis of cobalt ferrite impregnated ceramic membrane for sulfamethoxazole degradation via peroxymonosulfate activation. Chemical Engineering Journal, 343, 737–747. https://doi.org/10.1016/j.cej.2018.03.010

Cheng, X., Liang, H., Ding, A., Zhu, X., Tang, X., Gan, Z., Xing, J., Wu, D., & Li, G. (2017). Application of Fe(II)/peroxymonosulfate for improving ultrafiltration membrane performance in surface water treatment: Comparison with coagulation and ozonation. Water Research, 124, 298–307. https://doi.org/10.1016/j.watres.2017.07.062

Cheng, X., Wu, D., Liang, H., Zhu, X., Tang, X., Gan, Z., Xing, J., Luo, X., & Li, G. (2018). Effect of sulfate radical-based oxidation pretreatments for mitigating ceramic UF membrane fouling caused by algal extracellular organic matter. Water Research, 145, 39–49. https://doi.org/10.1016/j.watres.2018.08.018

Deng, Y., & Zhao, R. (2015). Advanced Oxidation Processes (AOPs) in Wastewater Treatment. Current Pollution Reports, 1(3), 167–176. https://doi.org/10.1007/s40726-015-0015-z

Erhayem, M., & Sohn, M. (2014). Stability studies for titanium dioxide nanoparticles upon adsorption of Suwannee River humic and fulvic acids and natural organic matter. Science of the Total Environment, 468–469, 249–257. https://doi.org/10.1016/j.scitotenv.2013.08.038

Freeman, S., & Shorney-Darby, H. (2011). What's the Buzz About Ceramic Membranes? Journal AWWA, 103(12), 12–13. https://doi.org/https://doi.org/10.1002/j.1551-8833.2011.tb11572.x

Karnik, B. S., Davies, S. H., Baumann, M. J., & Masten, S. J. (2005a). Fabrication of catalytic membranes for the treatment of drinking water using combined ozonation and ultrafiltration. Environmental Science and Technology, 39(19), 7656–7661. https://doi.org/10.1021/es0503938

Karnik, B. S., Davies, S. H., Baumann, M. J., & Masten, S. J. (2005b). The effects of combined ozonation and filtration on disinfection by-product formation. Water Research, 39(13), 2839–2850. https://doi.org/10.1016/j.watres.2005.04.073

Karnik, B. S., Davies, S. H., Baumann, M. J., & Masten, S. J. (2007). Use of salicylic acid as a model compound to investigate hydroxyl radical reaction in an ozonation-membrane filtration

hybrid process. Environmental Engineering Science, 24(6), 852–860. https://doi.org/10.1089/ees.2006.0156

Li, C., Sun, W., Lu, Z., Ao, X., & Li, S. (2020). Ceramic nanocomposite membranes and membrane fouling: A review. In Water Research (Vol. 175). Elsevier Ltd. https://doi.org/10.1016/j.watres.2020.115674

Li, N., Lu, X., He, M., Duan, X., Yan, B., Chen, G., & Wang, S. (2021). Catalytic membrane-based oxidation-filtration systems for organic wastewater purification: A review. Journal of Hazardous Materials, 414(135), 125478. https://doi.org/10.1016/j.jhazmat.2021.125478

Li, Z., Sun, Y., Huang, W., Xue, C., Zhu, Y., Wang, Q., & Liu, D. (2020). Innovatively employing magnetic CuO nanosheet to activate peroxymonosulfate for the treatment of high-salinity organic wastewater. Journal of Environmental Sciences (China), 88, 46–58. https://doi.org/10.1016/j.jes.2019.07.011

Liu, B., Qu, F., Yu, H., Tian, J., Chen, W., Liang, H., Li, G., & Van Der Bruggen, B. (2018). Membrane Fouling and Rejection of Organics during Algae-Laden Water Treatment Using Ultrafiltration: A Comparison between in Situ Pretreatment with Fe(II)/Persulfate and Ozone. Environmental Science and Technology, 52(2), 765–774. https://doi.org/10.1021/acs.est.7b03819

Peters, T. (2010). Membrane technology for water treatment. Chemical Engineering and Technology, 33(8), 1233–1240. https://doi.org/10.1002/ceat.201000139

Qing, W., Liu, F., Yao, H., Sun, S., Chen, C., & Zhang, W. (2020). Functional catalytic membrane development: A review of catalyst coating techniques. Advances in Colloid and Interface Science, 282. https://doi.org/10.1016/j.cis.2020.102207

Wu, H., Xu, X., Shi, L., Yin, Y., Zhang, L. C., Wu, Z., Duan, X., Wang, S., & Sun, H. (2019). Manganese oxide integrated catalytic ceramic membrane for degradation of organic pollutants using sulfate radicals. Water Research, 167. https://doi.org/10.1016/j.watres.2019.115110

Xu, H., Cheng, W., Chen, Z., Zhai, X., Ma, J., & Zhang, T. (2022). Selective oxidation of water pollutants by surface-complexed peroxymonosulfate during filtration with highly dispersed Co(II)-doped ceramic membrane. Chemical Engineering Journal, 448. https://doi.org/10.1016/j.cej.2022.137686

Yu, C., Xiong, Z., Zhou, H., Zhou, P., Zhang, H., Huang, R., Yao, G., & Lai, B. (2022). Marriage of membrane filtration and sulfate radical-advanced oxidation processes (SR-AOPs) for water purification: Current developments, challenges and prospects. Chemical Engineering Journal, 433(P3), 133802. https://doi.org/10.1016/j.cej.2021.133802

Zhao, Y., Lu, D., Xu, C., Zhong, J., Chen, M., Xu, S., Cao, Y., Zhao, Q., Yang, M., & Ma, J. (2020). Synergistic oxidation - filtration process analysis of catalytic CuFe2O4 - Tailored ceramic membrane filtration via peroxymonosulfate activation for humic acid treatment. Water Research, 171. https://doi.org/10.1016/j.watres.2019.115387

Zhu, R., Diaz, A. J., Shen, Y., Qi, F., Chang, X., Durkin, D. P., Sun, Y., Solares, S. D., & Shuai, D. (2018). Mechanism of humic acid fouling in a photocatalytic membrane system. Journal of Membrane Science, 563, 531–540. https://doi.org/10.1016/j.memsci.2018.06.017